Hot Mix Asphalt Surface Characteristics Related to Ride, Texture, Friction, Noise and Durability

Rebecca McDaniel, Principal Investigator
Institute for Safe, Quiet, and Durable Highways
North Central Superpave Center
Purdue University

February 2014

LRRB
LOCAL
ROAD RESEARCH
BOARD

Technical Report Documentation Page

1. Report No. 2014-07	2.	3. Recipients Accession No.	
4. Title and Subtitle Hot Mix Asphalt Surface Characteristics Related to Ride, Texture, Friction, Noise and Durability		5. Report Date February 2014	
		6.	
7. Author(s) Tyler Dare, Rebecca McDaniel, Ayesha Shah and Robert Bernhard		8. Performing Organization Report No.	
9. Performing Organization Name and Address North Central Superpave Center Joint Transportation Research Program, Purdue University School of Civil Engineering West Lafayette, IN 47907-1284		10. Project/Task/Work Unit No.	
		11. Contract (C) or Grant (G) No. (C) 98283	
12. Sponsoring Organization Name and Address Minnesota Department of Transportation Research Services & Library 395 John Ireland Boulevard, MS 330 St. Paul, MN 55155		13. Type of Report and Period Covered Final Report	
		14. Sponsoring Agency Code	
15. Supplementary Notes http://www.lrrb.org/pdf/201407.pdf			

16. Abstract (Limit: 250 words)

The objective of this investigation was to develop a model to predict on-board sound intensity (OBSI) on hot mix asphalt pavements using on-site and laboratory data. The data used included noise and physical property data collected on 25 asphalt-surfaced roadway test sections at the MnROAD pavement testing facility. These test sections were constructed mainly in 2007 and 2008 using a variety of materials, mixtures and layer thicknesses.

A modeling approach called the mechanism decomposition approach was used to develop the models. In this approach, the contributions of different noise mechanisms to the overall noise level and to noise in certain frequency ranges are modeled separately then are combined to form the total noise spectrum. Ultimately, two nonlinear statistical models were developed that predict one-third octave band and overall sound intensity levels on asphalt-surfaced pavements. The models incorporate the pavement parameters that were found to have the most significant effects on tire-pavement noise including pavement macrotexture, air temperature, modulus of the pavement surface layer, and the combined effect of temperature and modulus. The models differ in the type of texture data used as an input parameter.
The models have been found to predict the overall OBSI sound intensity level to within 1.5 dB and the one-third octave bands to within 2 dB for most of the pavements tested. Other metrics and evaluation of the model accuracy by cell, year, temperature and other factors are also reported. The models are provided in an Excel spreadsheet.

17. Document Analysis/Descriptors Tire/pavement noise, Sound intensity, Asphalt pavements, Texture		18. Availability Statement No restrictions. Document available from: National Technical Information Services, Alexandria, Virginia 22312	
19. Security Class (this report) Unclassified	20. Security Class (this page) Unclassified	21. No. of Pages 116	22. Price

Hot Mix Asphalt Surface Characteristics Related to Ride, Texture, Friction, Noise and Durability

Final Report

Prepared by:

Rebecca McDaniel
Ayesha Shah
Tyler Dare
Robert Bernhard

Institute for Safe, Quiet, and Durable Highways
North Central Superpave Center
Purdue University

February 2014

Published by:

St. Paul, MN 55155

Acknowledgements

Table of Contents

List of Figures

List of Tables

Executive Summary

Tire-pavement noise is a growing concern in many areas. The proliferation of noise walls along urban and suburban roadways is physical evidence of that fact. Noise walls are expensive features, however, and may have limited effectiveness. Controlling tire-pavement noise at its source, the tire-pavement interface, may be a more economical and effective approach to reducing noise.

Being able to predict the tire-pavement noise properties for various pavement surfaces based on properties of those surfaces would be advantageous. Using an accurate model, the effects of changing pavement surface properties could be evaluated prior to implementation. The long-term effects of various parameters could be estimated and appropriate designs developed.

This project, then, was initiated to explore a wealth of pavement and noise data available at the MnROAD pavement test facility to develop a noise model that would take the pavement surface properties into account. The specific objective of this investigation was to develop a model to predict on-board sound intensity (OBSI) on asphalt pavements using on-site and laboratory data. To develop such a prediction model, it was necessary to determine the effects of seasonal variations on asphalt surface characteristics and identify surface characteristics and material properties that affect tire-pavement noise generation.

Tire-Pavement Noise Mechanisms, Control and Measurement

Tire-pavement noise is generated and amplified through a variety of mechanisms, which are briefly summarized in this report. As the tire rolls over the pavement surface, the tread blocks impact the pavement, setting off vibrations in the tire carcass. Vibrations are also caused by friction between the tread blocks and the pavement. These vibrations create sound, which can be amplified by resonance within the tire cavity. Sound can also be created and amplified by air being forced into and out of the pavement and channels in the tire. Lastly, the curved shape of the tire at the pavement surface can act like the bell on a musical instrument, amplifying the sound and directing it away from the tire. Each of these mechanisms is affected differently by the properties of the pavement surface, and each contributes differently to noise. For example, friction-induced vibrations predominantly affect higher frequency noise (above 1000 Hz).

Controlling tire-pavement noise involves interfering with or disrupting these mechanisms. For example, air movement (pumping) can be reduced by using a porous asphalt surface where the air can be dissipated through the open pores in the pavement. Other properties of the pavement surface can affect the various noise generation and amplification mechanisms. Pavement properties that are thought to influence tire-pavement noise include: various types (wavelengths) of texture, friction, mechanical impedance or stiffness, resistance to airflow through the pavement, surface condition (or rating), porosity, sound absorption and wear. For asphalt pavements, the binder grade, aggregate gradation and maximum size, air void content, mixture type and other factors can affect the pavement surface properties.

Tire-pavement noise also depends on atmospheric conditions, which can vary daily or seasonally. Temperature has a great effect on the mixture stiffness, tire rubber stiffness and adhesion properties. Atmospheric and moisture conditions can affect the propagation of noise but these effects can be reduced by measuring the noise near the source. The effects of short-term and seasonal changes in atmospheric conditions are explored in this report.

There are a number of different ways to measure tire-pavement noise that are summarized in this report. The method of main interest for this project, however, is the On-

Board Sound Intensity (OBSI) method, because that is the method used routinely at MnROAD to collect tire-pavement noise data. In this method, microphones near the tire-pavement interface detect sound radiating from the tire. Since the noise is measured near the source, the impacts of climatic conditions on the propagation of sound are reduced, though effects of the climate on the generation mechanisms will still exist. OBSI data has been collected at MnROAD on different asphalt pavement test cells under varying climatic conditions over time.

Based on an extensive review of the literature on tire-pavement noise, the factors identified as potentially having an influence on tire-pavement noise were explored for possible inclusion in the model to be developed. That literature review also examined existing tire-pavement noise models developed in the U.S. and elsewhere and their applicability to the existing MnROAD test data.

Development of the Tire-Pavement Noise Models

A modeling approach called the mechanism decomposition approach was used in this study to develop a model to predict tire-pavement noise on asphalt pavements. In this approach, the contributions of different noise mechanisms to the overall noise level and to noise in certain frequency ranges are modeled separately then are combined to form the total noise spectrum. A change in one pavement parameter may increase noise caused by one mechanism but reduce noise from another mechanism. For example, an increase in pavement friction may cause increased noise from adhesion and friction-induced vibrations but a decrease in air pumping. The mechanism decomposition approach allows the effects of different mechanisms to be accounted for and for the noise from each mechanism to change independently. The mechanism-decomposition method was used to develop the models by considering the effects of changes in the pavement and test parameters on the low-, mid- and high-frequency noise spectra.

Using the available MnROAD data, a series of one- and two-parameter models was used to assess the significance of the potentially important pavement parameters on tire-pavement noise. These reduced parameter models were used to explore the effects of changes in each parameter on the noise in different frequency ranges. If a parameter was found to have a significant effect on noise in one or more frequency range, that parameter was considered further in the development of the full model. Parameters that were not found to have a significant impact on tire-pavement noise were dropped from consideration. The pavement parameters explored included temperature (alone and in combination with age and with modulus), texture (using various metrics and measurement techniques), absorption, friction and modulus (stiffness).

The parameters that were found to have a significant effect on tire-pavement noise included: temperature (on high-frequency noise), texture (at low-, mid- and high-frequencies) and friction (on low- and mid-frequencies). The combined effect of temperature and modulus was significant, so both parameters were considered in the final model development. Skewness was not found to have a significant impact on tire-pavement noise for the pavements studied. Absorption was included in the later modeling efforts but was later dropped; it is likely confounded with other parameters such as texture. Absorption could possibly have been found to be more important if more porous pavements were included in the data set.

Ultimately, data measured on MnROAD test sections was used to develop two nonlinear statistical models. The models predict one-third octave band and overall sound intensity levels on asphalt-surfaced pavements and incorporate the pavement parameters that were found to have the most significant effects on tire-pavement noise generation. Specifically, these models consider the effects of pavement macrotexture, air temperature, modulus of the pavement surface layer

and the combined effect of temperature and modulus. Sound intensity levels are predicted for both the leading and trailing edges of the tire. The models differ in the type of texture data used as an input parameter.

The models have been found to predict the overall OBSI sound intensity level to within 1.5 dB and the one-third octave bands to within 2 dB for most of the pavements tested. Other metrics and evaluation of the model accuracy by cell, year, temperature and other factors are also reported.

The models are provided in an Excel spreadsheet requiring three or four input values: 12.5 mm texture level, air temperature and surface modulus. When laser profiler data is used for the texture metric, the time between the texture measurement and the noise determination is also required. Changing the inputs results in automatic changes in the predicted overall OBSI sound intensity level and one-third octave band levels. The models are configured in such a way that future refinements in the data or test procedures can be incorporated, if desired.

1. Introduction

Tire-pavement noise is a growing concern in many areas. The proliferation of noise walls along urban and suburban roadways is physical evidence of that fact. Transportation related noise has been shown to affect human health and animal behavior, so its control and mitigation is important.

Being able to predict the tire-pavement noise properties for various pavement surfaces based on properties of those surfaces would be advantageous. Using an accurate model, the effects of changing pavement surface properties could be evaluated prior to implementation. The long-term effects of various parameters could be estimated and appropriate designs developed.

This project, then, was initiated to explore a wealth of pavement and noise data available at the MnROAD pavement test facility to develop a noise model that would take the pavement surface properties into account.

1.1 Objectives

The objective of this investigation was to develop a model to predict on-board sound intensity (OBSI) on hot mix asphalt (HMA) pavements using on-site and laboratory data. To develop such a prediction model, it was necessary to determine the effects of seasonal variations on asphalt surface characteristics and identify surface characteristics and material properties that affect tire-pavement noise generation.

Ultimately, data measured on MnROAD test sections was used to develop two nonlinear statistical models. The models predict one-third octave band and overall sound intensity levels on asphalt-surfaced pavements and incorporate the pavement parameters that were found to have the most significant effects on tire-pavement noise generation.

1.2 Scope

The models were developed based on noise and physical property data collected on 25 asphalt-surfaced roadway test sections at the MnROAD pavement testing facility. These test sections were constructed mainly in 2007 and 2008 using a variety of materials, mixtures and layer thicknesses. The surfacing materials include dense-graded Superpave mixtures with varying binder grades, warm mix asphalt, porous asphalt and Novachip.

In the years since construction, an extensive amount of data has been collected. The types of data available include measurements of noise, friction, surface texture, ride quality, temperature, distress and structural capacity, among other properties. This data was analyzed as appropriate to develop the models to predict OBSI noise levels based on the physical properties of the pavement.

The models were developed for the types of asphalt surfaces tested at MnROAD and based on the types of test data available. Applying these models to other surface types or with different input variables would require validation and perhaps revision of the models. However, the models were formulated and implemented (in an Excel spreadsheet) in such a way that future revisions can be readily accommodated.

1.3 Approach

The major tasks in completing the proposed investigation are outlined below. These tasks ultimately led to the development of two models to predict OBSI noise levels using different input variables. The findings of these tasks and the resulting models are described in this report.

- **Task 1:** Conduct a thorough review of the literature on state-of-the-art tire-pavement noise modeling efforts in the U.S. and abroad and the effect of pavement characteristics on tire-pavement noise.
- **Task 2:** Conduct an investigation into the effects of seasonal variations in temperature and moisture on surface characteristics of HMA pavements
- **Task 3:** Identify the variables significant to tire-pavement noise and whether they are positively or negatively correlated with OBSI.
- **Task 4:** Develop a mathematical model of OBSI using data measured on MnROAD test sections and determine the limitations of the model.
- **Task 5:** Write a draft final report including detailed information on the model, its development, and its use. Submit the model through the MnDOT/University of Minnesota Center for Transportation Studies publication process.
- **Task 6:** Write a final report addressing all comments and corrections from MnDOT and submit it for publication.

1.4 Organization of this Report

This report will summarize the findings of the various tasks of this research effort and describe the resulting tire-pavement noise prediction models and how to use them. The remainder of this report is organized as follows:

- Chapter 2 provides background information on how tire-pavement noise is measured by different researchers; tire-pavement noise generation and amplification mechanisms; the pavement and mixture properties that affect tire-pavement noise and how they are measured; and the effects of atmospheric conditions and seasonal variations on tire-pavement noise.
- Chapter 3 consists of a review of existing tire-pavement noise models, the applicability of those models to the MnROAD test data and, finally, the mechanism-decomposition approach used to develop new models based on the MnROAD data.
- Chapter 4 summarizes the variables that significantly affect tire-pavement noise in different frequency ranges and presents reduced parameter models of tire-pavement noise used to assess the impacts of various parameters on overall noise levels.
- Chapter 5 presents the final tire-pavement noise prediction models developed as a part of this research effort.
- Chapter 6 presents a summary of the findings, conclusions and future research and implementation needs.

A bibliography of cited references and appendices detailing certain efforts necessary for the development of the models are also included.

2. Background Information

When exploring the findings of the literature review, review of existing models and the other tasks of this project, it is important to understand the ways in which tire-pavement noise is measured; the mechanisms that cause tire-pavement noise; the pavement properties that significantly impact tire-pavement noise; and other factors, such as environmental conditions and seasonal variations, that also affect tire-pavement noise generation and propagation. This chapter provides a brief overview of those topics. In addition, Appendix A provides some definitions of terms used in this report.

2.1   Tire-Pavement Noise Measurement Techniques

There are a number of different methods to measure tire-pavement noise. The differences between these methods are largely due to differences in the equipment available, goals of the measurement efforts and preferences among researchers. Different noise prediction models, described in Chapter 3, use different measurements of tire-pavement noise. Therefore, a brief overview of the measurement techniques used by tire-pavement noise researchers follows.

There are five common methods of measuring tire-pavement noise on in-service pavements. Each method has advantages and disadvantages, primarily involving the equipment and time required and whether the method focuses on tire-pavement noise or traffic noise as a whole.

2.1.1   Statistical Pass-By

The statistical pass-by (SPB) method describes a technique for measuring the average traffic noise for a given section of pavement. As described in ISO 11819-1 [1], a microphone is placed 7.5 m from the center of the lane of traffic to be tested and 1.2 m above the ground. Vehicle speed and maximum sound pressure level (SPL) are measured for at least 100 passenger cars and 80 heavy vehicles. A linear interpolation is used to determine the average SPL at the desired speed. The principal advantage of the SPB method is that total traffic noise is measured, which can be used to estimate the noise received at nearby homes. In addition, the equipment needed to conduct the measurement is minimal and traffic control is not necessary. One disadvantage of SPB measurements is that they are time-consuming. A typical measurement can take two technicians several hours to conduct. In addition, researchers interested in only one component of traffic noise, such as tire-pavement noise or engine noise, are not able to isolate the desired component from SPB measurements. Results of the SPB method are more susceptible to variation with weather conditions than some other measurement techniques.

2.1.2   Controlled Pass-By

The controlled pass-by (CPB) method uses a similar microphone set up to the SPB method but uses a test vehicle instead of measuring noise from the existing traffic stream. Maximum pass-by SPL is recorded for several passes of the test vehicle. The principal advantage of the CPB method over the SPB method is that measurements taken at different locations can be easily compared because they are taken with identical test vehicles and tires. CPB takes less time at a single location than SPB. Since the CPB test requires that the test vehicle be isolated from surrounding traffic, this method may require traffic control depending on the density of traffic.

2.1.3   Coast-By

The coast-by (CB) method is similar to the CPB method, but the engine of the test vehicle is shut off as the vehicle reaches the test area. Any remaining noise is solely due to tire-pavement interaction.

2.1.4   Close-Proximity Trailer

The close-proximity (CPX) method is one of the most common methods for measuring tire-pavement noise at the source. As described in ISO 11819-2 [2], a trailer is towed behind a test vehicle at highway speeds. The trailer houses a test tire and an array of microphones. The tire is enclosed in a box of sound-absorbing material so that the microphones only measure tire-pavement noise. Because noise is measured close to the source, results of CPX testing are less susceptible to atmospheric variations than wayside testing. The primary disadvantage of CPX testing is that a larger investment must be made in microphones, data processing equipment, and the trailer.

2.1.5   On-Board Sound Intensity

The on-board sound intensity (OBSI) method is another common method of measuring tire-pavement noise at the source. Instead of the test trailer used in the CPX method, sound intensity probes, which consist of two phase-matched microphones, are placed near the rear passenger tire of the test vehicle itself. The sound intensity probes are placed so that only sound radiating away from the tire is measured, and other sounds such as engine noise and wind noise are excluded. The OBSI method requires intensity probes at the leading and trailing edge of the contact patch, so either four microphones must be used or additional passes of the test vehicle must be made compared to the CPX method. The OBSI method is described in AASHTO TP 76 [3]. Its advantages and disadvantages are similar to those of the CPX method.

2.1.6   Relationships between Measurement Techniques

Several studies have attempted to discover relationships between the different measurement techniques of tire-pavement noise. A large study found a good relationship between CPX and SPB measurements when considering overall sound pressure levels [4]. The relationship between CPX and CB measurements was found to depend on both microphone position and frequency, but the two methods were shown to give similar rank orders of tires and pavement [5]. Substantial testing of the relationship between OBSI and CPB tests had been conducted in the development of the OBSI method. It was found that CPB data can be predicted from OBSI data for a variety of pavement types within 0.5 dB on average [6]. Porous pavements have been shown to affect both noise generation, as measured by OBSI, and propagation to pass-by measurement locations, and so correlation between pass-by measurements and OBSI is weaker for porous pavements [7].

In general, correlations have been found for several pairs of measurement techniques. However, in the development of tire-pavement noise models, it is preferable to use a single technique to reduce measurement errors and simplify the model. In the case of the MnROAD data used in this project, that method is OBSI, because multiple measurements have been, and presumably will continue to be, made on the test sections. Only limited SPB data is available at MnROAD, so that data is not used here. In addition, the models developed are ultimately intended to investigate and compare pavement properties affecting tire-pavement noise, not necessarily to predict noise levels at or beyond the right-of-way, therefore, the OBSI method

provides noise measurements at the pavement surface that are less susceptible to variations caused by atmospheric conditions.

2.2   Tire-Pavement Noise Mechanisms

Tire-pavement noise is the result of several generation mechanisms, including tire carcass vibration, adhesion, slip-stick and air pumping. Each of these mechanisms is affected differently by changes in pavement parameters. Each mechanism may be strong or weak on any given pavement, so a model must account for these independent phenomena to accurately predict noise levels. In addition, there are several mechanisms by which generated sound is amplified, such as Helmholtz resonance and the horn effect. A thorough understanding of the tire-pavement noise mechanisms and how each is affected by changes in pavement parameters is a necessary component of a successful prediction model.

2.2.1   Generation Mechanisms

This section describes the mechanisms by which tire-pavement noise is generated. It also presents the frequency ranges where the mechanism has the greatest impact on noise and the pavement parameters that influence the mechanism. The relevant pavement and mixture properties affecting tire-pavement noise are described in Section 2.3.

2.2.1.1   Air Pumping

The air pumping mechanism is a major source of tire-pavement noise [8-12]. Air pumping occurs when air is forced from between two surfaces, such as between tread blocks and pavement. The air pumping mechanism can be thought of as similar to two hands clapping together, where the air is compressed and forced out at the edges of the hands, which creates the clapping sound. This mechanism is generally highest around 1000-2500 Hz or higher frequencies [13-15]. Researchers have found that increased pavement porosity or roughness can decrease air pumping noise by creating a path for air to escape while being compressed [12, 16-18].

Frequency range: 1000-2500 Hz, possibly higher

Relevant pavement characteristics: Porosity, macrotexture

2.2.1.2   Impact-Induced Vibration

Vibrations in the tire carcass are induced as tread blocks impact the pavement. This is analogous to striking a surface with a rubber hammer. Such vibrations can radiate sound and can be a major source of tire-pavement noise. Impact-induced vibrations are thought to affect noise below 1000 Hz [8, 17]. These vibrations can exist in the radial, tangential, or axial directions and depend primarily on surface macrotexture. The mechanical impedance of the pavement has also been shown to affect this mechanism [16].

Frequency range: Below 1000 Hz

Relevant pavement characteristics: Macrotexture, mechanical impedance

2.2.1.3   Friction-Induced Vibration

Tire carcass vibrations can also be induced by very smooth pavements through friction. Slip-stick motion between the pavement and tread blocks has been shown to cause noise in the 1000-

2500 Hz range and above [8, 19]. The squeaking of shoes on a basketball court is an example of the stick-slip mechanism. Friction can also build up shear forces in the tread blocks, which are released as the treads leave the contact patch [19, 20]. The free vibration of the tread blocks can then radiate sound. Friction is likely to be affected by pavement texture at all wavelengths and by whether the texture is positive or negative. In addition, rubber friction can be affected by temperature, so frictional noise characteristics could vary with changes in climate, even when using the same tire on the same pavement.

Frequency range: 1000-2500 Hz and above

Relevant pavement characteristics: Microtexture, macrotexture, positive/negative texture

2.2.1.4 Adhesion-Induced Vibrations

The adhesion mechanism occurs when tread blocks stick to pavement and then are stretched and released at the trailing edge of the contact patch. This can be thought of as similar to the pop when a suction cup releases from a surface. The mechanism can cause radial and tangential carcass vibrations, which can radiate sound near the trailing edge [21, 22]. Adhesion has been shown to be reduced by wet pavement and with increasing microtexture [23] but could also be affected by temperature. Adhesion is thought to be an important mechanism above 1000 Hz [8].

Frequency range: above 1000 Hz at trailing edge

Relevant pavement characteristics: Microtexture, macrotexture, positive/negative texture

2.2.2 *Amplification Mechanisms*

Once noise is generated there are other mechanisms that can serve to amplify the noise. Those mechanisms, the frequency ranges they affect and the pavement parameters that influence them are presented in this section.

2.2.2.1 Cavity Resonance

Acoustic resonances within the cavity of the tire are thought to lead to amplification of vibrations near the acoustic resonance frequency (200-250 Hz) [22]. However, some researchers have found that these resonances do not affect tire vibration [24] or are only important at pavement discontinuities, such as contraction joints [21].

Frequency range: 200-250 Hz

Relevant pavement characteristics: none

2.2.2.2 Pipe Resonance

Acoustic resonances can form in the channels between tread blocks, analogous to sound in organ pipes. This phenomenon has been measured on grooved tires [25, 26] and on modern treaded tires [21]. Estimates for the frequency of pipe resonances have ranged from 600-8000 Hz, but the mechanism is generally thought to occur at high frequencies [15, 27, 28]. The dimensions and shapes of the tread blocks can affect resonant frequencies [25]. Resonances are linked with the air pumping mechanism, and researchers have concluded that the two phenomena should not be considered to be independent [15, 29]. Pipe resonances have been shown to be more prominent on very smooth pavements and can be reduced by using porous pavement [26].

Frequency range: Generally high frequencies but estimates range from 600-8000 Hz

Relevant pavement characteristics: Porosity, macrotexture

2.2.2.3 Helmholtz Resonance

A Helmholtz resonance occurs when a trapped volume of air is connected to the outside via a channel [30]. This has been likened to the noise produced by blowing air across the top of a soda bottle. Resonance occurs at sharp peaks whose frequencies are determined by the cavity volume and channel dimensions. In a tire, a volume of air can be trapped between the tread blocks and the pavement, and a channel is formed as a tread is about to contact the pavement or has just lifted off. It has been noted that the Helmholtz resonance effect should not be separated from the air pumping mechanism [15]. Helmholtz resonances can be reduced by allowing the air to escape from the trapped volume through the use of porous or rough-textured pavements.

Frequency range: Generally high frequencies but estimates range from 600-8000 Hz

Relevant pavement characteristics: Porosity, macrotexture

2.2.2.4 Horn Effect

The horn effect is the mechanism by which sound is amplified by the horn-like shape formed between the pavement and the tire near the leading and trailing edge of the contact patch. Similar to the bell on many brass instruments, the horn shape acts as an impedance matching device between sound sources at the contact patch and the surrounding air [31]. The effect has been shown to amplify sound in the 2000-3000 Hz range [31], though some models of the horn amplification mechanism include all frequencies above 700 Hz [32]. The horn effect is reduced due to porosity [33] and other parameters affecting sound absorption by the pavement [34].

Frequency range: 700 Hz and above

Relevant pavement characteristics: Porosity, sound absorption

2.3 Pavement and Mixture Parameters and How They Are Measured

There are a number of pavement surface characteristics that may affect the generation and propagation of tire-pavement noise. (The generation and amplification mechanisms are described in Section 2.2 of this report.) Different parameters affect different generation and propagation mechanisms, and some are more important than others. Characteristics that are strongly related to tire-pavement noise include the surface texture, friction, air voids, sound absorption and mechanical impedance. Pavement surface characteristics also depend on some mixture characteristics, such as aggregate gradation, volumetrics and binder type. These characteristics may vary to some extent with seasonal changes in temperature and moisture conditions, as discussed in 2.4 and 2.5. Surface wear caused by the action of traffic may also affect tire-pavement noise but is typically not a seasonal variation. Factors of somewhat lesser importance include airflow resistance, roughness and surface rating.

The following is a discussion of the pavement and mixture parameters most commonly used in or potentially applicable to tire-pavement noise modeling. How those characteristics can be measured is also summarized.

2.3.1   Texture

As an overall category of pavement surface characteristics, texture has the greatest impact on tire-pavement noise. Pavement texture is included in virtually all tire-pavement noise models.

There are, however, different aspects of texture that must be considered; a single metric cannot adequately describe texture because different texture characteristics have different effects on the various noise mechanisms (as discussed in 2.2). Therefore, texture is generally broken down into different ranges of texture depending on the wavelength of the texture. Pavement microtexture is defined as "a deviation of a pavement surface from a true planar surface with characteristic dimensions along the surface of less than 0.5 mm" while the pavement macrotexture is defined as "a deviation of 0.5 - 50 mm." Megatexture is the term used to categorize larger scale texture in the range of 50 to 500 mm. Lastly, unevenness describes variations in the roadway profile greater than 500 mm in length [35, 36].

2.3.1.1   Texture Measurements

There are a number of different texture metrics used that are applicable to differing ranges of texture. One method of measuring texture profiles using a laser profiler is standardized in ISO 13473-4 [37]. A laser is used to measure the depth of the pavement at regularly spaced points along the direction of travel. The laser can be mounted on a track or on a rolling chassis. Several parallel lines of texture can be measured simultaneously to collect three-dimensional texture data. Texture data are used to calculate texture profile spectra in statistical models and are used as inputs to rolling contact finite element models. One profiler meeting the requirements of ISO 13473-4, which was used at MnROAD over three days in 2011, is the RoboTex texture profiler.

Another method uses the Circular Track Meter (CTM), sometimes called the Circular Texture Meter. The CTM is standardized in ASTM E2157 [38]. The CTM is a portable device allowing for macrotexture measurements. In the CTM device, a laser displacement sensor mounted on a 142 mm (5.6 in.) arm rotates around a central point at a fixed distance above the pavement and measures the change in elevation of points on the surface. During the measurement, data are collected by a personal computer attached to the tester and the mean profile depth (MPD) is determined. A very rough pavement would have high MPD and a smooth pavement low MPD. Efforts to correlate MPD with noise characteristics have gotten mixed results [39-41]. Texture profile scans of the circumference of the circle measured can be analyzed similarly to laser profiler data.

Historically, pavement surface texture has been determined using a sand patch test [42], where a known volume of sand is spread out and allowed to infiltrate the surface. The diameter of the patch is measured to calculate the mean texture depth (MTD). MTD has been shown to be highly correlated to the MPD determined using the CTM [38]. MPD is now preferred because of the speed of its determination and the fact that the electronic texture profiles provide much more information than the overall average texture measured using the sand patch test.

2.3.1.2   Microtexture

Microtexture is a function of the surface texture of the aggregate particles. High microtexture provides a gritty surface that disrupts the continuity of the water film and produces frictional resistance between the tire and pavement. The microtexture of the pavement surface affects noise generated by tire vibrations induced by friction and by the adhesion between the tire and the pavement surface. Sandberg and Ejsmont suggest that higher microtexture typically causes

8

increased friction, which increases the stick-slip noise generation mechanism. On the other hand, the increased microtexture also leads to a decrease in the adhesion, which results in a lowering of the stick-snap mechanism. These conflicting changes may explain why clear relations between microtexture and tire-pavement noise are not always observed [4]. Generally, microtexture features have been shown to affect tire-pavement noise at frequencies above 1000 Hz [43, 44].

Microtexture can be measured with a laser profiler but cannot be described by measurements such as mean profile depth (MPD) or International Roughness Index (IRI), which are determined primarily by textures of longer wavelengths.

2.3.1.3 Macrotexture

Macrotexture, with wavelengths between 0.5 mm and 50 mm, is determined by the overall properties of the pavement surface. It is related to the type of asphalt surface (e.g., dense versus porous), the gradation of the aggregates in the mixture, and presence of air voids at the surface. This larger scale texture provides channels at the surface through which water can travel away from the contact area between the tire and pavement, reducing the risk of hydroplaning [45, 46].

The macrotexture of the pavement is a major factor affecting tire-pavement noise because it can change the volume of air cavities in the pavement and influence tire vibrations related to impact and friction. Air pumping, impact-induced vibrations, friction-induced vibrations and adhesion between the tire and surface are the generation mechanisms most related to macrotexture, as described in 2.2. Pipe resonance and Helmholtz resonance are the amplification mechanisms impacted by macrotexture. Macrotexture has been shown to affect OBSI levels in the 630-1000 Hz range [47-49]. An increase of macrotexture in the range of 2 to 10 mm reportedly leads to a decrease in tire-pavement noise [50].

Macrotexture can be measured by several methods. Measurement with a laser profiler or CTM can be used to separate the effects of different texture wavelengths within the macrotexture range. However, the most common metric of macrotexture is MPD.

2.3.1.4 Megatexture and Unevenness

Megatexture and unevenness refer to even larger scale texture, with wavelengths greater than 50 mm. In general, megatexture is not considered to affect OBSI, except in cases of extreme roughness such as potholes. An increase in megatexture, however, has been related to an increase in interior vehicle noise [50]. High megatexture or unevenness is usually regarded as a construction defect or symptom of the approaching end of the pavement service life.

Megatexture and unevenness can be quantified by the International Roughness Index (IRI), which is a measure of ride quality. IRI can be calculated from longitudinal texture profiles. It is defined by a digital filter based on a model of a quarter car, and most of the texture information considered is in the 1.25-30 m range [51]. These texture wavelengths are generally not considered to influence tire-pavement noise, but IRI has been included in some tire-pavement noise models [52, 53].

2.3.1.5 Positive versus Negative Texture

One additional aspect of surface texture has an impact on tire-pavement noise of asphalt pavements; that is, whether the texture is positive or negative. Positive surface texture is characterized by aggregate particles that project above the overall level of the pavement surface. A chip seal would frequently provide a positive surface texture as the aggregate particles are embedded in a layer of asphalt binder at their base. Negative texture, on the other hand, consists

9

of channels or air voids that protrude into the surface. A fine graded asphalt mixture would typically exhibit a negative surface texture. If the surface texture is positive, vehicle tires deform around the protruding aggregates to some extent, affecting impact and adhesion mechanisms. More aggressive, positive surface textures also produce greater friction and, in turn, greater friction-induced vibration in the tires. Conversely, with negative texture, the tires tend to travel over the generally planar surface with little deformation and less noise generation [54]. Negative texture tends to reduce air pumping and resonance mechanisms.

Therefore, many tire-pavement noise prediction models distinguish between positive and negative textures. Two pavements with identical texture spectra, one with primarily positive texture and the other with negative texture, can induce different noise levels [55]. Many models incorporate an envelopment process to address the difference between positive and negative textures. High amplitude, negative texture features are filtered out before texture spectra are calculated. Envelopment calculations can be time consuming, so simpler methods of processing texture scans have been used to describe positive and negative texture. One approach is to use a measurement of shape factor, the percentage of pavement texture below 50% of the maximum depth. Low negative texture yields a high shape factor [55]. Other models use measurements of the heights and separation of pavement asperities [39] or the statistical distribution of texture heights [56].

2.3.1.6   Transverse Texture

Texture measurements with a laser profiler are almost always measured in the direction of travel. However, some tire-pavement noise models incorporate transverse texture in their predictions [57-59]. With some prediction models, there is little difference between predictions made with and without considering transverse texture. Transverse texture can affect generation mechanisms in the same way as longitudinal texture. Additionally, transverse texture can affect laser profiler and other measurements of longitudinal texture if the measurement is not lined up with longitudinal textural features. An example of this effect is with longitudinally grooved pavements. A laser dot may dip in and out of grooves if the profiler is not lined up exactly with groove lines, and the resultant measurement may not be an accurate representation of pavement texture. (The CTM measures texture around the circumference of a circle with a diameter of 284 mm (11.2 in) but different segments of that circumference can be analyzed to roughly correspond to longitudinal and transverse texture.) Transverse texture is more important on concrete surfaces or grooved asphalt surfaces on runways; texture on other asphalt surfaces is typically isotropic.

2.3.2   Friction

Pavement friction is closely related to texture. Friction is often used as a measurement of pavement safety, but it can also be used to predict noise levels. Changes in friction primarily affect the slip-stick mechanism, and so affect OBSI levels at high frequencies [23].

Pavement friction is typically used as a measurement of safety and braking distance but can also be used as a parameter in tire-pavement noise prediction models. Friction is most commonly measured in the U.S. using an ASTM towed friction trailer [60]. In this method, the torque produced when a full-scale test tire is locked and slid over the wet pavement surface is used to determine the frictional forces produced by the pavement on the tire. This method is well-suited to measuring frictional properties on a site or network level but can be challenging

and somewhat time consuming to use on short test sections because of the distance traversed during the skid and resetting for a second test.

Another standard test of wet friction is described in ASTM E1911 [61]. A dynamic friction tester is used to measure friction as a function of speed. The tester uses a spinning disk with three rubber sliders. The tester is brought up to the desired rotation speed, and the sliders are brought into contact with the pavement. Torque and rotation speed are used to calculate friction coefficients at speeds of 20, 40, 60, and 80 km/h. One advantage of the DFT is that it is a companion device to the CTM and together they can be used to calculate the International Friction Index (IFI) standardized in ASTM E1960 [62]. In addition, the DFT is a portable device that can be used to spot test friction and can easily be used on short test sections.

2.3.3 Mechanical Impedance

The mechanical impedance of the pavement is related to the flexibility and energy dissipation properties of the pavement surface. In an asphalt mixture, the mechanical impedance is related to the stiffness, or modulus, of the mixture. The modulus of the asphalt pavement materials is known to have a profound impact on the structural strength of the pavement. In addition, it is well known that asphalt mixtures are viscoelastic materials whose moduli change with changes in temperature and loading rate. The modulus of the pavement materials has an unknown effect on tire-pavement noise, but it is potentially a fairly important factor affecting impact-generated vibrations [4]. For this reason, modulus was examined further in the development of the noise prediction models as part of this research.

Mixture stiffness is affected by many factors, including the mixture type, aggregate gradation and mixture volumetrics, but the asphalt binder properties have a major impact on the modulus. A more elastic binder, such as a polymer modified binder, would be expected to produce a more flexible mixture. In fact, one group found than a granulated rubber pavement allowed high-frequency vibrations to discharge into the road surface [16]. In general, it has been found that rigid pavements tend to be louder than flexible pavements [63].

Asphalt mixture stiffness properties change as the temperature changes, so the mechanical impedance, as measured by the modulus, would also change over the course of a day or seasonally, as discussed further in Sections 2.4 and 2.5. Since asphalt binders age over time through oxidation, the mechanical impedance could also change over the life of the pavement as the mixture stiffens.

Modulus can be measured or estimated in a variety of ways. Laboratory measurement of dynamic or resilient modulus is very common, with dynamic modulus increasing in popularity with the implementation of the Mechanistic-Empirical Pavement Design Guide and the Asphalt Mixture Performance Tester (AMPT). Dynamic modulus can also be estimated using a variety of models based on mixture volumetrics and binder properties, most notably the Hirsch and Witczak models. Lastly, modulus can be measured or estimated in the field. Backcalculation of layer moduli from Falling Weight Deflectometer (FWD) readings is one of the most common methods of determining moduli in situ.

The complex dynamic modulus can be used to characterize mixture behavior over the range of temperatures and loads that pavements are exposed to in situ. Dynamic modulus testing is conducted in the laboratory on mixes at different temperatures and frequencies according to AASHTO T 342 [64]. Dynamic modulus master curves are then developed by applying shift factors with respect to a reference temperature and are used in mechanistic-empirical pavement design [65].

11

Alternatively, models have been developed by various researchers [66-68] to predict the modulus as a function of mixture properties in addition to frequency and temperature. For example, the Witczak model uses material properties and mixture volumetrics including the binder viscosity, air void content, effective binder volume and aggregate gradation, along with the loading frequency, to predict the mixture dynamic modulus. The Hirsch model uses the binder complex modulus, voids in the mineral aggregate and voids filled with asphalt to predict the dynamic modulus [69]. While there is some disagreement about how well these models work for predicting the modulus or which model is best, most agree that these two work fairly well in most cases [69-73]. So, volumetrics can be assumed to have an impact on the mechanical impedance of the pavement in which those mixtures are used.

In addition to measuring the stiffness of asphalt paving mixtures in the laboratory, it is also possible to estimate the stiffness of pavement layers by measuring the deflection of the pavement structure under a known load and backcalculating the stiffnesses of the individual pavement layers. The deflection is commonly measured using a Falling Weight Deflectometer (FWD). There are many different backcalculation programs available, but Evercalc was selected for use in this project based on work by Rao and Von Quintus [74]. The use of Evercalc to estimate pavement surface moduli for this project is described in Appendix B.

2.3.4   Airflow Resistance

Airflow resistance is a measure of how difficult it is for air to flow through a pavement. Airflow is measured according to ISO 9053 [75]. Air is forced through a sample, the pressure difference and flow rate are both measured, and flow resistivity is then calculated. Airflow resistance is related to air pumping and resonance mechanisms of tire-pavement noise and is often incorporated into models of acoustic impedance for pavement.

2.3.5   Surface Rating

Similar to pavement roughness, the pavement condition rating is considered to be a measure of distress at the pavement surface. The rating is typically highest immediately after construction or rehabilitation and gradually (or sometimes rapidly) decreases as cracking, rutting, raveling and other types of distress accumulate. As these distresses increase the texture or roughness of the pavement surface, they can impact the noise generation.

Surface rating (SR) is one measure of the distress on a pavement surface. SR is measured by counting the number of cracks and joint deterioration on a segment of road, and then calculating the SR metric by applying weighting factors [76].

2.3.6   Porosity and Sound Absorption

The porosity of an asphalt surface is largely determined by the presence and amount of air voids at the surface and interconnected voids within the mixture. Consequently, the porosity is related to the type of mixture. Open-graded mixtures tend to have more interconnected voids than dense-graded mixtures. These interconnected voids provide channels for air pressure to travel away from the tire-pavement contact area. Sound pressure energy can be dissipated through friction within these air voids, thus porosity is related to sound absorption within the pavement [54].

The porosity of the pavement surface impacts noise generation through air pumping since higher porosity provides more channels in which sound energy can be dissipated. There is less resistance to airflow, thus reducing the noise. Pavement porosity also affects the noise amplification mechanisms associated with pipe and Helmholtz resonances and the horn effect.

Air void content is a measure of pavement porosity and is used in many prediction models for tire-pavement noise. Air void content, V_A, is determined by the theoretical maximum specific gravity, G_{mm}, and the bulk specific gravity, G_{mb}, of compacted specimens or pavement cores according to the equation:

$$V_A = \frac{G_{mm} - G_{mb}}{G_{mm}} * 100\% \qquad\qquad \text{Eqn 1}$$

Calculation of G_{mm} is described in AASHTO T 209 [77] and involves measuring the mass and volume of the loose HMA mix. For porous mixes, G_{mb} is calculated per AASHTO T 331 [78], where a compacted specimen is vacuum sealed before a volume measurement is conducted.

Sound absorption of pavement is measured in one of two ways. First, a core sample of a pavement may be taken and the absorption measured in an impedance tube, as described in ASTM E1050 [79]. Alternatively, non-destructive tests of absorption have been developed by several different research teams. Sound absorption data are usually reported as narrow-band spectra. For the most common size of pavement specimen tested, absorption data are valid up to approximately 1600 Hz.

2.3.7 Traffic Wear

The action of traffic on the pavement surface produces wear in the wheelpaths. It is a well-known observation that the friction of asphalt surfaces initially increases as traffic wears off the binder film coating the aggregate particles. This typically happens within a few months, but the time varies depending on the level of traffic, type of binder and temperature. After the binder film on the aggregate surfaces is worn off, friction changes as the aggregate particles polish under the pneumatic tires. How rapidly the friction changes depends primarily on the type of aggregate at the surface and the amount of traffic [80]. Friction and noise are closely related since they both depend on the micro- and macrotexture of the pavement. Consequently, traffic wear is also expected to affect tire-pavement noise, and many field studies confirm this [80, 81].

Traffic also frequently affects the in situ volumetrics of an asphalt mixture. It is typical for the air void content of a mixture to exhibit a loss of air voids in the range of as much as 2 to 3% from the time of construction until several years later, depending on the mixture characteristics and components, traffic level and prevailing temperatures). This densification under traffic changes the air void content, voids filled with asphalt and voids in the mineral aggregate.

Traffic has historically been quantified using equivalent single axle loads (ESALs). Calculation of ESALs requires traffic count data and an estimate or count of the number of heavy trucks. A measurement of ESALs can be used to describe the amount of wear on a roadway section. More direct measurements of the effects of traffic are also possible. Changes in pavement texture or porosity, for example, can be detected using the measurement techniques described above and comparing the measurements over time.

2.3.8 Mixture Parameters Related to Tire-Pavement Noise

As noted above, various pavement surface parameters such as texture, friction, stiffness and porosity are influenced by the mixture type and volumetrics. Therefore, in analyzing the MnROAD tire-pavement noise data, the mixture characteristics in the individual test sections will need to be considered.

A paper by Kocak and Kutay [82] reported on a laboratory study to investigate the mixture parameters that had the greatest impact on tire-pavement noise. Though perhaps not definitive, the paper does provide some insight into mixture parameters that are likely to be significant variables impacting tire-pavement noise. The authors used a novel lab method called TIPANOS to measure the noise generated when cylindrical specimens are rotated between treaded tires. The noise generated is measured with an intensity microphone. The experiment involved comparisons of different nominal maximum aggregate sizes, aging conditions, air void contents, binder types, mixture types, aggregates and gradations. In addition to measuring the noise generated, the specimen volumetrics and certain mixture parameters were measured. The mixtures were evaluated in terms of dynamic modulus, phase angle, storage modulus and elastic modulus. The authors concluded that as the air void content and voids in the mineral aggregate (VMA) increased, the sound pressure level (SPL) decreased, presumably because of the increased presence of interconnected air voids. As binder content increased, SPL was observed to decrease. The authors surmised that an increase in binder content made the mixture more viscous and therefore quieter due to damping. They cautioned, however, that an increase in the binder content could decrease the air voids, which could increase the noise generation, so binder content should be optimized. A positive relationship between the coefficient of uniformity of the aggregate gradation and SPL was also observed. As the coefficient of uniformity increases, the aggregates are more densely packed, thus reducing the air void content and increasing the noise. Lastly, the authors found that the dynamic modulus, voids filled with asphalt, coefficient of uniformity of the aggregate gradation and binder content had statistically significant impacts on the SPL [82].

Volumetrics also have a great impact on the porosity of the pavement, and porosity is expected to have an impact on tire-pavement noise [4]. Many studies have shown, for example, the beneficial effects of porous, open-graded mixtures on noise properties [81, 83-87]. The porosity affects several noise generation and propagation mechanisms and is related to sound absorption as described in 2.2

2.4   Effects of Atmospheric Conditions and Moisture on Tire-Pavement Noise

Many of the pavement characteristics that influence tire-pavement noise can vary as atmospheric conditions and moisture levels in the pavement change. These changes in the pavement can, in turn, affect the noise generation and amplification mechanisms. Changes in atmospheric conditions can have a strong influence on the propagation of noise through the air, but those effects are minimized when noise is measured using the OBSI method because the propagation distance from the noise source to the receiver is very short. Atmospheric conditions have a much greater effect on noise levels measured by the SPB, CPB or CB methods. The potential effects of these changing conditions are summarized here, with an emphasis on the effects of the pavement parameters.

The parameters most sensitive to changes in temperature, age and rainfall include mechanical impedance, friction, texture and air voids. Air voids and friction can also be affected by wear, and mechanical impedance may be affected by aging. The relevant effects of changing parameters were explored during model development, as described in Chapter 4.

2.4.1   Direct Effects of Temperature on Tire-Pavement Noise

Changes in ambient temperature can have a strong effect on the propagation of tire-pavement noise, as measured by pass-by techniques. Additionally, temperature can affect tire-pavement

14

noise generation mechanisms. Increased temperature has been found to cause increases in high-frequency noise and decreases in low-frequency noise [8]. The low-frequency effect may be the result of changes in the mechanical impedance of the pavement, affecting impact mechanisms, while the high-frequency effect may be due to changes in adhesion or friction characteristics. It is difficult to separate the effects of changes in tire temperature from the effects of changes in pavement temperature, since tire temperature is difficult to measure on a moving vehicle [88] and the tire may change temperature over the course of several tests. Rubber tread compounds can change properties with temperature [89], which can affect several generation mechanisms.

2.4.2   Modulus

The response of an HMA pavement to traffic load is determined primarily by its modulus, which in turn is highly dependent on the loading frequency and pavement temperature because asphalt is a viscoelastic material. At high temperatures and low loading frequencies (as in slow-moving traffic), the pavement has low stiffness and will tend to deform more under these conditions. On the other hand, at low temperatures and high frequencies, the stiffness of the pavement is greater and, correspondingly, the deflections are lower. The pavement response may also change as the binder oxidizes or stiffens over time (age hardens).

2.4.3   Air Voids

Air voids can change with changes in the pavement temperature, though in most cases the variation in the air void content is relatively minor in well-designed mixtures. An extreme example of a change in the air void content would be with an over-asphalted or low air void mixture that flushes or bleeds when the pavement temperature is very high and the volume of asphalt binder expands. As the binder volume begins to exceed the volume of air voids, excess binder is pushed out onto the surface of the pavement, which could affect the frictional properties, adhesion and porosity of the pavement. Once bleeding occurs on the surface because of the increased binder volume, however, the change is not reversible. In addition, daily or seasonal temperature increases that cause an increase in binder volume may fill voids in the mineral aggregate and may therefore have some influence on noise.

2.4.4   Friction

Seasonal and short-term variations in pavement friction have been reported and widely studied [90-96]. The lowest values typically occur towards the end of summer and the highest during the winter. Short-term variations are typically caused by temperature fluctuations and precipitation. A nonlinear relationship to model seasonal friction variation has been proposed [97]. Other authors [98] have proposed using a fuzzy clustering approach as a mathematical description of the seasonal friction variation. Friction changes were also found to be affected by seasonal changes in the grading of abrasive material lying on the road or embedded in vehicle tires [99. 100].

In addition to seasonal variations in friction, the action of traffic (wear) also results in changes in the friction and texture of the pavement surface. It is commonly reported that the frictional properties of a newly paved surface improve markedly over the first few months of service. One study, for example, showed substantial increases in the friction value of a new HMA surface from the time it was opened to traffic to 35 weeks later [101]. This phenomenon was most likely caused by improvement of the surface microtexture resulting from wearing off (due to tire action) the binder film coating the aggregates on the surface of the pavement.

Results of a laboratory study [102] showed that the shape of the polishing curve may sometimes exhibit a high rate of friction loss after the binder film is worn off. After this initial loss, the friction may continue to decrease at a lower rate, eventually leveling off. The high rate of friction loss may be due to polishing of the initially sharp edges of the exposed aggregate; as these edges are worn off or reoriented, the friction decreases.

2.5 Investigation of Effects of Seasonal Variations (Task 2)

The pavement and material properties discussed above may also exhibit seasonal or cyclic changes. In developing a model to predict tire-pavement noise, it is important to understand how these parameters may vary with seasonal changes in temperature and moisture conditions. Therefore, this section summarizes the results of a review of the literature regarding seasonal variations in asphalt pavement surface parameters and how these parameters relate to tire-pavement noise. The most important pavement surface characteristics that affect tire-pavement noise are identified.

A recent interim report on the SPS8 experiment in the Long-Term Pavement Performance (LTPP) program summarizes the key factors that cause asphalt pavement distress related to environmental factors in the absence of heavy loads. Changing moisture conditions were determined to contribute to alligator cracking, bleeding, block cracking, corrugations, depressions, edge cracking, potholes, pumping, raveling, rutting, shoving and swelling/bumps; however, moisture was not the primary cause of any of these distresses. Temperature change was concluded to be the primary cause of thermal cracks and a contributing factor in the development of alligator cracking, bleeding, block cracking, corrugations, longitudinal cracking in and outside the wheelpath, raveling, rutting, shoving and swelling/bumps. Environmental changes in the subgrade were primarily to blame for swelling/bumps and edge cracking; they also contributed to alligator cracking, depressions, longitudinal cracking, pumping and rutting [103].

These distresses may contribute to increased megatexture and/or unevenness of the pavement surface and to changes in the condition rating so may have some impact on noise. Most of them, however, are not seasonal variations; that is, once they occur, they do not heal, so they would contribute not to a cyclic change in noise but instead to a gradual increase in noise. Some moisture and subgrade conditions may vary seasonally, however. Therefore, while these distresses were considered in the development of the model, other surface parameters were found to have a greater impact on noise.

2.5.1 Texture and Friction

The seasonal variability of friction is widely recognized and has been the subject of many research efforts. Friction has been studied much more widely than changes in the pavement surface texture, perhaps because it has historically been more feasible to measure friction at high speeds on a network level.

As one example, seasonal variation was observed in Indiana, where the cyclic variation was described as "very apparent." Repeated testing of 14 asphalt pavement sections showed that the friction was highest in the spring, decreased markedly in the summer, and began to recover in late fall [104].

Hill and Henry observed both short- and long-term seasonal variations in friction on test pavement surfaces in State College, Pennsylvania. They noted that the friction (skid number, SN) was generally higher in the winter and spring than in summer and fall. They attributed the short-

term variations to the number of days since the last significant rainfall and to the pavement temperature. They also said that the microtexture, traffic volume and mechanical effects of winter traffic (such as studded tire abrasion) determine the skid resistance at the beginning of summer [105]. A further study of the same Pennsylvania sections plus ten sites in Tennessee and North Carolina confirmed the significance of time since last rainfall and pavement temperature [106].

A study in Mississippi also documented the fact that friction increases in the late fall and winter and decreases in late spring and summer. The author observed that shorter term variations occur within the seasonal variation cycle and were attributed predominantly to the time since the last rain [107].

The impacts of temperature and rain were also observed in a study of four sites with widely differing climates (ranging from cool temperate to subtropical) in Australia. The strength of correlations varied depending on the climates and frequency of rainfall at the sites [108].

Wang and Flintsch reported on a six-year study of variations in pavement surface conditions at the Virginia Smart Road. The surfaces investigated included several Superpave mixes, an open-graded friction course and an SMA. As noted in previous studies, this data confirmed that the friction was lowest in the late summer and started to rebound in fall, however, they observed different trends in the friction at high and low speeds. They ascribed this to the higher temperature in summer. At low speed, where adhesion is believed to be the controlling factor, higher temperatures will soften and expand the asphalt binder, creating a thicker binder film coating the aggregate. This presumably decreases adhesion and causes a lower low speed friction number in the summer. At high speeds, where hysteresis is more dominant, a decrease in the stiffness of the tire rubber because of the higher temperature in summer could lead to more hysteresis due to more tire and pavement deformation. The authors also acknowledge an alternate explanation related to snow removal operations increasing the microtexture during the winter which may be lost over the summer [96].

In the same study, Wang and Flintsch also looked at changes in the pavement macrotexture using a high speed laser profiler. They observed very minimal changes in macrotexture over the course of a year. There was a slight decrease in macrotexture in August compared to measurements in February and May; the authors suggest that this slight decrease coupled with the increase in friction at high speed in summer imply that the change in hysteresis is related to changes in the tire rubber properties as well as the characteristics of the pavement surface. Longer-term changes in the macrotexture were observed. The macrotexture slowly increased as the pavements aged, probably due to loss of fines [96].

A paper from 1998 [109] summarized the conceptual explanation of seasonal variation in friction while acknowledging that the fundamental mechanisms controlling this type of variation are not known. The basic concept is that during the dry period in summer, fines are polished off the surface of the pavement resulting in decreases in the micro- and macrotexture of the pavement. Contamination of the surface from oil and grease dripping from vehicles can also cause a decrease in friction during the summer. During the winter, the use of deicing salts and abrasives scours the pavement and exposes new aggregate faces, causing an increase in the micro- and macrotexture. When heavy rains fall in the spring, the pavement is cleaned of the fine particles that abrade the pavement in the winter. The paper went on to show that seasonal variations in friction exist even in no-freeze pavements in Texas and follow the same trends noted earlier. Biweekly friction measurements at six sites in Texas showed that higher friction measurements were observed after significant rainfall, lending credence to the concept that

rainfall washes away fines and increases the surface texture. Temperature was also shown to be a significant factor [109].

A study by Ahammed and Tighe came to somewhat different conclusions. They looked at both concrete and asphalt pavements and found similar trends in month to month friction levels, leading them to conclude that the seasonal differences were more related to changes in the tire rubber stiffness than to changes in the pavement surface characteristics. They also concluded that the length of time since the last rainfall did not have a statistically significant effect on friction. However, they did not evaluate the potential effects of surface contamination. The authors observed a statistically significant effect of temperature on friction, which they attributed to changes in the tire rubber stiffness [110].

2.5.2   Mechanical Impedance

One Long-Term Pavement Performance (LTPP) program Seasonal Monitoring Program (SMP) site in Texas was examined to look at seasonal variations in pavement structural properties [111]. The backcalculated elastic layer moduli from the site were analyzed and compared over the course of a year. A strong correlation was observed between temperature and modulus of the asphalt layer; as the temperature increased, the modulus decreased. There were also strong correlations between the temperatures measured at different locations within the pavement, meaning that only one pavement temperature was needed to model the modulus. Another study looking at data from the same SMP site determined that the seasonal variation in elastic moduli followed a sinusoidal pattern similar to that of temperature [112].

There are many models to predict pavement modulus based on temperatures measured at various locations. As one example, a 2004 paper reports on an analysis of data from the LTPP program to examine seasonal variations in the modulus of asphalt pavements. The study looked at data from 11 LTPP sites located in areas with freezing and non-freezing climates. The authors found a strong correlation between backcalculated modulus and pavement temperature (measured at middepth, in this case), but temperature alone was not enough to accurately predict the modulus. The air void content, layer thickness, bulk specific gravity of the mix and binder grade were also found to affect the modulus [113].

2.5.3   Mixture Volumetrics

Mixture volumetrics are typically measured only at mix design or during construction as a quality control/quality assurance measure. (Sometimes for research or forensics, volumetrics are determined from cores or though in situ testing during the service life.) Under traffic, some non-reversible densification usually occurs, resulting in a change in the volumetrics, particularly the air void content, voids in the mineral aggregate (VMA) and voids filled with asphalt (VFA). The binder volume can expand with an increase in temperature resulting in a decrease in the air void content and VFA. Except in cases of poor void structure and bleeding, however, these changes are usually expected to be relatively small.

2.5.4   Moisture Conditions

Most research related to the effects of changes in moisture conditions has focused on the changes in the structural strength of the pavement layers, especially of unbound materials. The unbound materials may be subject to frost heave and swelling with changes in moisture at different temperatures. Exceptions to this include studies looking at the effects of rainfall on friction and studies of moisture damage in the bound pavement layers.

One study, however, was found that looked at the effect of subgrade moisture on longitudinal profile [114]. (Since profile is related to megatexture and/or unevenness, it is conceivable that changes in subgrade moisture could have some impact on noise levels if the profile is affected at relevant wavelengths.) This study examined data from 43 LTPP Seasonal Monitoring Sites with asphalt pavements. The study found that moisture in the subgrade did have a significant effect on pavement roughness in the range of 5.0 to 31.2 m for sites in freezing climates and 5.0 to 39.0 m in sites in non-freezing climates. Thus, subgrade moisture affects the pavement unevenness, which is not expected to contribute significantly to tire-pavement noise.

So, as seen in the discussion of friction, most researchers agree that a rainfall event may clean the pavement and affect the surface texture. Severe distresses caused by moisture damage in the pavement structure, such as potholes, stripping, swelling or depressions, may cause increases in roughness that can impact noise in extreme cases. The physical presence of moisture in the pavement structure, however, is not expected to influence tire-pavement noise as long as the voids in the surface are not saturated with moisture.

3. Tire-Pavement Noise Models (Task 1)

Over the past several decades, many statistical models have been developed to predict tire-pavement noise from pavement properties. While the following is not an exhaustive list, it will illustrate the typical methods, inputs and results of noise models from both the United States and abroad. It should be noted that many of the models discussed here are acknowledged by the authors to be works in progress with room for improvement by incorporating more inputs or more mechanisms. A summary of the inputs and outputs of the models described is shown in Table 1 at the end of this section.

Section 3.4 describes the mechanism decomposition approach used to develop the new tire-pavement noise predictions models in this study.

3.1 Tire-Pavement Noise Models Developed in the United States

Noise models developed in the United States and the inputs to those models are presented here. Models developed overseas are presented in the next section.

3.1.1 Khazanovich and Izevbekhai

Khazanovich and Izevbekhai [52] have developed a statistical model for tire-pavement noise using input data from 51 different test cells at the MnROAD test facility. OBSI levels were measured with the Standard Reference Test Tire (SRTT) [115] at 60 mph, and the inputs to the model were surface rating, pavement age, IRI, friction and ESALs. Different models were developed for different types of pavement, such as tined concrete and asphalt, but all models were of the form:

$$I = ESAL^{\alpha} Age^{\beta} IRI^{\gamma} SR^{\delta} \qquad \text{Eqn 2}$$

where I is the overall sound intensity, SR is surface rating, and α, β, γ, and δ are model parameters. Although Khazanovich and Izevbekhai present residual errors for some of the input pavements, it is difficult to determine an average dB error for all of the pavements.

3.1.2 Ongel, Kohler, and Harvey

Ongel, Kohler, and Harvey [53] have developed a statistical model of noise generation on asphalt pavements. A total of 72 open-graded, dense-graded, rubberized open-graded and rubberized gap-graded asphalt pavements were used as inputs to the model. The pavements were 0-8 years old. The authors found that many of the input parameters are highly correlated with each other, such as IRI and pavement age. The model includes pavement age, mix type, air void content, IRI, fineness modulus, uniformity, MPD, raveling, transverse cracking and layer thickness. The model is given by:

$$
\begin{aligned}
L = 107.6 &+ 0.172(Age) - 1.74(Mix\ Type) - 0.10(AVC) - 0.48(IRI) \\
&- 1.25(Fineness\ modulus) - 0.005 C_u + 0.004(MPD) \\
&+ 1.84(Presence\ of\ Raveling) \\
&- 0.09(Presence\ of\ Transverse\ Cracking) \\
&+ 0.003(Surface\ Layer\ Thickness)
\end{aligned}
\qquad \text{Eqn 3}
$$

where L is the overall OBSI level and C_u is the coefficient of uniformity. The Presence of Raveling and Presence of Transverse Cracking variables are input as either 1 or 0, depending on if the phenomenon is present in the roadway. The model produced a standard error of about 1 dB, and the pavements' OBSI levels covered a total range of about 7 dB.

20

3.1.3 Rasmussen

Rasmussen [116] has developed a statistical model for tire-pavement noise that focuses on the effect of pavement texture. The inputs to the model were 3-D texture profiles measured with the RoboTex line laser profiler. While the author mentions that models for many types of pavements are being developed, a model for OBSI level on concrete pavements with burlap drag was presented. The model includes texture levels for 40 and 50 mm wavelength pavement features (measured according to ISO 13473-4 [117]), texture skew in the transverse direction [118] and core roughness depth in the transverse direction (ISO 13565-2 [119]). A standard error of 0.6 dB was reported. Several test sections from each pavement were included in the analysis, although the number of distinct pavements used and the range of their OBSI levels were not reported.

3.1.4 Reyes and Harvey

One of the most recently published models for tire-pavement noise was developed by Reyes and Harvey [120]. The model is unique in that it only requires inputs from pavement core samples and not from field test sections. Among models developed in the United States, it is one of the few that can be used to predict one-third octave band intensity data. The inputs required are MPD and airflow resistivity, both of which are measured on pavement cores. A separate linear model is used for each one-third octave band between 500 and 5000 Hz. The statistical inputs to the model were 16 different pavement core samples from open-graded and gap-graded asphalt pavements. The authors do not provide standard error numbers for overall OBSI levels but do mention that a low coefficient of determination was obtained for the 800 and 1000 Hz bands, which generally have a high influence on overall OBSI levels.

3.2 Tire-Pavement Noise Models Developed in Europe and Asia

Models developed in Europe and Asia are presented here.

3.2.1 Brinkmeier et al.

Brinkmeier et al. [121, 122] have approached tire-pavement noise modeling by constructing a complete finite element model of the tire and using the boundary element method to predict radiated sound. Their research is part of the "Leiser Straßenverkehr" (silent traffic) project in Germany. Their finite element model involves the computation of tire vibration in the rolling process, which is nonlinear because of large deformation and contact mechanics. The authors point out that the model is not valid at high frequencies, where relative motion between tread blocks and tire carcass becomes important. The model has been used to predict noise generation on smooth and rough drum surfaces with several different tires. The model correctly predicted the ranking of the tires from quietest to loudest, but the measured overall noise levels varied from predictions by 6-17 dB.

3.2.2 Fujikawa et al.

Fujikawa et al. [39, 40, 56, 123-126] have been developing a model for tire-pavement noise for several years. In the model, a laser profiler is used to measure surface profiles, and texture metrics such as asperity height, spacing, and unevenness are all calculated. A statistical model is used to predict octave band spectra in the 500-4000 Hz range. The model inputs are MPD and asperity height unevenness. In contrast to most other statistical models of noise, the linear model is used to predict mean square acoustic pressure instead of decibel sound pressure or intensity. Nine pavements were used in developing the model, including six dense-graded asphalt

pavements, two open-graded asphalt pavements and one polished surface. The model predictions match measured spectra within 2 dB at all frequency bands, with a variation among the samples of 5-8 dB across the bands.

3.2.3 SPERoN

The SPERoN model (Statistical Physical Explanation of Rolling Noise) has been developed in recent years by researchers at Chalmers University and consulting firms M+P and Müller-BBM [55, 57, 127-129]. The SPERoN model aims to predict coast-by levels from road surface parameters. The model uses a 3-D contact model to obtain the one-third octave band contact pressure spectrum, which is then used as an input to the statistical portion of the model. The inputs to the contact model are pavement surface profiles and 3-D tread profile data, and additional statistical inputs are airflow resistivity and vehicle speed. Data for the model are taken from the Sperenberg project database, which contains 3200 coast-by spectra with 16 tires, 38 dense pavements, and rolling speeds from 50-120 km/h. The SPERoN model uses a mechanism-based approach, where pressure spectra from four sound generation mechanisms are added together. The four mechanisms considered by the model are:
- Vibration, which is assumed to be related to airflow resistance, contact force, tire width and tread stiffness;
- Airflow, related to contact force, airflow resistance, tread stiffness, tire width and vehicle speed;
- Cavity resonances, related to tread pattern; and
- Aerodynamic noise, related to vehicle speed.

The SPERoN model is only valid at 20°C, so temperature correction must be applied to measured data. The model appears to perform well for a wide range of vehicle speeds but average prediction errors have not been published by the authors. More recent iterations of the model have included acoustic absorption and mechanical impedance data.

3.2.4 HyRoNE

Similar to the SPERoN model, the HyRoNE model [128-130] uses a linear relationship between contact force and sound pressure to predict pass-by levels. The HyRoNE model also uses a 3-D contact model but also uses raw texture spectra to predict noise at frequencies above 1250 Hz. Inputs to the model are 2-D texture data, the acoustical impedance of the surface and vehicle speed. The prediction accuracy of the HyRoNE model is similar to the SPERoN model, and predictions get slightly better when temperature correction is applied.

3.2.5 TRIAS

TRIAS (Tyre-Road Interaction Acoustic Simulation) is a purely physical model for tire vibration and noise emission [131-136]. The model uses finite and boundary element modeling to predict one-third octave band pressure spectra near the tire. A submodel to TRIAS called RODAS (Road Design Acoustic Simulation) is used to estimate road texture, porosity, and sound absorption from HMA mix properties. Another submodel, TYDAS (TYre Design Acoustic Simulation) simulates model inputs from known tire parameters if all necessary inputs are not known. Dense and porous HMA pavements and ISO test tracks were used to validate the TRIAS model. Noise on the dense asphalt surfaces was predicted to within 2 dB overall. Noise on porous surfaces was predicted to within 5 dB, and the model mostly over-predicted the noise. Measured and predicted noise spectra have not been presented.

3.3 Applicability of Models to MnROAD Test Data

As illustrated in Table 1 below, the various models of tire-pavement noise all have different requirements as far as inputs, outputs, and data processing. It would be informative to apply the existing noise models to the MnROAD data set and determine the accuracy of the predictions. Unfortunately, there is not complete overlap between the MnROAD data set and the requirements of any of the models. For example, the popular European models require a 2-D or 3-D texture profile of the pavement surface and output coast-by or close proximity pressure predictions. While there is texture data on many cells, the noise data is either OBSI or, to a lesser extent, SPB, not CB or CPX data. So it is not possible to determine the accuracy of the European models with respect to MnROAD test surfaces. The prediction models developed in the U.S. all use OBSI as the noise metric, but the models either require pavement survey results [52, 53], 3-D texture profiles [116], or flow resistivity [119]. Without a complete overlap of data, it is not possible to compare the accuracy of the various models.

Table 1. Comparison of inputs and outputs for tire-pavement noise models. Variables included in the MnROAD database are shaded.

	Measured pavement texture properties					Surveyed pavement texture properties			Other pavement properties								Tire props.		Outputs				
	Mean profile depth (MPD)	Asperity height unevenness	International roughness index (IRI)	2-D texture profile	3-D texture profile	Surface rating (SR)	Raveling	Transverse cracking	Equivalent single axle loads (ESALs)	Age	Mix type	Surface layer thickness	Air void content (V_A)	Fineness modulus	Uniformity	Flow resistivity	3-D tire profile	Vehicle speed	Overall OBSI Level	1/3rd octave band OBSI level	Overall nearfield pressure	1/3rd octave band coast-by levels	1/3rd octave band CPB levels
Khazanovich and Izevbekhai			X			X			X	X									X				
Ongel, Kohler, and Harvey	X		X				X	X	X	X	X	X	X	X	X				X				
Rasmussen					X														X				
Reyes and Harvey	X															X			X	X			
Brinkmeier					X												X					X	
Fujikawa	X	X																				X	
SPERoN					X											X	X	X				X	
HyRoNE				X						X													X

24

3.4 The Mechanism Decomposition Approach

The most common approach in tire-pavement noise modeling is to use linear regression analysis to correlate overall on-board sound intensity levels with the measured pavement parameters [52, 53]. The model takes the form

$$L_{noise} = c_0 + c_1 P_1 + c_2 P_2 + c_3 P_3 + \cdots \qquad \text{Eqn 4}$$

where L_{noise} is the overall noise level of the pavement measured using OBSI; P_i are parameters such as texture level, mean profile depth, vehicle speed, pavement age, traffic volume and acoustical properties; and c_i are coefficients determined by the regression analysis.

Unfortunately, there are assumptions and oversimplifications inherently made in this approach. One shortcoming of this statistical model is that it is only used to predict overall sound levels. Tire-pavement noise is complex and controlled by several independent phenomena. These phenomena may be either strong or weak on any given HMA pavement. Thus, a model must be able to properly account for these independent phenomena to predict overall sound intensity levels. To predict overall sound intensity level, it is necessary to do a reasonably accurate prediction of the one-third band spectrum.

Tire-pavement noise is the result of several generation mechanisms, including tire carcass vibration, adhesion, slip-stick and air pumping [4] and described in Chapter 2. Each of these mechanisms is affected differently by changes in pavement parameters. For example, consider two pavements with identical macrotexture but different friction. A tire rolling on the pavement with higher friction will experience more vibration and adhesion than on the pavement with lower friction, but air pumping will be reduced. The result of an increase in only one variable (friction) is a complicated shift in the shape of the tire-pavement noise spectrum. The effect of the shift on the overall noise levels depends on which of the several generation mechanisms is most prominent. A successful model of tire-pavement noise must take into account the different mechanisms and allow for the noise from each mechanism to change independently of the others.

There is, however, another method for modeling tire-pavement noise that does not have the same oversimplification issues. In the mechanism decomposition method, a hybrid statistical-experimental approach is used to model tire-pavement noise. The fundamental theory of this method is that a tire-pavement sound intensity spectrum can be decomposed into several constituent spectra, each representing the contribution from a generation mechanism [43]. Since each mechanism is an independent noise source, the constituent spectra are added logarithmically to form the total tire-pavement noise spectrum. The magnitude of each constituent spectrum is a function of a subset of the pavement parameters. The model can be mathematically represented by

$$L_{noise}(f) = \big(L_1(f) + c_{1,0} + c_{1,1}P_1 + c_{1,2}P_2 + \cdots\big) \oplus \big(L_2(f) + c_{2,0} + c_{2,1}P_1 + c_{2,2}P_2 + \cdots\big) \oplus \ldots \qquad \text{Eqn 5}$$

where $L_{noise}(f)$ is the predicted noise level but is now a function of frequency; P_i are measured pavement parameters; $c_{i,j}$ are coefficients determined by a non-linear least squares method; and $L_j(f)$ are constituent spectra that are the same for all pavements. $\oplus$ represents a logarithmic sum, defined as:

$$a \oplus b = 10 log_{10}\big(10^{a/10} + 10^{b/10}\big) \qquad \text{Eqn 6}$$

3.4.1 Example of Mechanism Decomposition

The mechanism decomposition approach is best illustrated through an example. In this example, three constituent spectra are used, as shown in Figure 1. The level of the low-frequency spectrum (blue, a) represents the contributions determined by macrotexture levels. The mid-frequency spectrum (red, b) contributions are determined by porosity. The high-frequency spectrum (green, c) represents noise determined by friction.
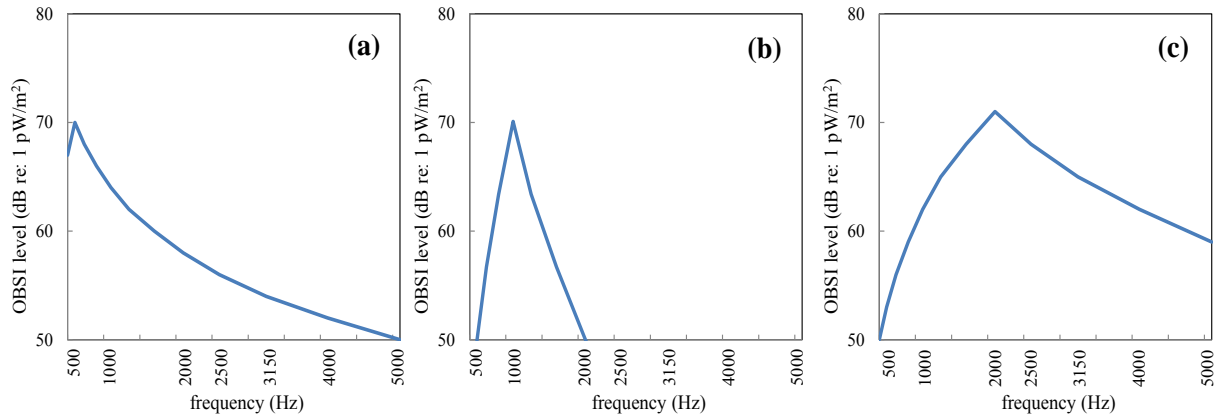
Figure 1. Example constituent spectra. (a) low-frequency spectrum, affected by macrotexture; (b) mid-frequency spectrum, affected by porosity; (c) high-frequency spectrum, affected by friction.

In this hypothetical example, noise spectra on three pavements were measured, as shown in Figure 2. Assume each of the three pavements is identical except for varying porosity. The measured spectra are shown in the solid line behind the dotted line (magenta in color) for the three different pavements (a), (b) and (c). Since the mid-frequency spectrum is the only one affected by porosity, the low- and high-frequency spectra are held constant while the mid-frequency spectrum is shifted such that the total spectrum (black dotted line) best matches with the measured noise. The shift in the mid-frequency spectrum is then correlated to the porosity of the pavement.
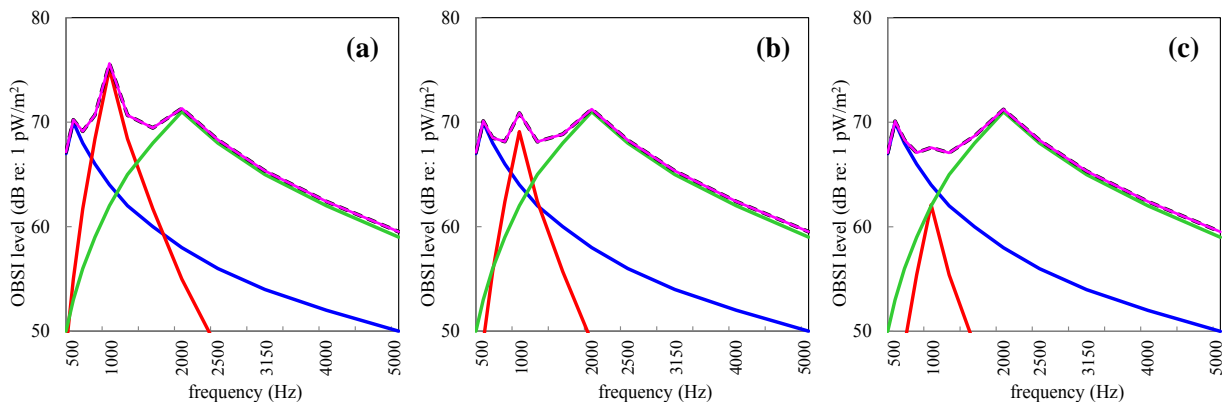
Figure 2. Fitting constituent spectra to measured noise. The mid-frequency spectrum (red) is adjusted higher or lower such that the sum of the three constituent spectra (black dotted) matches the measured spectrum (magenta) for each of the three pavements (a), (b) and (c)

The results of the mechanism decomposition approach and the overall level approach are compared in Figure 3. Using mechanism decomposition (a), the mid-frequency spectrum decreases dramatically with increasing porosity. However, the overall levels (b) are shown to only decrease slightly with increasing porosity due to the effects of the other mechanisms. A researcher only investigating the effect of porosity on overall levels might erroneously conclude that porosity was not an important variable to tire-pavement noise, when, in reality, the effect was masked by other mechanisms. If noise from other mechanisms were reduced, porosity would become increasingly important to overall levels.
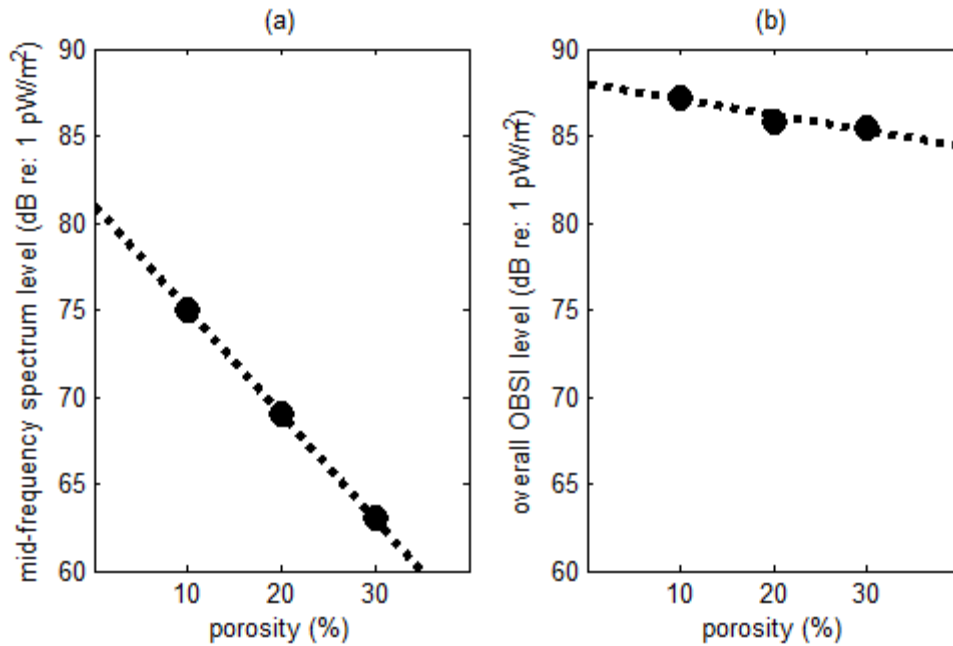

Figure 3. Comparison of the level of the mid-frequency component results from (a) mechanism decomposition approach and (b) overall level approach. The mechanism decomposition approach leads to better insights about the effects of porosity on the three pavements.

As the preceding hypothetical example shows, using a model to predict only overall levels may lead to misleading trends and erroneous conclusions. A mechanism decomposition approach, including prediction of one-third octave band OBSI spectra, is crucial to accurate modeling of tire-pavement noise.

3.5   MnROAD Test Sections and Data Availability

This study will include data from as many as 25 test cells at MnROAD; 15 on the Mainline and ten on the Low Volume Road. The cells include Ultrathin Bonded Wearing Courses; 12.5 mm Superpave mixes with and without RAP and with and without Warm Mix; 4.75 mm HMA with taconite aggregate; porous HMA; and chip seals. There is a wealth of data of various types from these test sections. One complication, however, is the availability of complementary data about different parameters at about the same time period, to facilitate the examination of seasonal variability in the parameters that affect tire-pavement noise. Another potential complication is that some parameters are confounded. For example, both pervious HMA sections have the same

thickness, so it will not be possible to separate out the effects of pervious HMA and layer thickness based solely on the MnROAD data. The different surface types include varying binder grades, but comparison of the effects of binder grade may not be possible in most cases because binder grade is confounded with other variables, such as surface type.

Not all of the cells have the same types of data collected at the same time because they were designed for different research efforts. Therefore, different cells are used in different analyses. Table 2 lists the cells used in various parts of the project and describes the surface type represented by that cell. Specific information on which cells were used in various facets of the project is provided in Section 4.2 for the reduced-parameter models and in figures in Chapter 5 for the full models.

Table 2. Cells Used in Model Analysis and Development

Cell	Surface Type	Binder	Spec/Designation
1	75-Blow Marshall Mix Mill & Inlay	PG52-34	SPWEB340A
2	Ultrathin Bonded Wearing Course	Novachip	--
3	Ultrathin Bonded Wearing Course	Novachip	--
4	Hot Mix Asphalt	PG64-34	SPWEB440F
6	4.75mm Taconite Mix	PG64-34	2360
15	Warm Mix Asphalt	PG58-34	SPWEB440C
16	Warm Mix Asphalt	PG58-34	SPWEB440C
17	Warm Mix Asphalt	PG58-34	SPWEB440C
18	Warm Mix Asphalt	PG58-34	SPWEB440C
19	Warm Mix Asphalt	PG58-34	SPWEB440C
20	Hot Mix Asphalt with RAP	PG58-28	SPWEB440B
21	Hot Mix Asphalt with Fractionated RAP	PG58-28	SPWEB440B
22	Hot Mix Asphalt with Fractionated RAP	PG58-28	SPWEB440B
23	Warm Mix Asphalt	PG58-34	SPWEB440C
24*	Warm Mix Asphalt – Aging Study	PG58-34	SPWEB440C
27*	Hot Mix Asphalt (Chip Seal in 2009)	PG58-34	SPWEB340C
28*	Hot Mix Asphalt (Double Chip Seal in 2011)	PG58-34	SPWEB340C 2356
31*	Hot Mix Asphalt – Taconite Aggregate	PG64-34	SPWEB240F
33*	Hot Mix Asphalt	PG58-34 PPA	SPWEB340C
34*	Hot Mix Asphalt	PG58-34 SBS+PPA	SPWEB340C
35*	Hot Mix Asphalt	PG58-34 SBS	SPWEB340C
70	Hot Mix Asphalt	PG64-34	SPWEB440F
77*	Hot Mix Asphalt	PG58-34 Elvaloy+PPA	SPWEB340C
86*	Pervious HMA	PG70-28	2360
88*	Pervious HMA	PG70-28	2360

*Cells on Low Volume Road; all others on Mainline.

In terms of those parameters that are expected to be significant factors affecting tire-pavement noise, the following briefly summarizes the available data in the test sections of interest.

3.5.1 Texture and Friction

Texture measurements were taken using the sand patch method on some cells in the fall of 2008, near the time of construction. Since then, texture measurements using the Circular Track Meter (CTM) have been collected one to two times a year, in general. RoboTex data was collected on 22 cells a single time, in October-November 2011.

Friction measurements were performed in and between the wheelpaths in some cells using the Dynamic Friction Tester (DFT) since 2008. The towed friction trailer data has been collected one to three times yearly.

3.5.2 Volumetric Properties

Overall, there is no direct measure of volumetric data on the in-place asphalt mixtures over time at MnROAD. Volumetrics were examined at the time of construction but typically not after that. Determining the volumetric properties in situ is either impossible or requires destructive testing (coring). Changes in density could conceivably be measured with a nuclear gauge, but the expected changes due to something like binder expansion at high service temperature are likely to be very small and may be lost in the overall measurement variability. Even if cores were pulled from the pavement during different environmental conditions, by the time they were returned to the lab for testing, some properties would have changed.

Since the volumetric data available is from the mix designs or during construction, consideration of the effects of changes in air void content, for example, with changes in temperature would have to be based on predictions of expected changes in these properties over time. This approach was considered but abandoned because of the imprecise nature of any estimates of changes in air voids, gradation or binder properties during construction or over the service life of the test sections.

3.5.3 Porosity

No direct measurements of porosity of the mixtures have been made, with the exception of permeability tests that were conducted several times on the pervious HMA sections (cells 86 and 88). The researchers searched for predictive models of porosity that could be used with the available data, but no reliable predictive models could be identified. If the models were to be used for porous pavements, porosity and related sound absorption would likely become more important to consider. Since most of the MnROAD test sections, however, are dense graded, the lack of porosity information is not as critical.

3.5.4 Mechanical Impedance

While some measurements of dynamic modulus and ultrasonic modulus have been made on the asphalt mixtures used in various cells, these measurements were made near the time of construction. In situ measurements that would allow estimation of the changes in the stiffness of the mixes daily, seasonally or over the pavement life have not been made, with the exception of Falling Weight Deflectometer (FWD) measurements. One possibility explored in this project was to use a model like the Hirsch or Witczak models to characterize the modulus but, as with the mixture volumetrics, the in situ volumetrics and binder properties are unknown, so the predictions would have been imprecise at best. The FWD data, then, was the best option for considering changes in asphalt concrete modulus over time – both seasonally and as the asphalt ages.

The FWD data was used to backcalculate the asphalt layer moduli. Numerous backcalculation programs exist, and various assumptions are required, so backcalculation is not an exact science. A recent LTPP report compared several different backcalculation programs to recommend which method should be used to determine computed modulus values to incorporate in the LTPP database [74]. One of the programs recommended for HMA analysis is Evercalc, developed by the Washington State Department of Transportation [137]. Based on this recommendation, Evercalc seems to be a reasonable choice for further analysis of the FWD data for this project. The assumptions used in performing the backcalculation are described in Appendix B.

3.5.5 *Condition Rating and Ride Quality*

As with the FWD data, there is a significant amount of data available about the pavement surface condition and ride quality. Data exists on the development of rutting collected roughly every two to three months during the spring through fall from 2009-2011. Visual distress data was collected every year as well. Ride quality data was also collected multiple times each year with the Pathways vehicle and the Lightweight Inertial Surface Analyzer (LISA). For the most part, however, the test sections are relatively smooth, so there are not great differences in ride quality or condition overall.

3.6   Summary

Based on the analysis of literature regarding pavement parameters that affect tire-pavement noise and consideration of the physical data available for the appropriate MnROAD test cells, the following conclusions and plans were made to guide the model development efforts in Chapters 4 and 5.

- Some of the potentially interesting variables have not been measured periodically over time, such as density, air void content and porosity, binder properties, and mixture stiffness. These properties are generally difficult to measure and often require destructive testing (coring).
- The effects of changes in texture were examined on a limited number of cells using the CTM data collected repeatedly. RoboTex data is available on more cells but was only collected once.
- Ride quality data has been measured several times per year and was examined to see if there is a relationship to tire-pavement noise.
- The best data set for exploring the relationship between mechanical impedance and tire-pavement noise was the FWD data. It was necessary to backcalculate the asphalt layer moduli from this data to look for changes in stiffness seasonally and over the pavement service life. Evercalc was used for backcalculation and the non-asphalt layers were grouped into one or two layers to simplify the analysis. Backcalculated moduli were examined to explore the effects of changing temperatures and time on mechanical impedance.
- The Hirsch model was considered as a means to estimate the surface moduli and to explore the effects of possible changes in mixture moduli with changes in volumetrics caused by traffic densification or seasonal changes (binder expansion, etc.). The data to support this model is mainly from mix design or construction, however, not from later in

the pavement life when the noise measurements were made. Therefore, this approach was abandoned.

- In Task 3, the relationships between the various surface parameters and noise (absorption and OBSI data) were explored further to determine which surface parameters are most important and whether they are positively or negatively correlated with noise level.

4. Identification of Variables Significant to Tire-Pavement Noise (Task 3)

Many different parameters have been shown in the literature to affect tire-pavement noise to one extent or another. For efficient model development, however, the variables with significant effects on tire-pavement noise needed to be identified. These variables were identified by developing a series of simplified models for tire-pavement noise using MnROAD data. Each simplified model involved only one or two variables, and all of the other variables were controlled. For example, to identify the effects of temperature on tire-pavement noise, a model was developed using OBSI data measured at MnROAD several times over the course of a single day, thereby eliminating the effects of pavement age. Separate temperature models were developed for each pavement tested to control for differences in texture and sound absorption. By controlling for all other parameters, the effect of air temperature alone could be identified. Simplified models were developed for as many different pavement and atmospheric parameters as possible. Using the findings from these simplified models, a set of significant variables was identified.

4.1   The Mechanism Decomposition Approach to Modeling Tire-Pavement Noise

A series of experiments was designed and used to identify the constituent spectra for different mechanisms of tire-pavement noise. Three spectra were identified, each associated with a different generation mechanism. The spectra for the leading edge are shown in Figure 4. Spectra for the trailing edge are similar and are omitted from this section for brevity. All results for the trailing OBSI probe location are shown in Appendix C.
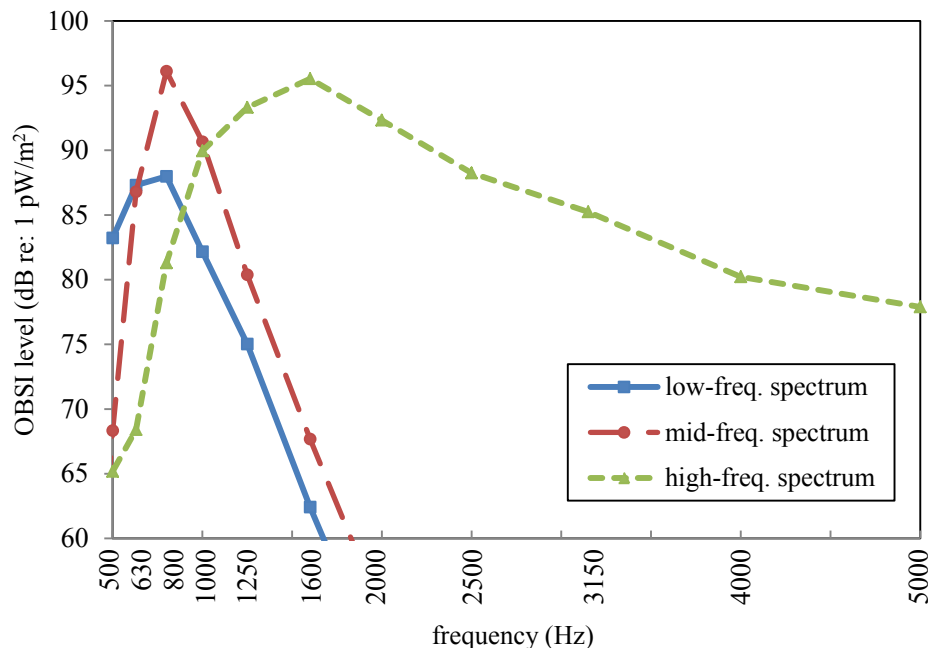

Figure 4: Low-, mid-, and high-frequency constituent spectra.

4.1.1   Low-Frequency Constituent Spectrum

The low-frequency portion of a measured OBSI spectrum is governed by noise generated by a tire's vibrating sidewall. The spectrum (Figure 4, solid line) increases by approximately 7 dB/octave in the 500-800 Hz range. The spectrum has a peak at 800 Hz and decreases at a steeper slope above this frequency.

4.1.2   Mid-Frequency Constituent Spectrum

At frequencies between approximately 800-1250 Hz, a measured OBSI spectrum is determined primarily by noise generated from the vibrations of the treadband. Similar to the sidewall-dominated low-frequency spectrum, the mid-frequency spectrum has a peak at approximately 800 Hz. However, the mid-frequency spectrum (Figure 4, dashed line) rolls off more quickly at higher and lower frequencies. Previous research [138] has shown that the sidewall (low-frequency) and treadband (mid-frequency) sources cannot be considered independent noise sources. To address this issue, the phase relationship between these two sources was determined experimentally [138]. The phase difference between the low- and mid-frequency sources is shown in Figure 5. This phase relationship is important because destructive interference exists between sources at the sidewall and treadband at some frequencies.
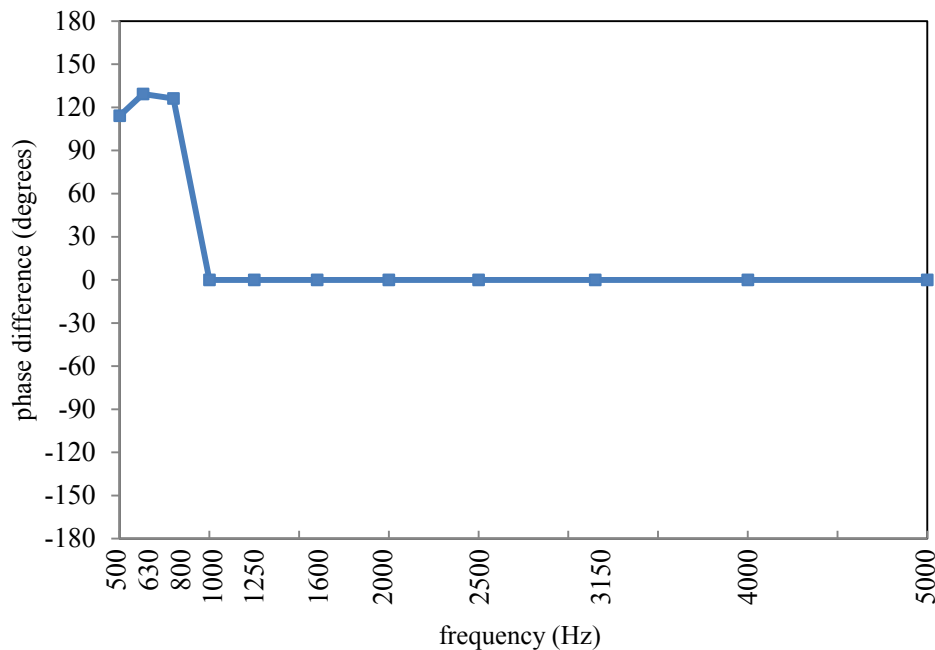

Figure 5: Phase difference between low- and mid-frequency sources.

4.1.3   High-Frequency Constituent Spectrum

At frequencies above approximately 1250 Hz, OBSI noise is dominated by the mechanisms of air pumping and tangential tread block vibrations. The spectra resulting from these sources are similar and can be combined into one high-frequency constituent spectrum. This spectrum (Figure 4, dotted line) peaks at approximately 1600 Hz, with a roll off of approximately 10 dB/octave at higher frequencies. Air pumping and tangential tread block vibration sources are independent from treadband and sidewall sources, so there is no need to consider the phase relationship between the high-frequency spectrum and the other two constituent spectra.

4.1.4 Combination of Constituent Spectra

As described in 3.4, the mechanism decomposition approach allows the individual spectra to be added logarithmically. Therefore, the low-, mid-, and high-frequency constituent spectra are combined to form the total OBSI spectrum according to Equation 7.

$$L_{\text{total}} = 10 \log_{10} \left(10^{\frac{L_{\text{low}}}{10}} + 10^{\frac{L_{\text{mid}}}{10}} + 2\sqrt{10^{\frac{L_{\text{low}}}{10}} 10^{\frac{L_{\text{mid}}}{10}} \cos\phi} + 10^{\frac{L_{\text{high}}}{10}} \right) \qquad \text{Eqn 7}$$

where L_{total} is the total OBSI spectrum; L_{low}, L_{mid}, and L_{high} are the low-, mid- and high-frequency constituent spectra, respectively; and ϕ is the phase difference between the low- and mid-frequency sources [138]. An example of how the three constituent spectra can be combined to fit different OBSI spectra is shown in Figure 6.
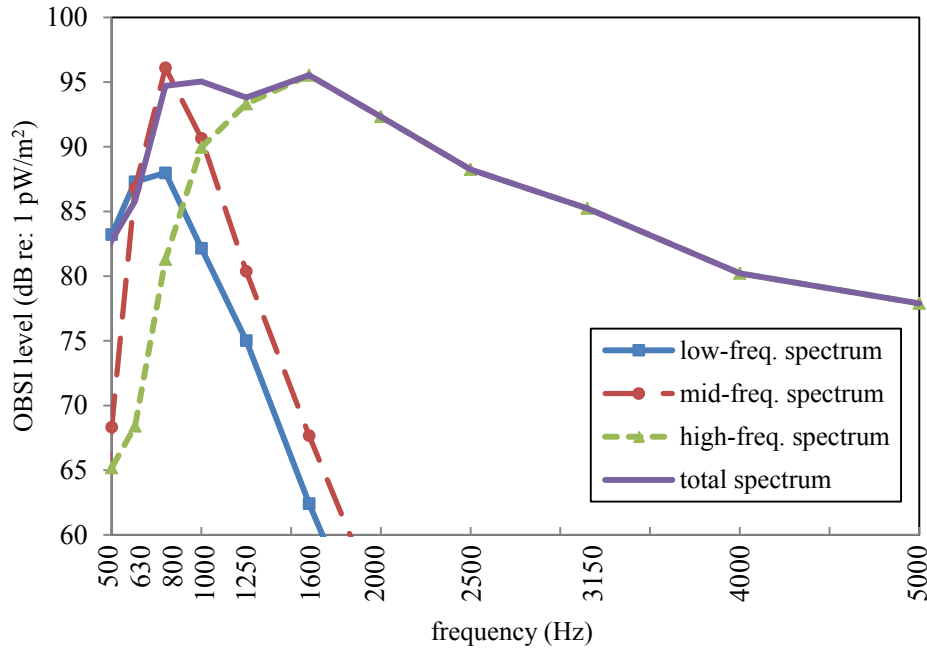

Figure 6: Combination of constituent spectra to form total OBSI spectrum.

4.1.5 Statistical Modeling with the Mechanism Decomposition Method

A fundamental principle of the mechanism decomposition method is that although a change in pavement parameters may cause a complicated change in the shape of an OBSI spectrum, the shapes of the underlying constituent spectra do not change significantly. It is assumed that changes in pavement parameters may change the magnitudes, but not the shapes, of the constituent spectra. Statistical techniques can be used to determine the effect of pavement parameters. For example, a simple one-parameter model of tire-pavement noise may be defined using Equations 8.

$$L_{\text{low}}^* = L_{\text{low}} + \beta_1 \alpha + \beta_2 \qquad \qquad \text{Eqn 8a}$$
$$L_{\text{mid}}^* = L_{\text{mid}} + \beta_3 \alpha + \beta_4 \qquad \qquad \text{Eqn 8b}$$
$$L_{\text{high}}^* = L_{\text{high}} + \beta_5 \alpha + \beta_6 \qquad \qquad \text{Eqn 8c}$$

34

where L_{low}^*, L_{mid}^*, and L_{high}^* are modified constituent spectra; α is a pavement or atmospheric parameter such as mean profile depth, air temperature, or porosity; and β_{1-6} are best-fit coefficients determined through nonlinear least-squares curve fitting. A predicted total OBSI spectrum is formed from the modified spectra according to Equation 7. This predicted spectrum can then be compared to the OBSI spectrum on a given pavement. The fit coefficients, β_{1-6}, are determined by comparing measured and predicted OBSI spectra for a number of different pavements, each having a different parameter α. For this research project, the coefficients were determined by minimizing the total squared error between the measured and predicted one-third octave band levels using the lsqnonlin function in MATLAB. It is possible to use the mechanism decomposition method to develop multi-parameter models to predict OBSI levels. In this case, additional pavement parameters (α_1, α_2, etc.) and additional coefficients (β) can be used. However, nonlinear least-squares methods are susceptible to finding local minima instead of global best-fit coefficients. Therefore, it is important to reduce the number of pavement parameters as much as possible before attempting to develop a multi-parameter model. In Section 4.2, a series of one- and two-parameter models is used to determine the pavement parameters that most affect each of the three constituent spectra.

4.2 Reduced Parameter Models of Tire-Pavement Noise

A series of one- and two-parameter models was developed to identify the pavement parameters that most affect tire-pavement noise. For each model, the variables not under consideration were controlled as much as possible. Qualitative conclusions were then made about the effects of each pavement parameter on OBSI levels. As with the previous section, detailed results and discussion are limited to the leading edge OBSI probe for brevity. Results for the trailing edge are shown in Appendix C. The cells that provided the data used in the various models are shown in Table 3.

Table 3. Cell data used in one- and two-parameter models

Cell number	1	2	3	4	6	15	16	17	18	19	20	21	22	23	24	27	28	31	33	34	35	70	77	86	88
Temperature		X	X	X		X	X	X	X	X	X	X	X	X									X		
RoboTex Texture	X	X	X	X		X	X	X	X	X	X	X	X	X	X	X	X	X	X	X	X		X		X
CTM Texture*		X	X	X		X	X	X	X	X	X	X	X	X										X	X
Absorption		X	X	X						X			X		X	X								X	X
Friction	X	X	X	X		X	X	X	X	X	X	X	X	X											
Temp.-Age	X	X	X	X	X	X	X	X	X	X	X	X	X	X	X	X	X	X	X	X	X				
Temp.-Modulus		X	X	X		X	X	X	X	X	X	X	X	X											

*Repeated measurements, CTM data used in final model only.

4.2.1 One-parameter temperature model

To examine the effects of air and pavement temperature on OBSI levels, a one-parameter model was developed according to Equations 7 and 8 using the available MnROAD data. The parameter α was chosen to be atmospheric or pavement temperature (in °C). Pavement age and wear are known to affect noise levels. To control for these parameters, OBSI [3] and temperature measurements were taken on a large number of pavements (see Table 3) over the course of

approximately 14 hours. Measurements were taken approximately every hour on 21 different test surfaces. The texture of the pavements was assumed to not vary over this short time frame. The experiment was conducted twice. For the first test, conducted in April 2011, atmospheric temperature varied from 0.7-11.0°C, and pavement temperature varied from 5.0-27.5°C. During the second test, conducted in June 2011, air temperature varied from 19.9-33.9°C, and pavement temperature varied from 17.9-48.9°C. The result of these experiments was OBSI levels measured with a wide range of air temperatures, while controlling for pavement texture and age.

One-third octave band OBSI spectra for a typical pavement measured over the course of a day are shown in Figure 7. The total variation with temperature for this experiment was 2-5 dB, depending on frequency. For some frequency ranges, colder temperatures consistently resulted in higher OBSI levels than warmer temperatures. However, in the 1000 Hz band, the temperature effect is less clear. This is an indication that the mid-frequency mechanism may be less dependent on temperature than the high-frequency mechanism.
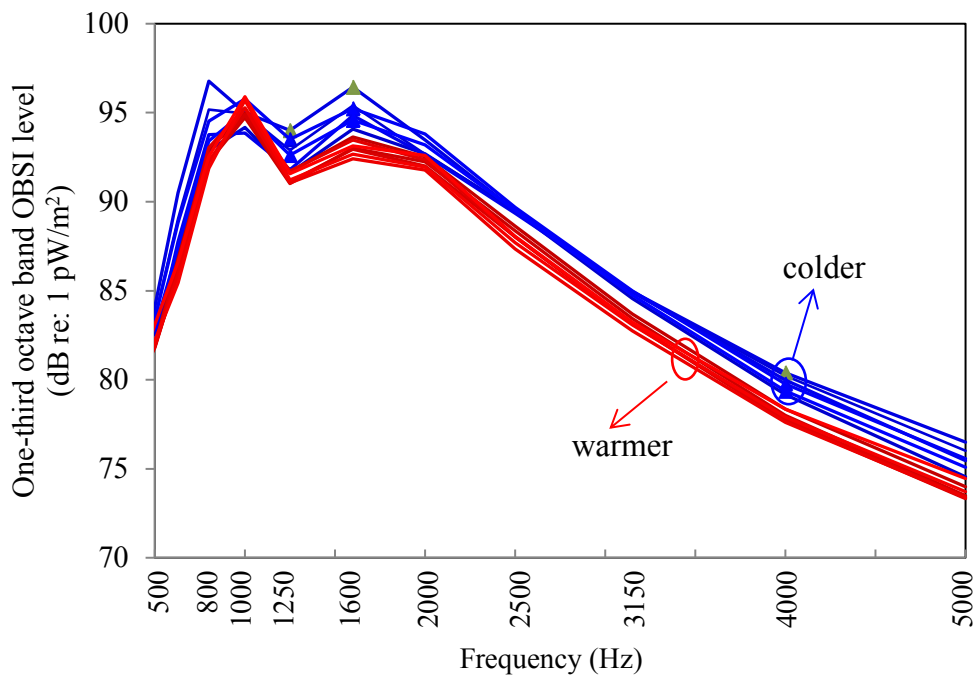

Figure 7: Variation in OBSI spectra with pavement temperature for cell 19. Blue lines correspond to colder temperatures (near 0°C); red lines correspond to warmer temperatures (near 10°C).

A one-parameter model was developed for each pavement. Separate models were developed for the June and April 2011 data sets. Separate models were also developed using air and pavement temperatures as input parameters. For each model, a best-fit temperature coefficient (in dB/°C) was derived for each of the three constituent spectra. The temperature coefficients for all models using air temperatures are shown in Figure 8. For this plot, a temperature coefficient of zero indicates no effect of temperature on noise levels for a given mechanism. There is wide variation among the different pavements when air temperature is used as the input to the model. The low- and mid-frequency constituent spectra have positive temperature coefficients for some pavements and negative for others. The high-frequency temperature coefficients are more consistent among the different pavements, with negative temperature coefficients found for all cases.
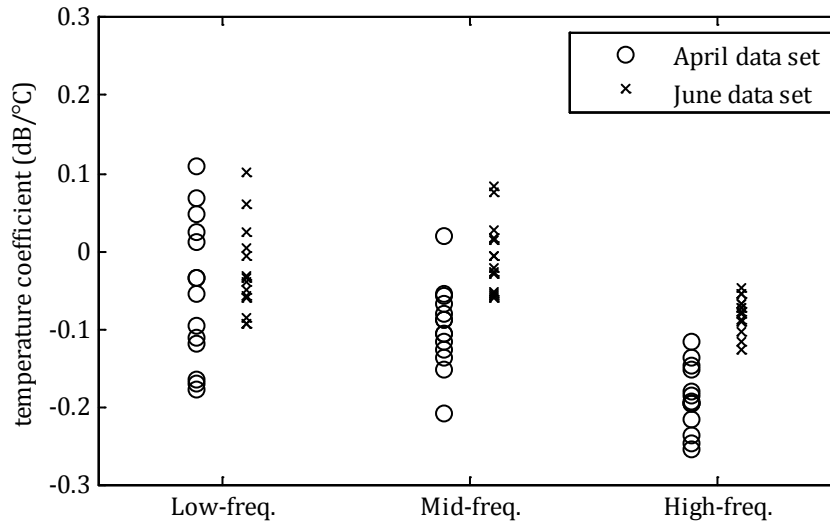
36

Figure 8: Constituent spectra temperature coefficients using air temperature.

The temperature coefficients for all models using pavement temperature, instead of air temperature, as the model input are shown in Figure 9. Using pavement temperature, the temperature coefficients are more consistent across pavements and between the April and June data sets. Again, the low- and mid-frequency spectra are affected less by temperature changes than the high-frequency spectrum. The average temperature coefficients for the low-, mid- and high-frequency constituent spectra were -0.016, -0.030, and -0.078 dB/°C, respectively. For an annual temperature variation of 50°C, these coefficients would yield OBSI variations of 0.8, 1.5, and 3.9 dB for the three constituent spectra. Therefore, temperature effects on the low- and mid-frequency spectra (0.8 and 1.5 dB annual variation) do not need to be considered in future modeling efforts. Temperature effects on the high-frequency spectrum (3.9 dB variation) should be considered.
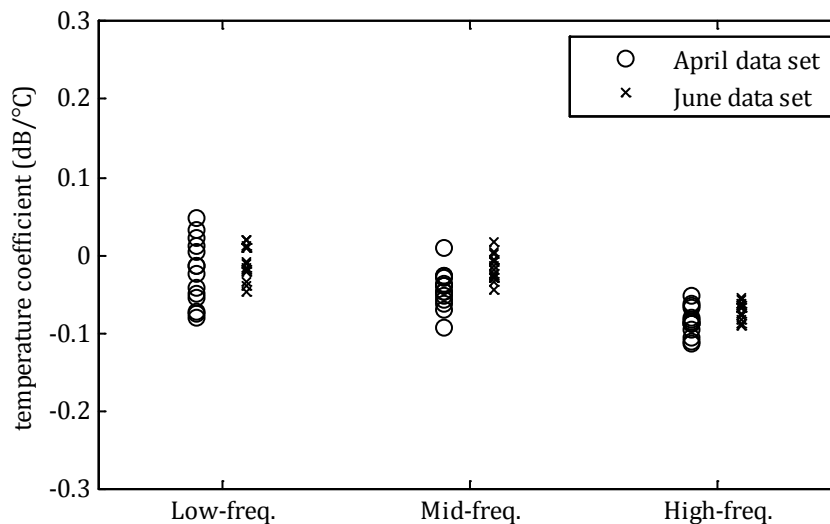

Figure 9: Constituent spectra temperature coefficients using pavement temperature.

4.2.2 One-Parameter Texture Models

A series of one-parameter models was developed to examine the effect of various texture metrics on OBSI levels. Three-dimensional RoboTex texture profiles were measured on 22 different MnROAD test cells in November 2011 (see Table 3). From these profiles, texture spectra were calculated according to ISO 13473-4 [116], and mean profile depths (MPD) were calculated. Texture spectra for all pavements are shown in Figure 10. Most of the pavements tested had similarly shaped spectra. One consequence of this fact is that texture levels at different wavelengths are highly correlated. The porous pavement, Cell 88, had the highest texture, as expected. The ultrathin wearing courses (Cells 2 and 3) and Cell 27, which was chip sealed in 2011, were the next highest followed by Cell 28 with the double chip seal.
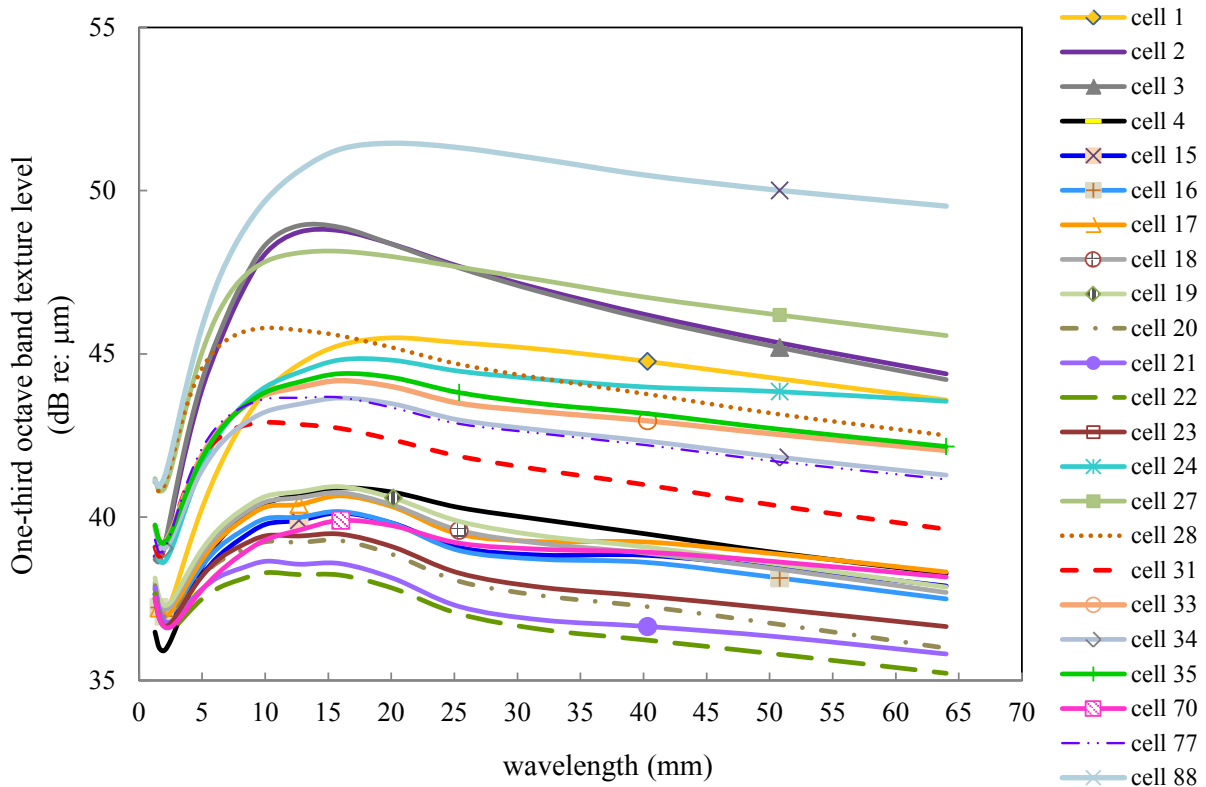

Figure 10: One-third octave band texture levels 22 pavements included in one-parameter texture model.

The effect of pavement texture was isolated from other factors, such as temperature and wear, by considering OBSI data measured in a single day close to the time the texture profiles were measured (September 2011). OBSI spectra for all pavements tested are shown in Figure 11. In general, there was more variation among the different pavements than was measured with the same pavement at different temperatures (Figure 7). There was approximately 10 dB variation among the pavements at each one-third octave band. The pavements with the highest peaks included the two chip sealed sections (Cells 27 and 28) and the cell from the aging study that was periodically sealed (Cell 24).
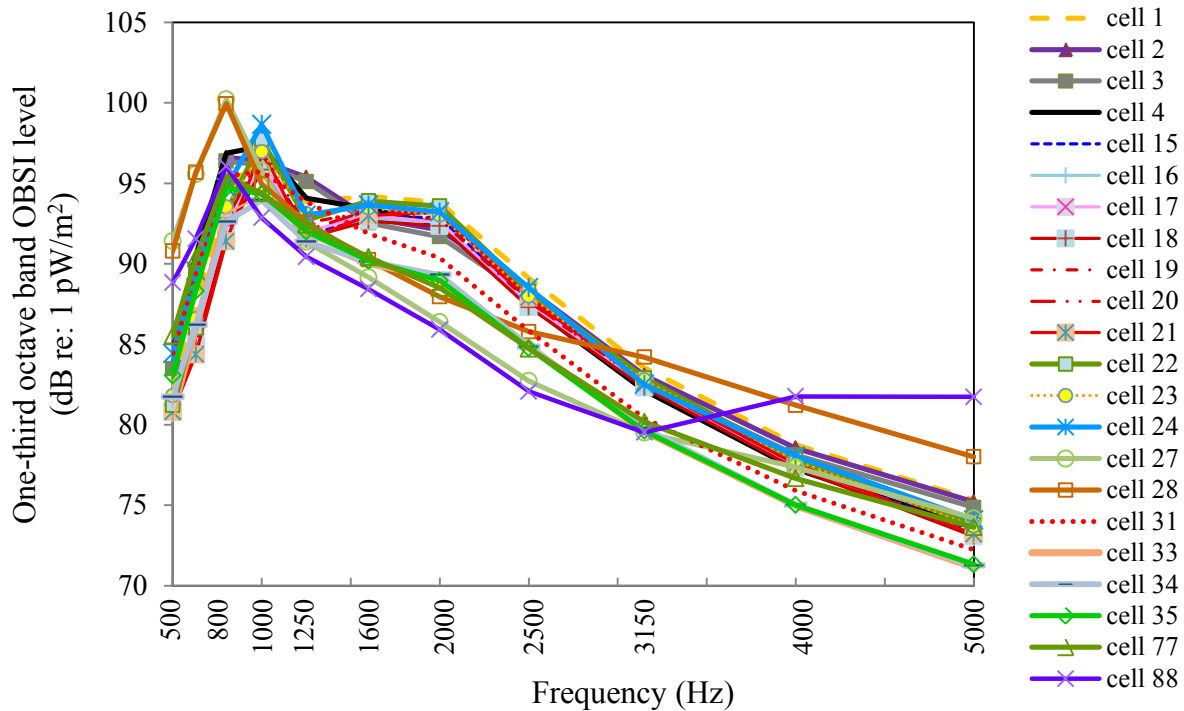
Figure 11: OBSI spectra for 22 pavements included in one-parameter texture model.

For each texture wavelength, a one-parameter model was developed according to Equations 7 and 8, using texture level as the parameter, α. For each model, a best-fit texture level coefficient (in units of $\frac{dB_{OBSI}}{dB_{texture}}$) was calculated for each of the three constituent spectra. The texture coefficients for all texture wavelengths are shown in Figure 12. The texture coefficients for the low- and mid-frequency spectra are positive for all wavelengths, meaning that increased texture at any wavelength is predicted to increase noise at 1000 Hz and lower frequencies. The coefficients for the high-frequency spectrum are consistently negative, meaning that increased texture at any wavelength is predicted to decrease noise above approximately 1600 Hz. With the variations seen in texture levels among pavements (approximately 15 dB), all three spectra can be expected to vary significantly with differences in pavement texture. Therefore, texture level was considered in all subsequent models. In addition, since the predicted effect of texture changes with wavelength, texture levels at multiple wavelengths were considered.
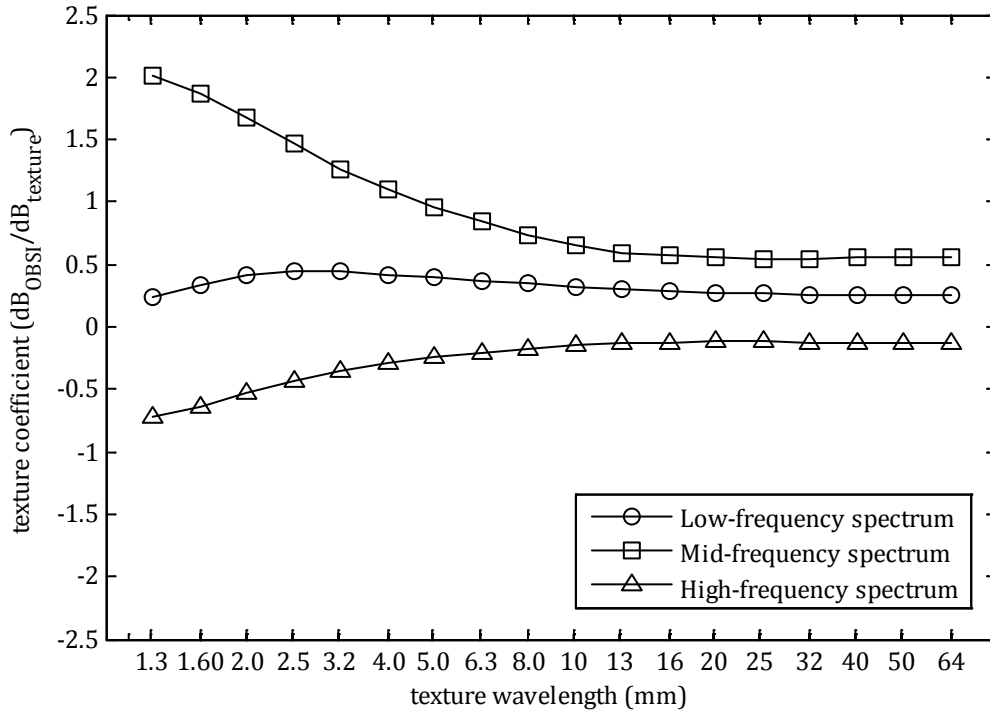
Figure 12: Best-fit texture coefficients for each texture wavelength.

One-parameter models were also developed for MPD and texture skewness. Measured MPDs for all 22 pavements tested are shown in Figure 13, and skewness values are shown in Figure 14. Most of the MPDs are between 0.5-1.0 mm, and most skewness values were negative, indicating predominately negative texture.
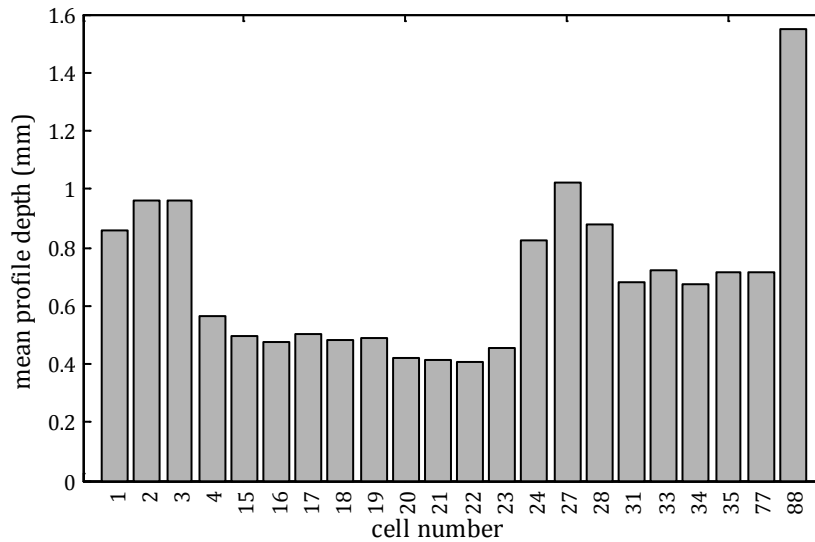

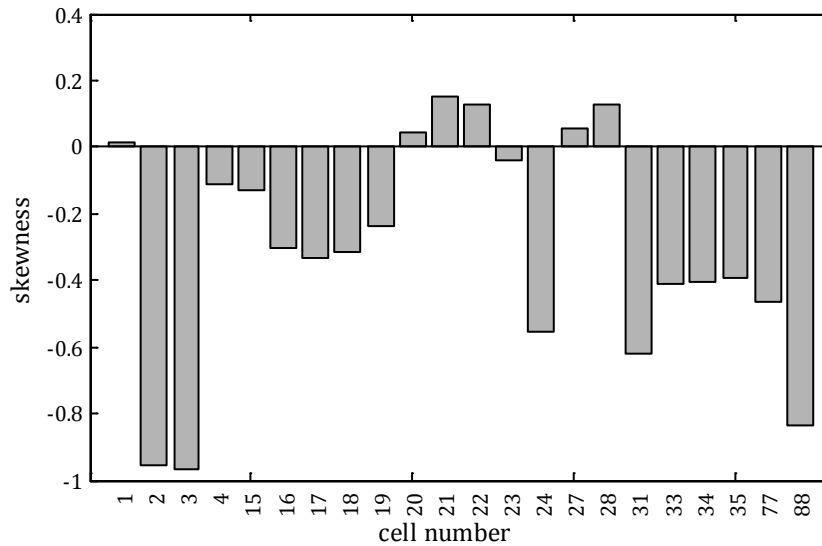Figure 13: MPD for 22 pavements included in one-parameter MPD model.

Figure 14: Skewness for 22 pavements included in one-parameter skewness model.

A one-parameter model was developed using MPD as the input parameter. Best-fit coefficients for the MPD model were found to be 3.46, 7.35, and -1.44 dB/mm for the low-, mid- and high-frequency constituent spectra, respectively. Using the variations in MPD measured on the test pavements, MPD is predicted to vary the three constituent spectra by 4, 8, and 2 dB, respectively. Therefore, MPD can be considered an important input to later models. However, redundancy between MPD and texture spectra will also be explored, since both metrics may not be necessary. Increased MPD is predicted to increase the low- and mid-frequency spectra but is predicted to decrease high-frequency noise.

A one-parameter model was developed using skewness as the input parameter. Best-fit coefficients were found to be -0.42, -0.84, and 0.62 dB for the low-, mid- and high-frequency spectra, yielding a predicted variation with skewness less than 1 dB for the three spectra. Therefore, skewness did not appear to affect any of the three constituent spectra significantly and was not included in later models.

4.2.3   One-Parameter Absorption Model

Sound absorption data were measured on nine different pavements according to ASTM E1050 [79]. The absorption spectra are shown in Figure 15. Most of the pavements had low absorption across all frequencies below the 1600 Hz band. Two porous asphalt pavements, Cells 86 and 88, had absorption of approximately 0.5-0.8 across all frequencies. One pavement (Cell 27) had a sharp increase in absorption in the 800 Hz band; this cell had a 0.5 in. chip seal applied in 2009.
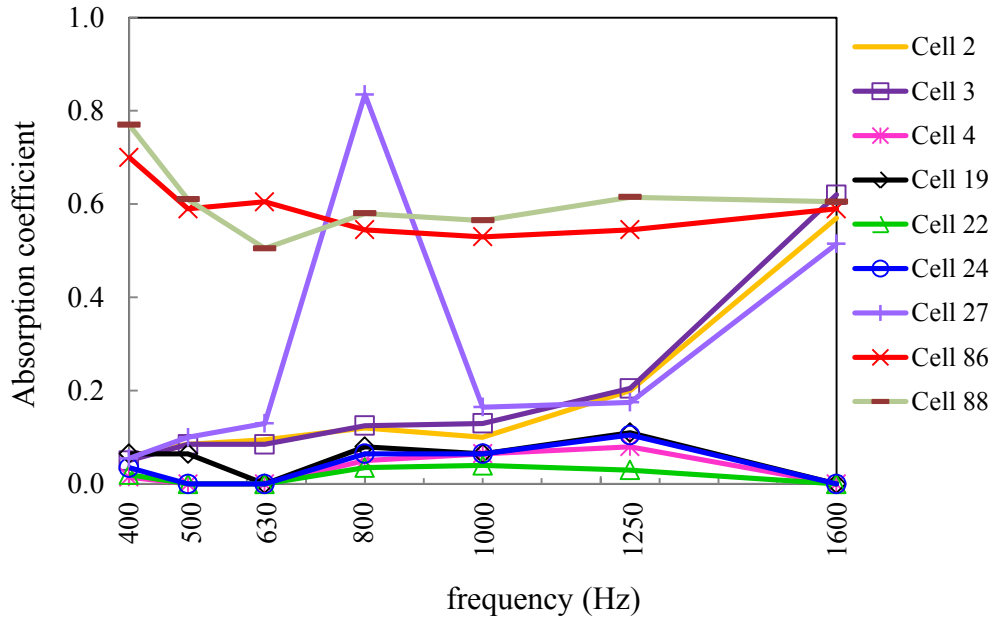
41

Figure 15: Absorption spectra for nine pavements included in one-parameter absorption model.

A series of one-parameter models was developed using sound absorption as the input parameter. Similar to the models developed with texture wavelength, a model was developed for each frequency in the absorption spectrum. A best-fit coefficient (in dB) was found for each absorption frequency for each of the three constituent spectra, as shown in Figure 16. The coefficients for the low- and high-frequency constituent spectra are generally negative; meaning that an increase in absorption is predicted to yield a decrease in noise. However, the mid-frequency coefficients are positive; meaning that an increase in absorption would yield an increase in noise, which is counterintuitive. It is likely that absorption is related to other parameters, such as pavement texture, which also affect tire-pavement noise. Therefore, absorption cannot be used as the sole parameter in models. Given the values shown in Figure 16 and noting that absorption spectra must be in the range of 0-1, absorption may affect OBSI levels by 5 dB or more. Therefore, absorption was included in subsequent modeling efforts.
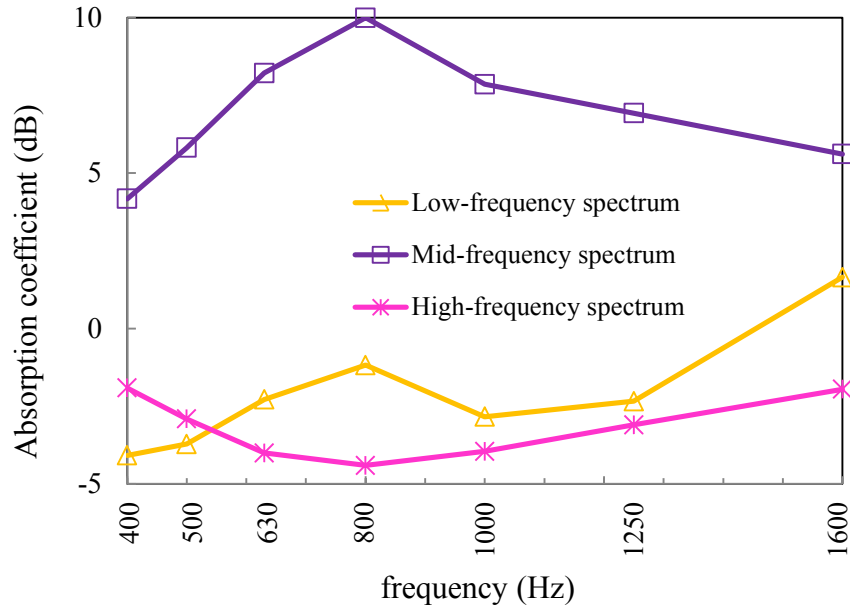
Figure 16: Best-fit coefficients for each absorption frequency.

4.2.4   One-Parameter Friction Model

Friction numbers were measured on 13 different pavement samples according to ASTM E1911 [61]. The friction numbers are shown in Figure 17. The friction numbers for all pavements tested were from 42-61.
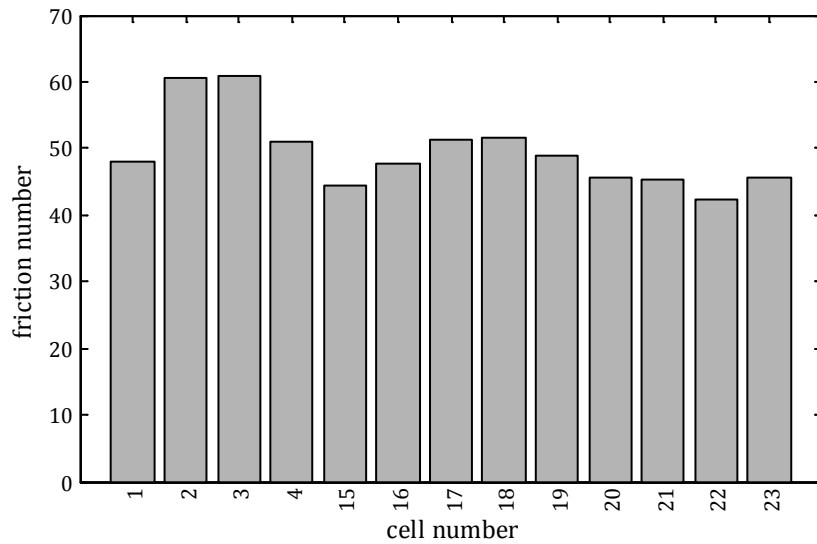
Figure 17: Friction numbers for 13 pavements used in one-parameter friction model.

A one-parameter model was developed using friction number as the input parameter. Best-fit coefficients for the low-, mid-, and high-frequency constituent spectra were found to be 0.211, 0.153, and -0.0027 dB, respectively. Therefore, increased friction is predicted to increase noise below approximately 1600 Hz. The range in friction numbers was approximately 19,

yielding a maximum effect of approximately 4, 3, and 0.05 dB for the three spectra. Therefore, later models considered incorporating friction number into the low- and mid-frequency models but not as a parameter for the high-frequency model. It is likely that friction is correlated with pavement texture, so it was recognized that it might not be necessary to include friction in a model where multiple texture parameters are included as inputs.

4.2.5   Two-Parameter Temperature and Age Model

A series of two-parameter models was developed to investigate the combined effect of temperature and pavement age on the three constituent spectra. A two-parameter model was used because OBSI measurements were taken at MnROAD at different seasons throughout the year. As with the one-parameter temperature models described above, a different model was developed for each pavement to control for variations in texture. For 21 different pavements, up to 11 different OBSI measurements were taken between July 2008 and July 2011. Measurements were taken every 2-5 months. Only atmospheric temperature data were available for this model. For each pavement, best-fit coefficients for the age effect (in units of $\frac{dB}{year}$) and the temperature effect (in units of $\frac{dB}{°C}$) were calculated for each of the three constituent spectra. Temperature coefficients are shown in Figure 18. The coefficients were similar to those calculated for the one-parameter model (Figure 8), with little dependence on temperature for the low-frequency spectrum and moderate dependence for the mid- and high-frequency spectra.
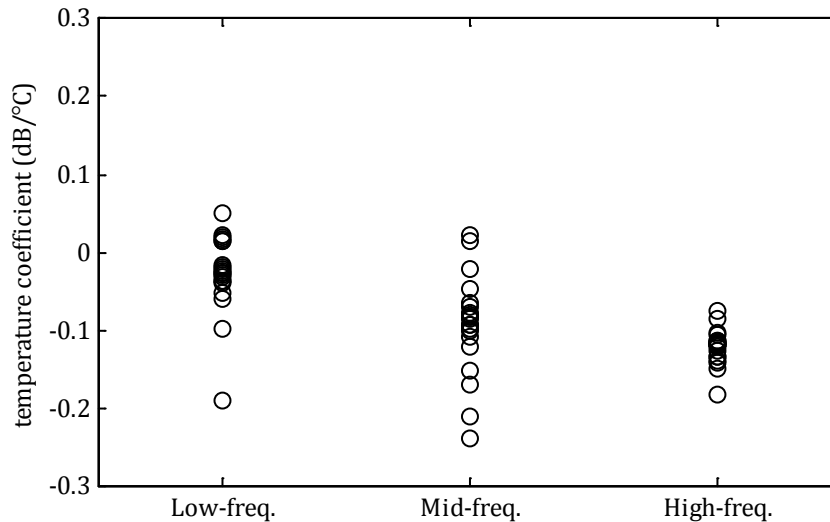
Figure 18: Best-fit temperature coefficients for two-parameter age-temperature model.

Best fit pavement age coefficients are shown in Figure 19. For most of the pavements, the age coefficient is positive for all three constituent spectra. Therefore, OBSI levels are predicted to increase over time. The average coefficients across all pavements were found to be 1.67, 1.96, and 0.71 $\frac{dB}{year}$ for the low-, mid- and high-frequency constituent spectra, respectively. Though noise across the entire frequency range is predicted to increase, noise above 1600 Hz is predicted to increase less due to changes in age and temperature.
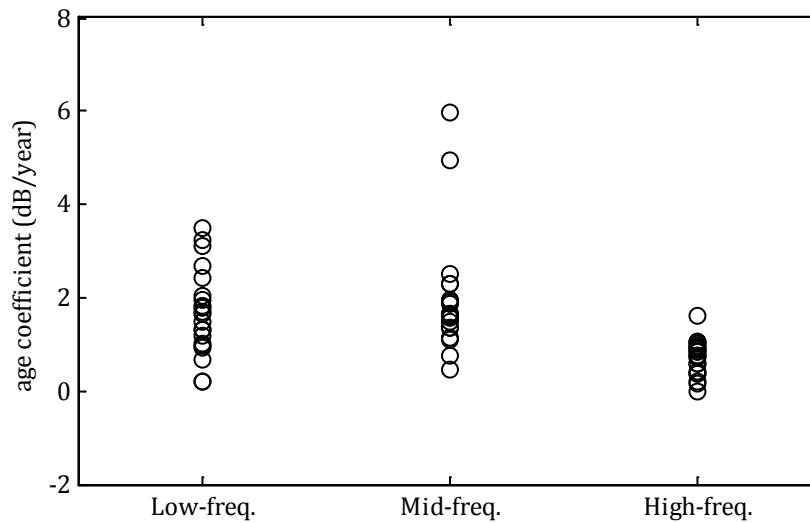
Figure 19: Best-fit pavement age coefficients for two-parameter age-temperature model.

To illustrate the effect of pavement age and temperature on the three constituent spectra, predictions of the change in OBSI noise over time were made using historical weather data. Hourly atmospheric temperatures measured at the MnROAD facility were used with the average temperature and age coefficients to predict the increase in the three constituent spectra between July 2008 and July 2011. The results are shown in Figure 20. Because of the positive age coefficients, the three constituent spectra are all predicted to increase gradually with time. The mid-frequency spectrum is predicted to have much less seasonal variation than the low- and high-frequency spectra. In addition, the high-frequency spectrum is predicted to increase less over time than the other two. Because of the dependence on temperature, the day-to-day variation in levels is approximately 2 dB for the low- and high-frequency spectra and less than 0.5 dB for the mid-frequency spectrum. This result illustrates the benefits of a mechanism decomposition approach: depending on which constituent spectrum is dominant, the levels of seasonal and day-to-day variations in the total OBSI spectrum will change. Accurate predictions can only be made by separating the constituent spectra.
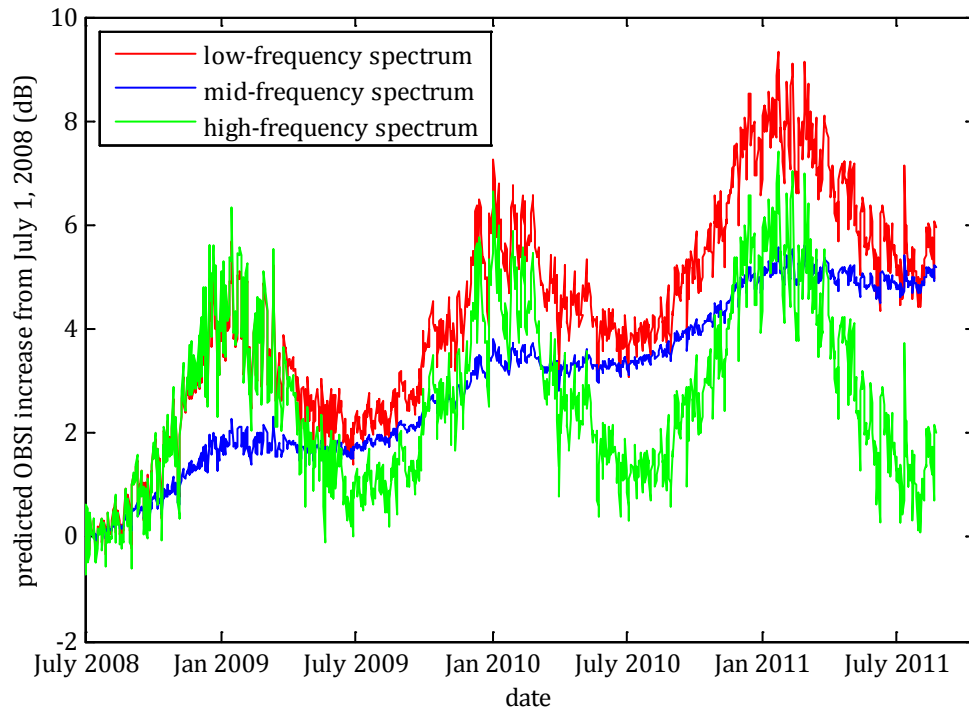
Figure 20: Predicted increase in constituent spectra from two-parameter age-temperature model from July 1, 2008.

4.2.6   *Two-Parameter Temperature and Modulus Model*

As discussed in Chapter 2, the mechanical impedance (stiffness or modulus) has an unknown but potentially significant effect on tire-pavement noise. Since asphalt mixtures are viscoelastic materials, however, the modulus will be strongly affected by temperature. Figure 21 shows one example of the deflection basins measured in Cell 2 at different times of the year, illustrating the significant changes in the mixture stiffness with temperature. In the development of the final models, the need to include both temperature and modulus because of this correlation was considered.

Figure 21: FWD deflection basins for Cell 2 (backcalculated) from February through October 2011.
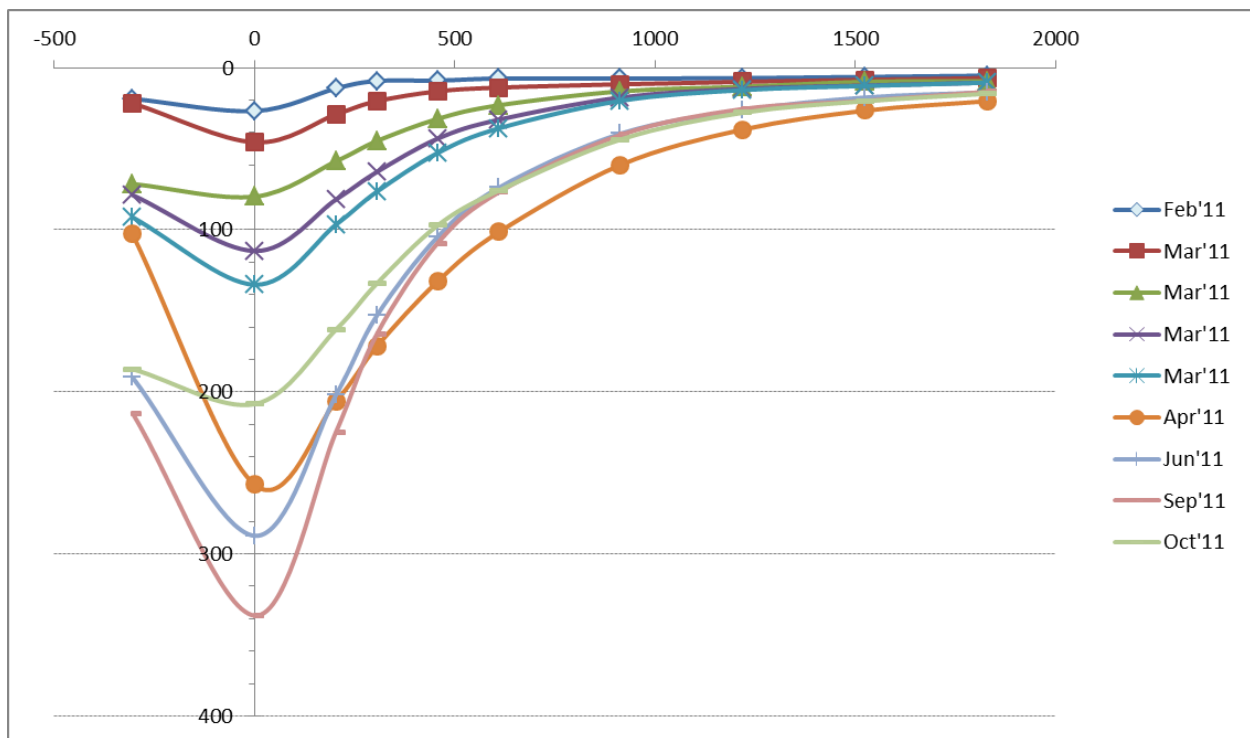
The best MnROAD data available for evaluating the effect of stiffness is the FWD data collected in the field because that is the only data set that includes the effects of any changes in the mixture properties during construction and over time. The only other available data, such as dynamic modulus and ultrasonic modulus, was obtained by testing mixture samples at the time of construction. The same was true for data to input into predictive models like the Hirsch model; the volumetric and binder properties were not available over time so could not be used reliably to predict changing stiffness over time. Therefore, the FWD data was analyzed to backcalculate the pavement stiffness using Evercalc, as described in more detail in Appendix B. By using the FWD data, it was possible to estimate the modulus of the in situ pavement materials to explore any relationship to noise.

Figure 22 shows the effect of changes in temperature on the backcalculated moduli for different cells tested. This figure shows that some cells are more sensitive to changes in modulus than others. In general, the stiffer materials tend to show the greatest changes in moduli as the temperature increases. Since the stiffness of an asphalt mixture depends both on the stiffness of the binder and of the aggregate structure, there will be, in effect, a limiting stiffness; when the binder becomes less stiff, the aggregate structure provides the mixture stiffness (provided the mixture does not become soft enough to experience plastic flow). The aggregates are unaffected by changes in temperature. The models developed in Chapter 5 will consider the effects of changing temperature and moduli on tire-pavement noise.
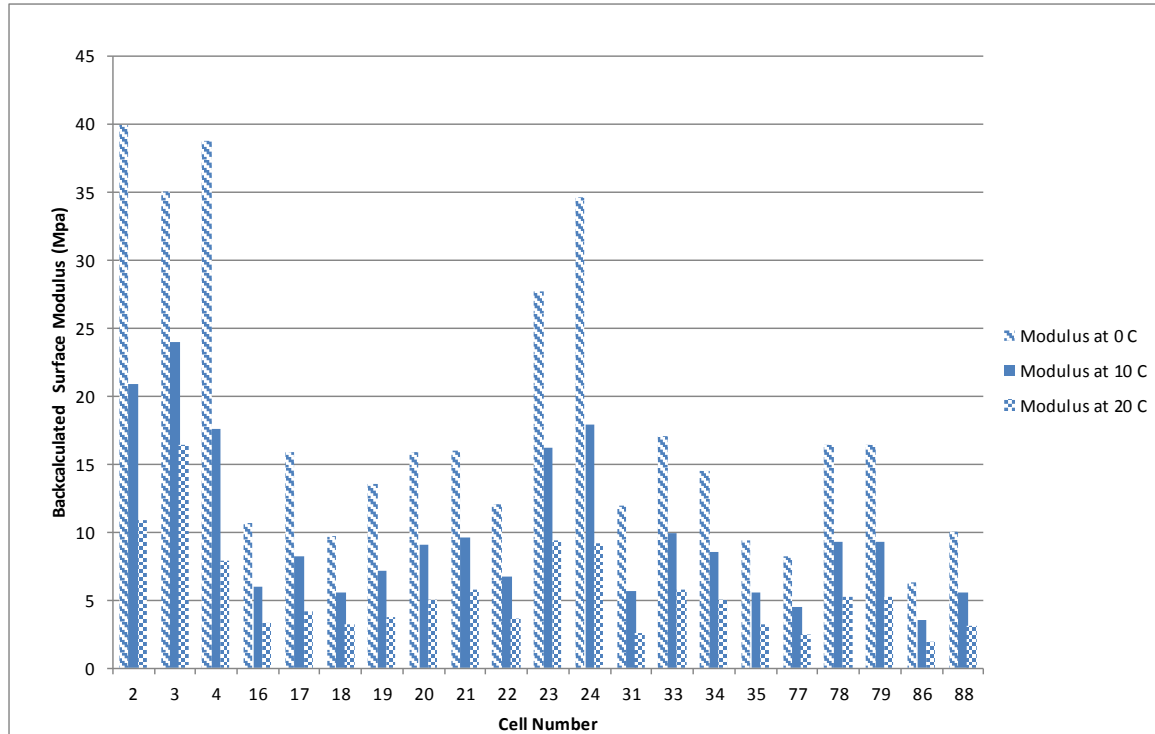
Figure 22: Change in backcalculated moduli at different temperatures

A series of two-parameter models were developed to investigate the combined effect of pavement temperature and modulus. Modulus depends on both material parameters and pavement temperature. The combined effect of modulus and temperature was investigated using the same data set described in Section 4.2.1. For this data set, OBSI and temperature data were measured hourly over the course of a day. For each pavement in this data set, any variation in noise is caused only by the change in air and pavement temperature. Since other parameters, such as pavement texture and absorption, were not constant across the pavements, a separate model was developed for each pavement. For each pavement, best-fit temperature ($\frac{dB}{°C}$) and modulus ($\frac{dB}{GPa}$) were calculated. As described in Section 4.2.1, separate coefficients were found for the April and June 2011 data sets.

Best-fit coefficients for the temperature-modulus model are shown in Figure 23 and Figure 24. For the low- and mid-frequency spectra, there is a large amount of scatter in the pavement temperature coefficients compared to the one-parameter temperature model. The high-frequency coefficients are much less scattered, which is similar to the results shown in Figure 9. The average pavement temperature coefficients were 0.001, -0.027, and -0.080 dB/°C for the low- mid- and high-frequency spectra, respectively. The average modulus coefficients were found to be 0.194, 0.029, and 0.036 dB/GPa for the three spectra. The average coefficients can be interpreted to mean that once the effect of a change in modulus is taken into account, temperature has little effect on the low-frequency spectrum. However, both modulus and temperature have an effect on the high-frequency spectrum. In further model development, modulus was considered for all spectra.
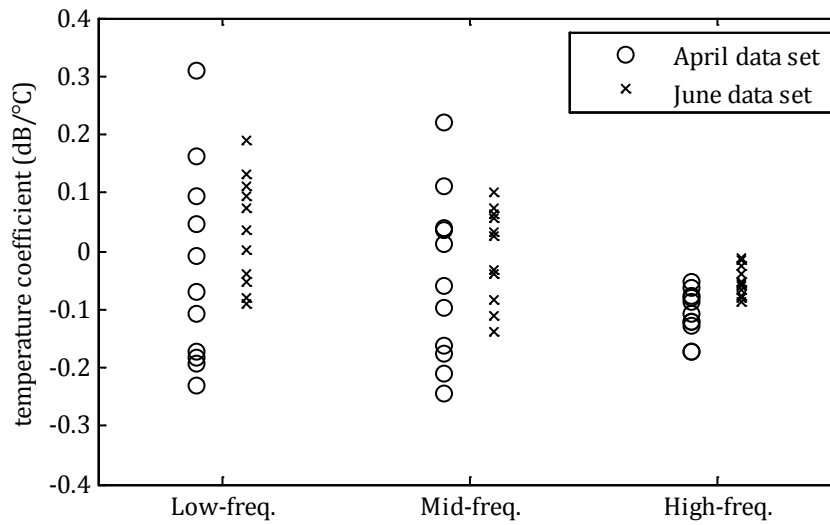
48

Figure 23: Best-fit pavement temperature coefficients for two-parameter temperature-modulus model.
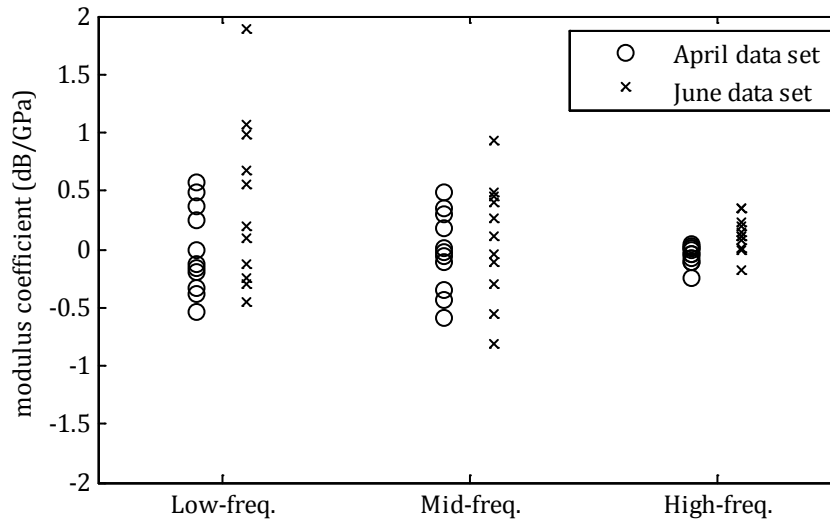
Figure 24: Best-fit modulus coefficients for two-parameter temperature-modulus model.

4.3   Summary of Parameter Effects

The model coefficients for all one-parameter models considered are shown in Table 4. For each parameter, the range of values is also shown, along with the maximum potential dB effect on each of the three constituent spectra. For each parameter, the maximum dB effect was found by multiplying the model coefficient by the range in the parameter found in the data set. For example, the leading edge, low-frequency coefficient for MPD was found to be 3.46 dB/mm. The range in MPD measured for all pavements was 1.1 mm, giving a maximum potential effect of 3.8 dB. In the table, maximum effects of greater than 4 dB are highlighted in red (with bold, italic type), indicating a significant effect on noise levels. Effects between 2 and 4 dB are shown

in yellow (with bold type), indicating a moderate effect. Effects of less than 2 dB are shown in green (with italic type) to indicate that the parameter has little effect on the constituent spectrum. In general, the low-frequency spectrum is affected most by macrotexture parameters (MPD, 64-mm wavelength) and is less affected by microtexture, absorption and temperature. The mid-frequency spectrum is affected by all texture parameters and absorption. The high-frequency spectrum is most affected by microtexture and air temperature. Using the two-parameter age-temperature model, it was shown that age significantly affects the low- and mid-frequency spectra but not the high-frequency spectrum. The two-parameter temperature-modulus model was used to show that modulus and temperature must both be considered for the high-frequency spectrum but not necessarily for the low-frequency spectrum. The amount of available data varied among the cells, so the number of cells used varied among the models. The cells used in each model are shown in Table 3.

The reduced-parameter models were valuable in determining which pavement parameters should be included in a comprehensive OBSI prediction model. Some variables were found not to be necessary for each of the three constituent spectra. For example, air and pavement temperature do not affect low-frequency noise, so these variables were not included in the later models. After eliminating the variables which are not likely to have a large effect, there were still many pavement parameters left to consider. Many pairs of parameters, such as 12.5 mm texture and MPD, are highly correlated, so the need to include both in the final model was explored. The significant variables identified in this chapter were used as preliminary inputs to the model for subsequent development of a full model.

Table 4. One-parameter model coefficients, parameter ranges, and maximum dB effects.

		MPD (mm)		skew		$\lambda_{1.25\,mm}$ (dB)		$\lambda_{12.5\,mm}$ (dB)		$\lambda_{64\,mm}$ (dB)	
		Lead	Trail	Lead	Trail	Lead	Trail	Lead	Trail	Lead	Trail
Model coefficient (dB/EU)	Low-freq.	3.46	4.97	-0.42	-0.13	0.24	0.97	0.30	0.40	0.25	0.37
	Mid-freq.	7.35	7.70	-0.84	-0.98	2.02	1.77	0.59	0.58	0.56	0.56
	High-freq.	-1.44	-1.31	0.62	0.04	-0.72	-0.79	-0.12	-0.10	-0.13	-0.12
Parameter range	Maximum	1.5	1.5	0.15	0.15	41.2	41.2	50.6	50.6	49.5	49.5
	Minimum	0.4	0.4	-0.97	-0.97	36.5	36.5	38.2	38.2	35.2	35.2
	Range	1.1	1.1	1.1	1.1	4.7	4.7	12.4	12.4	14.3	14.3
Maximum effect (dB)	Low-freq.	3.8	5.5	0.5	0.1	1.1	4.6	3.7	5.0	3.6	5.3
	Mid-freq.	8.1	8.5	0.9	1.1	9.5	8.3	7.3	7.2	8.0	8.0
	High-freq.	1.6	1.4	0.7	0.1	3.4	3.7	1.6	1.3	1.9	1.6

		FN		$\alpha_{1000\,Hz}$		T_{pav} (°C)		T_{air} (°C)	
		Lead	Trail	Lead	Trail	Lead	Trail	Lead	Trail
Model coefficient (dB/EU)	Low-freq.	0.21	0.17	-2.84	1.87	-0.016	-0.010	-0.038	-0.016
	Mid-freq.	0.15	0.16	7.85	9.19	-0.030	-0.065	-0.053	-0.098
	High-freq.	0.00	0.03	-3.95	-4.77	-0.078	-0.063	-0.13	-0.109
Parameter range	Maximum	60.9	60.9	0.6	0.6	48.9	48.9	33.9	33.9
	Minimum	42.3	42.3	0.0	0.0	5.0	5.0	0.7	0.7
	Range	18.6	18.6	0.5	0.5	44.0	44.0	33.2	33.2
Maximum effect (dB)	Low-freq.	3.9	3.1	1.5	1.0	0.7	0.5	1.3	0.6
	Mid-freq.	2.8	3.0	4.1	4.8	1.3	3.2	1.7	3.3
	High-freq.	0.1	0.5	2.1	2.5	3.4	3.1	4.5	3.7

5. Development of the Final Mechanism Decomposition Models

Using the mechanism decomposition approach described in Chapter 3, the significant variables described in Chapter 4 and the available MnROAD data summarized in Table 3 for the cells described in Table 2, two models to predict tire-pavement noise were developed and are described here. The first method is based on using the RoboTex texture data, and the second uses CTM texture data in a similar fashion. The models, their factors and accuracy are outlined in this chapter.

5.1   Combination of Constituent Spectra

Recall that in the mechanism decomposition approach, the low-, mid-, and high-frequency constituent spectra are combined to form the total OBSI spectrum according to Equation 7, repeated here.

$$L_{\text{total}} = 10 \log_{10} \left(10^{\frac{L_{\text{low}}}{10}} + 10^{\frac{L_{\text{mid}}}{10}} + 2\sqrt{10^{\frac{L_{\text{low}}}{10}} 10^{\frac{L_{\text{mid}}}{10}}} \cos \phi + 10^{\frac{L_{\text{high}}}{10}} \right) \quad \text{Eqn 7}$$

where L_{total} is the total OBSI spectrum; L_{low}, L_{mid}, and L_{high} are the low-, mid- and high-frequency constituent spectra, respectively; and ϕ is the phase difference between the low- and mid-frequency sources [1]. Several different forms of the model were tested to find the model that could best predict OBSI levels with the fewest variables.

5.2   Statistical Model of OBSI Levels Using RoboTex Data

The final form of the model using RoboTex data is shown in Equations 9a-c.

$$L_{\text{low}}^* = L_{\text{low}} + \beta_1 L_M + \beta_2 T + \beta_3 Y + \beta_4 E + \beta_5 \qquad \text{Eqn 9a}$$
$$L_{\text{mid}}^* = L_{\text{mid}} + \beta_6 L_M + \beta_7 Y + \beta_8 E + \beta_9 \qquad \text{Eqn 9b}$$
$$L_{\text{high}}^* = L_{\text{high}} + \beta_{10} L_M + \beta_{11} T + \beta_{12} Y + \beta_{13} \qquad \text{Eqn 9c}$$

where L_{low}^*, L_{mid}^*, and L_{high}^* are modified constituent spectra; L_M is macrotexture level (dB at 12.5 mm wavelength); T is air temperature (°C); Y is the number of years since the pavement texture was measured; and E is the pavement modulus (GPa) backcalculated from FWD data using Evercalc. β_{1-13} are best-fit coefficients determined through nonlinear least-squares curve fitting. A predicted total OBSI spectrum is formed from the modified spectra according to Equation 7. This predicted spectrum can then be compared to the OBSI spectrum on a given pavement. The fit coefficients, β_{1-13}, are determined by comparing measured and predicted OBSI spectra for a number of different pavements. For this research project, the coefficients were determined by minimizing the total squared error between the measured and predicted one-third octave band levels using the lsqnonlin function in MATLAB. The form of the model for the leading and trailing edges is the same, but the best-fit coefficients are different. The final RoboTex model, including the best-fit coefficients, is shown in Equations 10 and 11, with the subscripts LE and TE representing terms at leading and trailing edges respectively.

$$L_{\text{LE, low}}^* = L_{\text{LE, low}} + 0.50 L_M - 0.050 T + 1.29 Y + 0.073 E - 18.3 \text{ dB} \qquad \text{Eqn 10a}$$
$$L_{\text{LE, mid}}^* = L_{\text{LE, mid}} + 0.024 L_M + 1.12 Y + 0.030 E - 0.3 \text{ dB} \qquad \text{Eqn 10b}$$

$$L^*_{\text{LE, high}} = L_{\text{LE, high}} - 0.28L_M - 0.10T + 0.60Y + 11.2 \text{ dB} \qquad \text{Eqn 10c}$$

$$L^*_{\text{TE, low}} = L_{\text{TE, low}} + 0.38L_M - 0.069T + 1.44Y + 0.074E - 14.0 \text{ dB} \qquad \text{Eqn 11a}$$
$$L^*_{\text{TE, mid}} = L_{\text{TE, mid}} + 0.11L_M + 0.91Y + 0.042E - 4.3 \text{ dB} \qquad \text{Eqn 11b}$$
$$L^*_{\text{TE, high}} = L_{\text{TE, high}} - 0.29L_M - 0.073T + 0.67Y + 11.5 \text{ dB} \qquad \text{Eqn 11c}$$

The model described by Equations 10 and 11 (together with Equation 7) is complex, yet its individual terms can be interpreted physically.

5.2.1 Effect of Macrotexture

The macrotexture term, L_M, is the dB level from a texture spectrum in the 12.5 mm wavelength one-third octave band. Values for the pavements included in the data set ranged from 38-51 dB. The positive coefficient for the low-frequency spectrum seen in both the leading and trailing edges (Eqns. 10a and 11a) means that low-frequency noise is expected to increase with increasing macrotexture. The macrotexture terms in the mid-frequency spectra have much smaller coefficients, meaning that macrotexture is predicted to have a smaller effect in the mid-frequency range. These results match previous findings by Sandberg and Ejsmont [4]. Though the macrotexture terms in the high-frequency spectra (Eqn. 10c and 11c) have negative coefficients, the larger coefficients in the low-frequency spectrum will dominate, and overall noise will increase.

The predicted effect of an increase in macrotexture of 6 dB is shown in Figure 25. The low- and mid-frequency content increases, with more effect seen near 500-630 Hz. The high-frequency content decreases due to the negative coefficient for macrotexture in Eqn. 11c. The overall level is predicted to increase by approximately 0.5 dB.
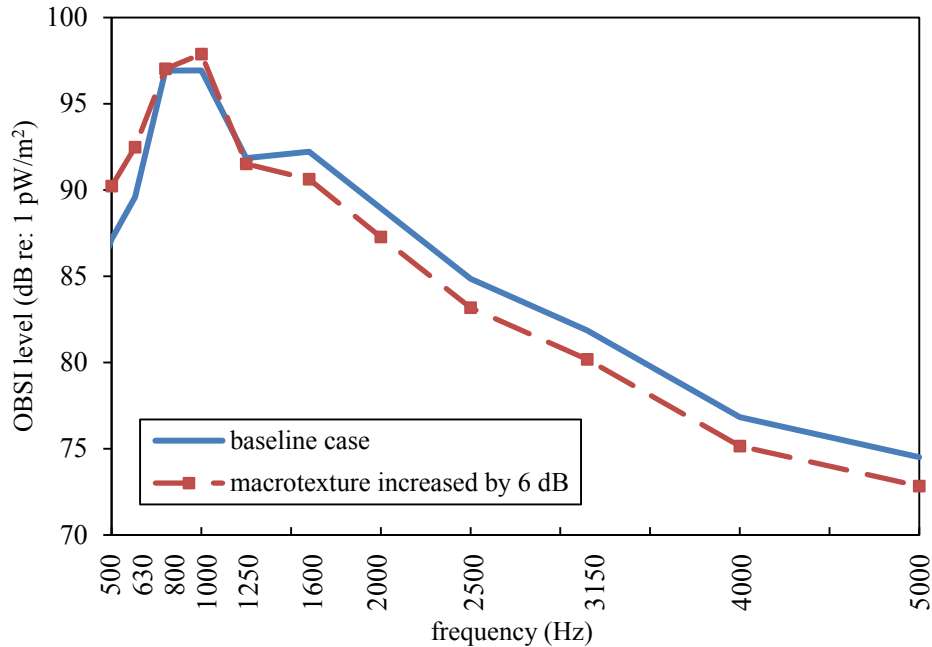

Figure 25: Effect of increased macrotexture (RoboTex).

5.2.2 Effect of Air Temperature

The air temperature term, T, is the ambient air temperature in °C at the time of OBSI testing. The negative coefficients mean that noise is expected to decrease with increasing temperature. This is consistent with findings by other researchers [139].

The predicted effect of an increase in temperature of 10°C is shown in Figure 26. The increased temperature primarily affects the high-frequency region and has little effect on the 1000 Hz peak. The result is a decrease in overall levels by approximately 0.3 dB. Though this is a small effect, the effect of temperature change on pavement modulus can lead to larger changes in noise with temperature. This effect is described in Section 5.2.5.
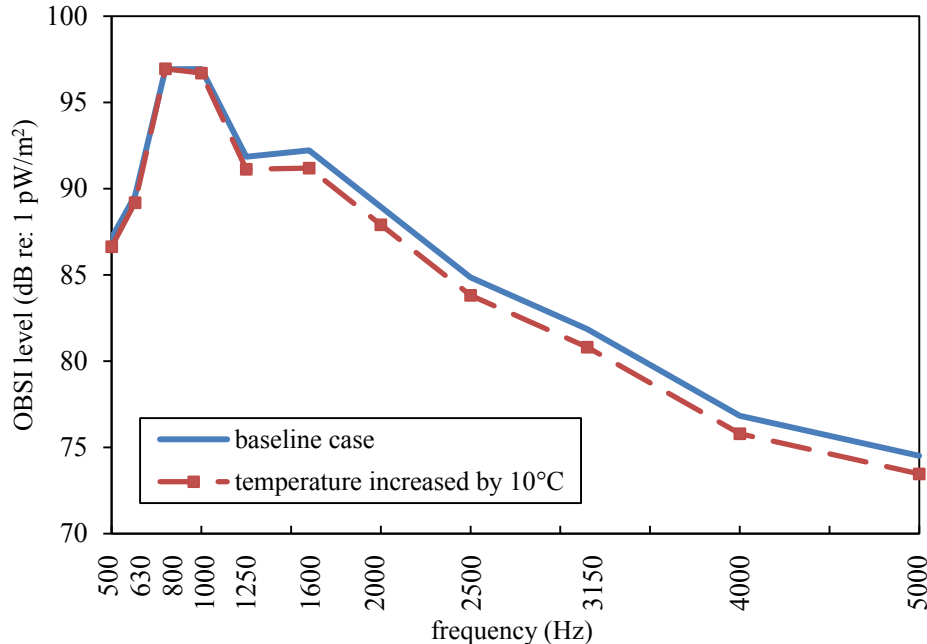

Figure 26: Effect of increased temperature (RoboTex).

5.2.3 Effect of Time

The time term, Y, represents the number of years since the texture measurement used to compute the macrotexture term was made. This is not the same as the age of the pavement since installation, unless the texture scan was performed at that time. Any effects of pavement aging on texture, such as increased texture due to freeze-thaw damage or decreased texture due to polishing, are incorporated into the texture measurements. The time correction term represents the expected variation in noise levels since the last texture scan. It can be thought of as a reliability term in the sense that the prediction is more accurate when the texture measurements were made close to the time of the noise measurements. If texture measurements were performed at the time of each OBSI measurement, a time correction term would not be necessary. The term is not necessarily positive; Y will be negative if OBSI measurements were made before texture measurements. For example, when comparing a data set with OBSI measured in May 2011 with texture measured in November 2011, the age term would be -0.5 years. The age coefficients in the model are all between 0.60-1.44 dB/year, which is slightly above previous findings by Donavan [139].

The effect of aging a pavement three years is illustrated in Figure 27. Since the coefficients are similar for each frequency range, the result is a broadband increase in noise by approximately 2-4 dB. The overall level is predicted to increase by 3.1 dB.
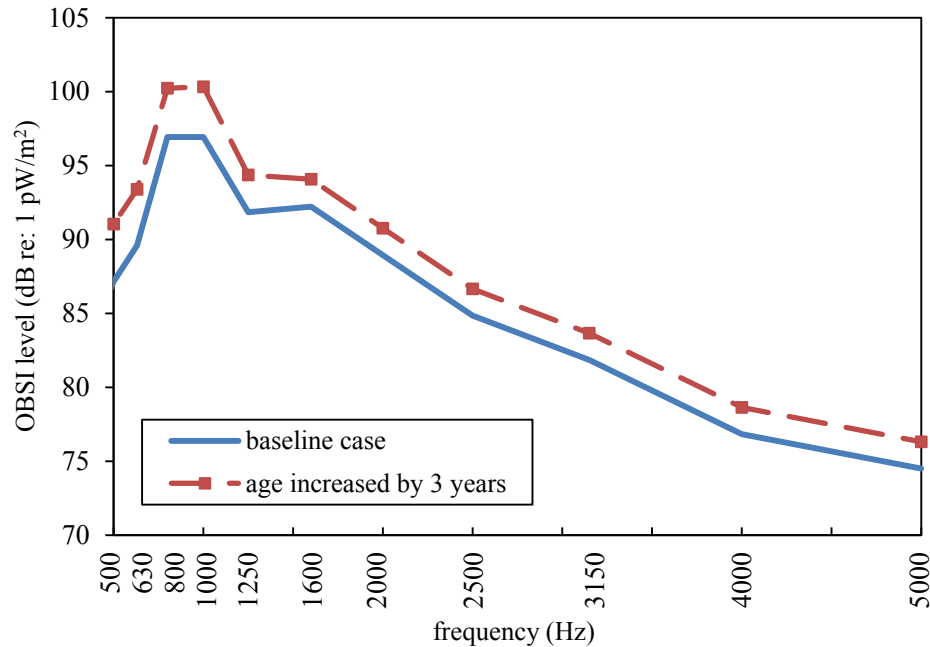

Figure 27: Effect of increased pavement age (RoboTex).

5.2.4   Effect of Modulus

The modulus term, E, represents the modulus of the top layer of pavement in GPa. Pavement stiffness is expected to only affect the low- and mid-frequency regions, which are dominated by carcass vibration mechanisms. The high-frequency region is dominated by aeroacoustic sources, and is not affected by pavement modulus. Modulus for the pavements used to generate the model ranged from 0.84-74 GPa. The positive modulus coefficients mean that stiffer pavements are expected to increase noise in the low- and mid-frequency regions.

The effect of an increase in modulus of 10 GPa is shown in Figure 28. The low-frequency region is affected more than the mid-frequency region, but there is still an increase in noise at the peak. The overall noise level is predicted to increase by approximately 0.5 dB.

The effect of an increase in modulus over time because of binder oxidation was explored in this task by comparing backcalculated surface moduli measured at different times over more than five years at similar temperatures. While the results did show an increase in modulus, this effect was greatly overshadowed by the change in modulus with temperature and did not significantly improve the model. Therefore, an aging term was not included in the model.
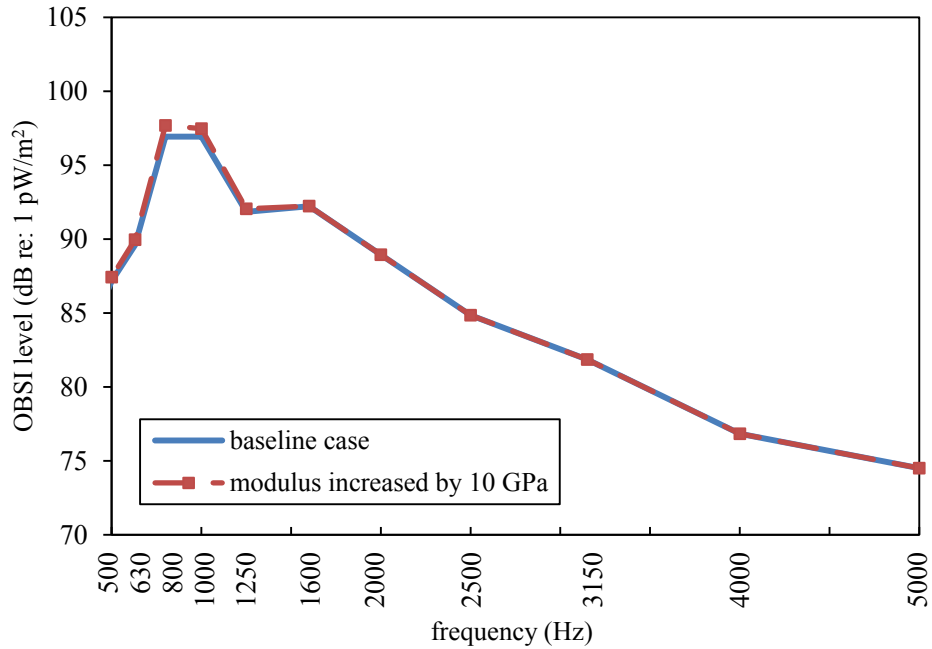
55

Figure 28: Effect of increased modulus (RoboTex).

5.2.5　Combined Effect of Temperature and Modulus

In Section 4.2.6, it was shown that surface modulus and temperature are related. Modulus will decrease with increasing temperature. For a given pavement, it is possible to predict the effect of temperature, taking the effect of changing modulus into account. Figure 29 shows the effect of the same 10°C increase in temperature as was shown in Figure 26 but accounts for the change in modulus. The increased temperature leads to a decreased modulus and a subsequent decrease in low- and mid-frequency levels. As shown in Figure 22, the stiffer materials generally showed a greater sensitivity to changes in temperature. The temperature coefficient affects the high-frequency region, and decreases it by a similar amount. The result is a decrease in overall levels of approximately 1.8 dB.
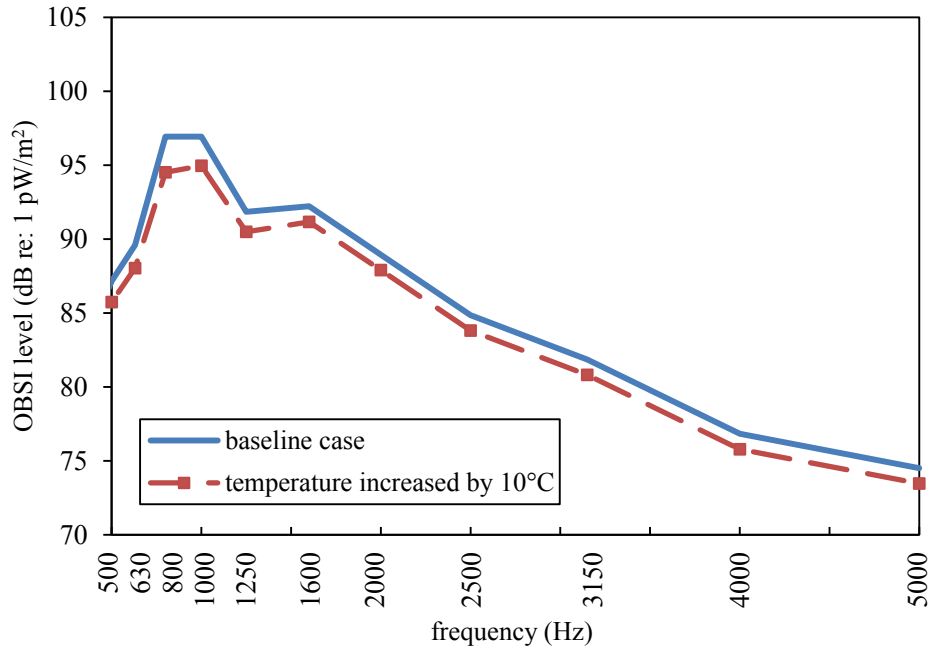
Figure 29: Effect of increased temperature, taking change in modulus into account (RoboTex).

5.2.6 Combined Effect of Temperature, Modulus, and Age

The model can be used to predict how noise levels will change for a given pavement over a time span, taking into account the effects of time, temperature and modulus changes. The predicted change in a typical pavement over time is shown in Figure 30. This figure was generated using texture data and the temperature-modulus curve for Cell 2. The temperatures were taken from MnROAD weather station data over a five-year period. There are variations between the summer and winter months of approximately 5 dB and a steady increase over time of approximately 1 dB/year.
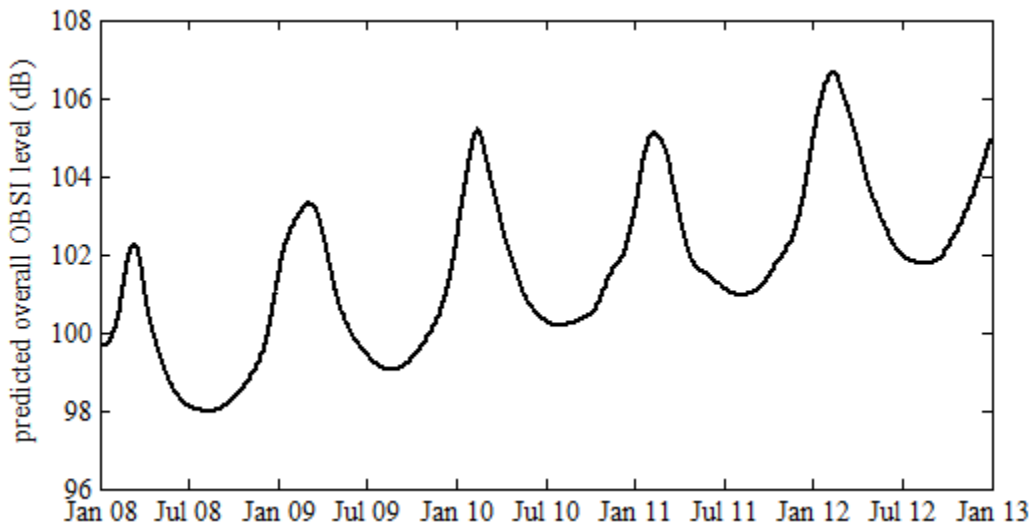

Figure 30: Predicted change in overall OBSI level of a typical pavement over time (RoboTex).

5.3   Statistical Model of OBSI Levels Using CTM Data

Because RoboTex data was collected only once and is not likely to be collected often in the future, a model using CTM data was considered desirable. CTM data is more frequently collected and can essentially be collected whenever it is needed by MnROAD personnel. Using CTM data allowed deletion of the time term from the model because the difference in time between texture and OBSI measurements was greatly reduced. Therefore, the final version of the model is shown in Equations 12a-c.

$$L^*_{\text{low}} = L_{\text{low}} + \beta_1 L_M + \beta_2 T + \beta_3 E + \beta_4 \qquad \text{Eqn 12a}$$
$$L^*_{\text{mid}} = L_{\text{mid}} + \beta_5 L_M + \beta_6 E + \beta_7 \qquad \text{Eqn 12b}$$
$$L^*_{\text{high}} = L_{\text{high}} + \beta_8 L_M + \beta_9 T + \beta_{10} \qquad \text{Eqn 12c}$$

Most of the terms are as described in 5.2; that is L^*_{low}, L^*_{mid}, and L^*_{high} are modified constituent spectra, T is pavement surface temperature (°C), E is the pavement modulus (GPa) and β_{1-10} are best-fit coefficients determined through nonlinear least-squares curve fitting. In this case, however, the macrotexture term L_M (dB at 12.5 mm wavelength) is determined based on CTM data.

A predicted total OBSI spectrum is formed according to Equation 7 and compared to the OBSI spectrum on a given pavement to determine the fit coefficients, β_{1-10}, as before. The final model, including the best-fit coefficients, is shown in Equations 13 and 14, with the subscripts LE and TE representing terms at leading and trailing edges respectively.

$$L^*_{\text{LE, low}} = L_{\text{LE, low}} + 0.11 L_M + 0.031 T + 0.098 E - 4.2 \text{ dB} \qquad \text{Eqn 13a}$$
$$L^*_{\text{LE, mid}} = L_{\text{LE, mid}} - 0.12 L_M + 0.068 E + 5.8 \text{ dB} \qquad \text{Eqn 13b}$$
$$L^*_{\text{LE, high}} = L_{\text{LE, high}} - 0.20 L_M - 0.060 T + 7.2 \text{ dB} \qquad \text{Eqn 13c}$$

$$L^*_{\text{TE, low}} = L_{\text{TE, low}} + 0.22 L_M - 0.016 T + 0.039 E - 6.7 \text{ dB} \qquad \text{Eqn 14a}$$
$$L^*_{\text{TE, mid}} = L_{\text{TE, mid}} + 0.098 L_M + 0.096 E - 3.1 \text{ dB} \qquad \text{Eqn 14b}$$
$$L^*_{\text{TE, high}} = L_{\text{TE, high}} - 0.36 L_M - 0.017 T + 18.2 \text{ dB} \qquad \text{Eqn 14c}$$

As with the model using RoboTex data, the model described by Equations 13 and 14 (together with Equation 7) is complex, yet its individual terms can be interpreted physically. There are many similarities between the effects of the various parameters on the two models, as there should be.

5.3.1   Effect of Macrotexture

Similar to the RoboTex model, when the CTM is used to measure macrotexture, the positive coefficient for the low-frequency spectrum seen in both the leading and trailing edge means that low-frequency noise is expected to increase with increasing macrotexture. Macrotexture is predicted to have a smaller effect in the mid-frequency range, and the high-frequency content decreases due to negative coefficients for macrotexture in Eqn. 13c and 14c. The predicted effect of an increase in macrotexture of 6 dB is shown in Figure 31. The low-frequency content

increases slightly but the mid- and high-frequency content decreases. The overall level is predicted to decrease by approximately 0.3 dB.
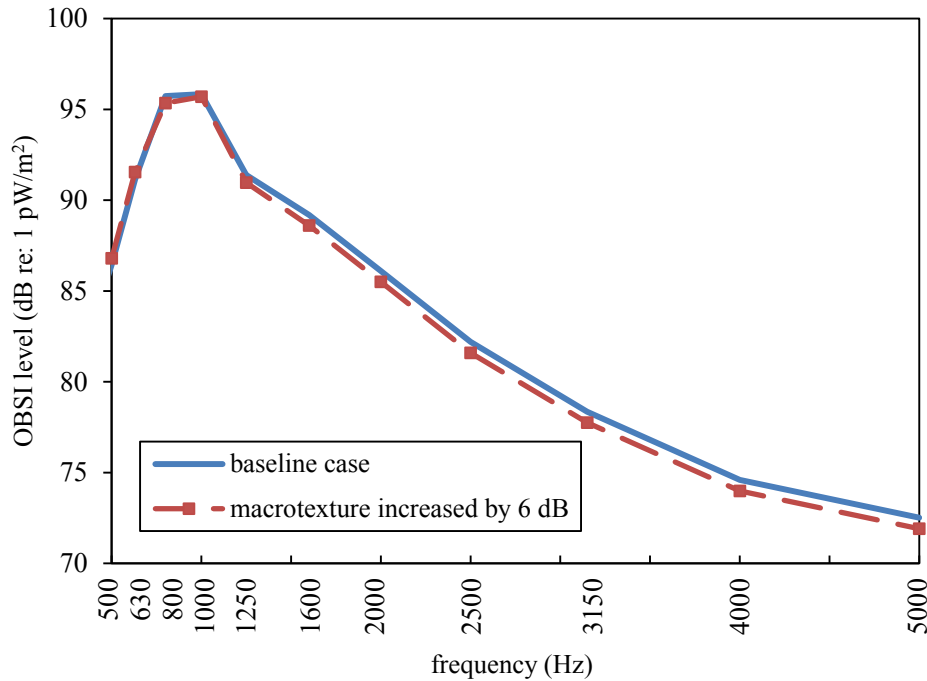

Figure 31. Effect of increased macrotexture (CTM).

5.3.2 *Effect of Temperature*

The temperature term, T, is the pavement temperature in °C at the time of OBSI testing, measured either by thermocouple or infrared thermometer. The negative coefficients mean that noise is expected to decrease with increasing temperature. This is consistent with findings by other researchers [138].

The predicted effect of an increase in temperature of 10°C is shown in Figure 32. The increased temperature primarily affects the high-frequency region and has little effect on the 1000 Hz peak. The result is a decrease in overall levels by approximately 0.1 dB, but again, the effect of temperature change on pavement modulus can lead to larger changes in noise with temperature as described in Section 5.2.5.
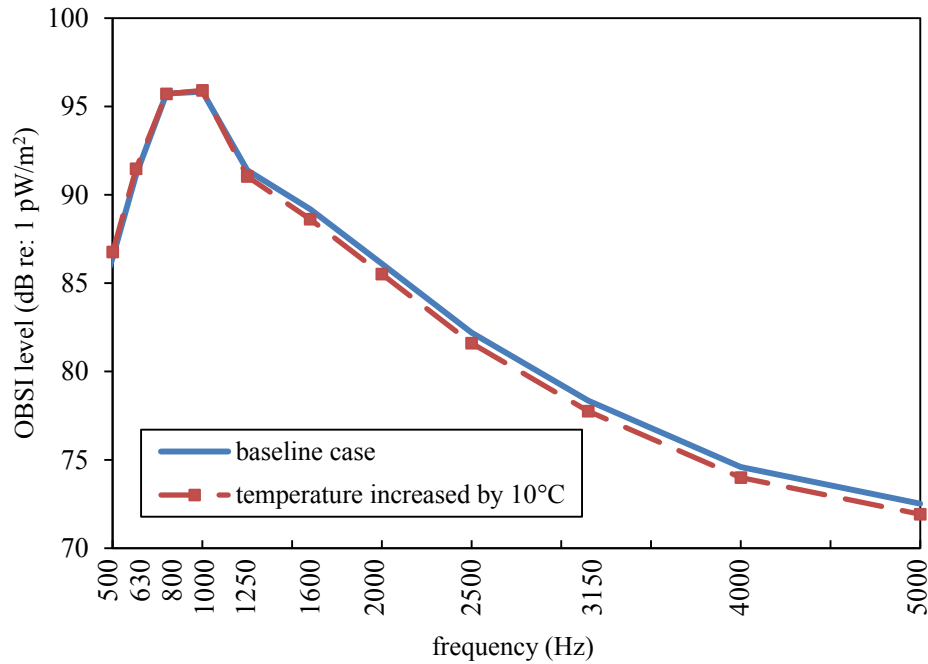
Figure 32. Effect of increased temperature (CTM).

5.3.3 *Effect of Modulus*

The effects of the modulus term, E, are very similar between the two models. As before, the positive modulus coefficients mean that stiffer pavements are expected to have increased noise in the low- and mid-frequency regions. Modulus has little to no effect on the high-frequency range, so there is no E term in Eqns. 13c and 14c.

The effect of an increase in modulus of 10 GPa is shown in Figure 33. The low-frequency region is affected more than the mid-frequency region, but there is still an increase in noise at the peak. The overall noise level is predicted to increase by approximately 0.5 dB.
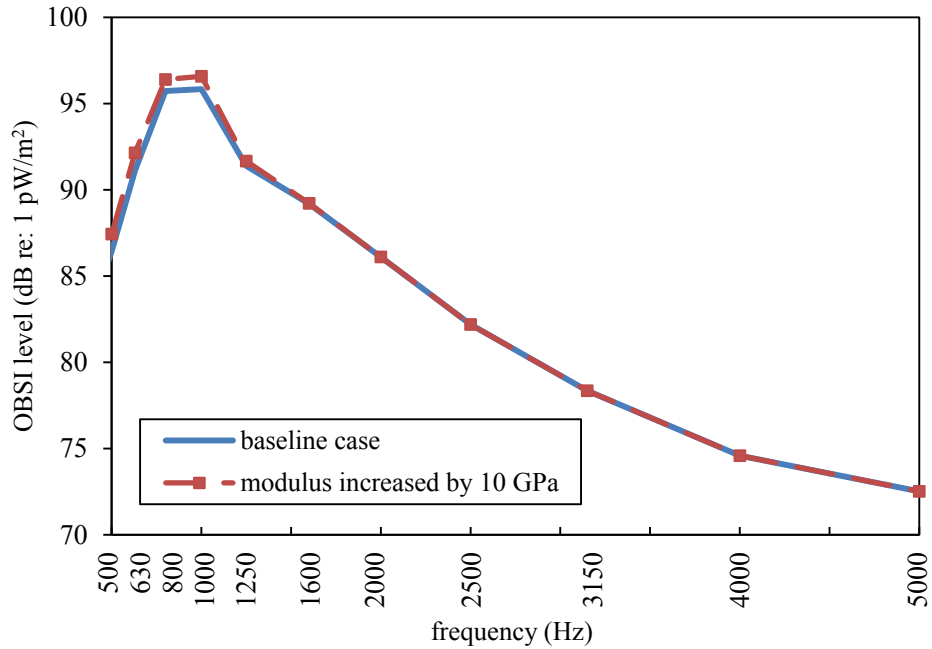
Figure 33. Effect of increased modulus (CTM).

5.3.4 Combined Effect of Temperature and Modulus

Like the RoboTex model, the CTM model also indicates that modulus will decrease with increasing temperature. Figure 34 shows the effect of the same 10°C increase in temperature as was shown in Figure 32 but accounts for the change in modulus. The increased temperature leads to a decreased modulus and a subsequent decrease in low- and mid-frequency levels. The temperature coefficient affects the high-frequency region and decreases it by a similar amount. The result is a decrease in overall levels of approximately 0.7 dB, somewhat less than with the RoboTex model.
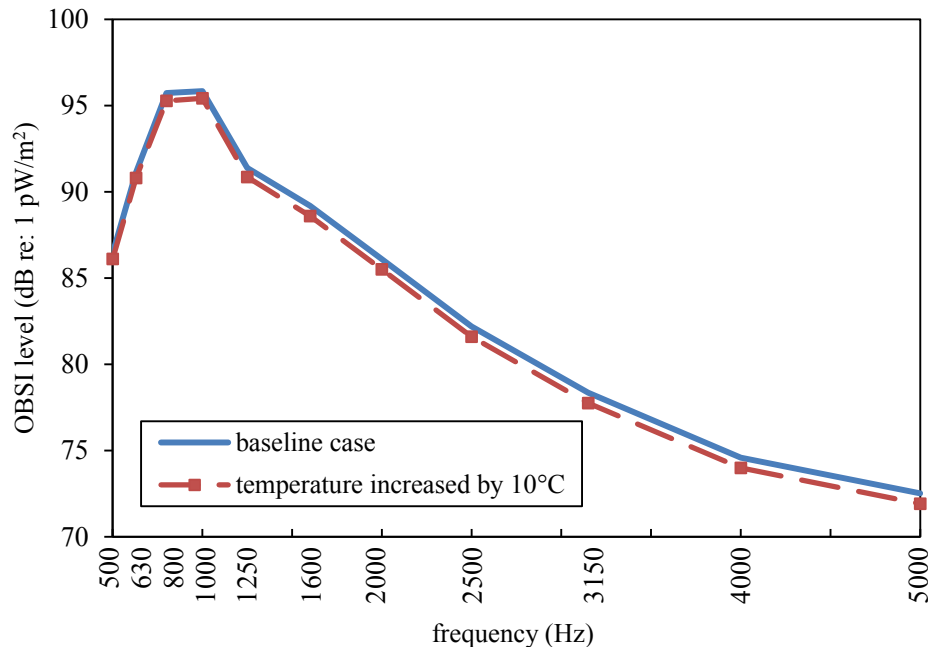
Figure 34. Effect of increased temperature, taking change in modulus into account (CTM).

5.4   Model Accuracy

Several different metrics were used to judge the accuracy of the models. For the types of pavements tested, the model can be used to predict overall levels to within 1 dB on average and one-third octave bands to within 2 dB on average. The model is more accurate with a recent texture scan and less accurate with extreme temperatures.

5.4.1   Overall Level Accuracy

The accuracy of the overall level predictions was judged by comparing model predictions to measured OBSI data.

For the RoboTex model, a total of 20 different asphalt pavements were used, because those asphalt sections were scanned using the RoboTex equipment. Sound levels were measured on each pavement several times over more than five years, for a total of 1421 different measurements of leading and trailing OBSI noise. The measured and predicted OBSI levels at both the leading and trailing edge sound intensity probes are shown in Figure 35 and Figure 36. In general, there is good match between the measured and predicted levels at both the leading and trailing edges. The model performs worst for loud pavements, which are sometimes predicted to be quiet. This may be a fault of the model or may be the result of faulty input data. For example, if the texture scan was performed on a smoother section of pavement than the OBSI measurements, predicted noise would be lower than measured noise. The average error in overall levels is 0.8 dB at the leading edge and 0.7 dB at the trailing edge. For comparison, the run-to-run variation in overall octave bands for data used in this study was approximately 0.6 dB. This corresponds to the average difference in overall OBSI levels for two different measurements of the same pavement made on the same day. The model matches the measured OBSI levels to within 1.5 dB for 87% of pavements at the leading edge and 90% at the trailing edge.

62

For the CTM model, a total of 13 different asphalt pavements had texture data measured at different times. The sound levels were measured on these cells several times over more than five years, for a total of 441 different measurements of leading and trailing OBSI noise. The measured and predicted OBSI levels at the leading and trailing edge sound intensity probes are shown in Figures 37 and 38. The average error in overall levels is 1.0 dB at the leading edge and 0.9 dB at the trailing edge. As before, the run-to-run variation in overall octave bands for data used in this study was approximately 0.6 dB. The model matches the measured OBSI levels to within 1.5 dB for 81% of pavements at the leading edge and 82% at the trailing edge.
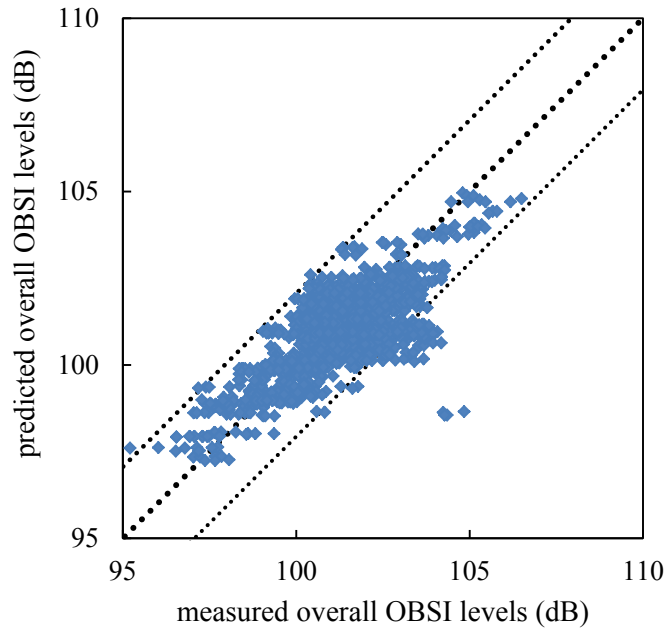

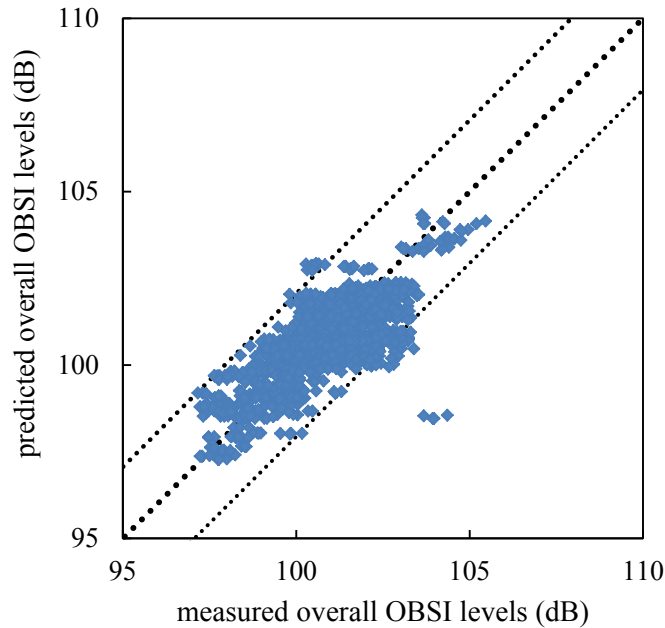Figure 35. Measured and predicted overall OBSI levels, leading edge, RoboTex data. Dotted line: 1:1.

Figure 36: Measured and predicted overall OBSI levels, trailing edge, RoboTex data. Dotted line: 1:1.
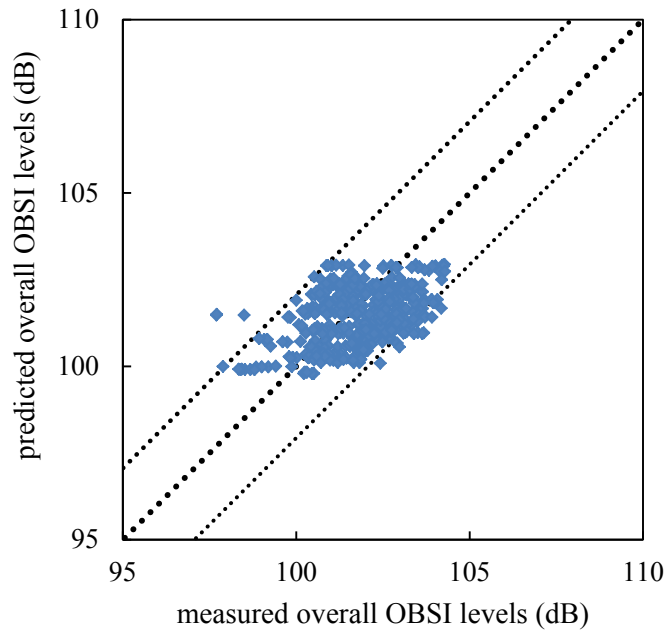
Figure 37. Measured and predicted overall OBSI levels, leading edge, CTM data. Dotted line: 1:1.

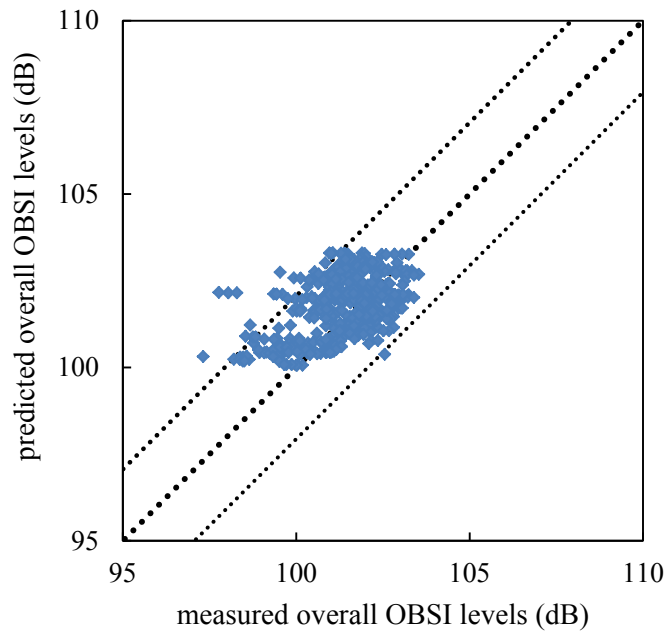Figure 38: Measured and predicted overall OBSI levels, trailing edge, CTM data. Dotted line: 1:1.

5.4.2   *Accuracy by Cell*

The average residual errors between the measured and predicted levels are shown separated by test cell in Figure 39 and Figure 40 for the RoboTex and CTM models respectively. In general, most pavements are predicted equally well. Cells 86 and 88 are porous pavements, which are

predicted accurately. However, if more porous pavements were included in the data set, another parameter, such as sound absorption, might need to be considered.
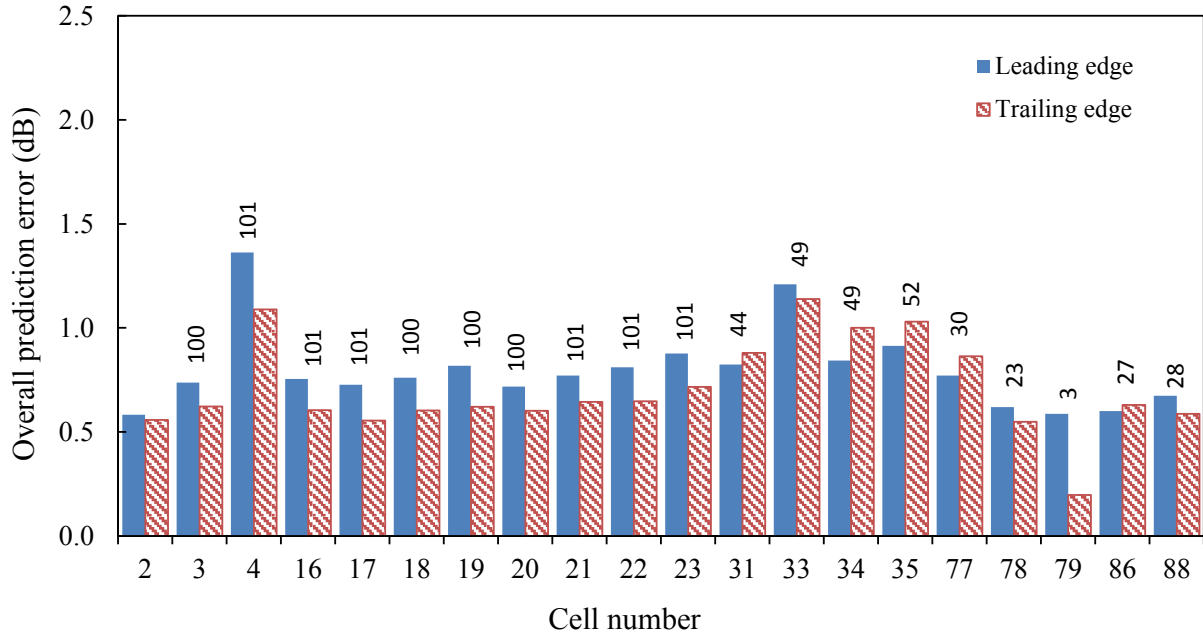

Figure 39: RoboTex Model accuracy by cell. Numbers above the bars indicate the number of OBSI measurements included for that cell in the model.
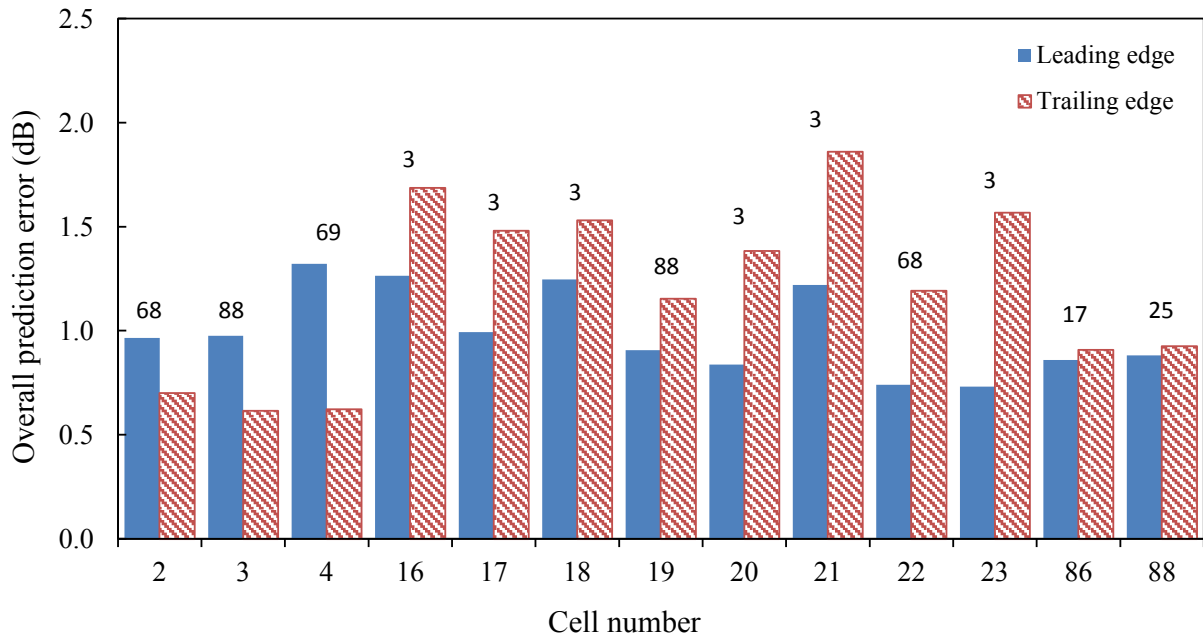

Figure 40. CTM Model accuracy by cell. Numbers above the bars indicate the number of OBSI measurements included for that cell in the model.

Comparison of Figures 39 and 40 shows that the overall residual prediction error is greater when the CTM model is used. The RoboTex model has residual errors less than 1.5 dB for all the cells in that model, whereas the CTM model has prediction errors less than 2 dB.

5.4.3 Accuracy by Year

The average residual error is shown separated by year in Figure 41 for the RoboTex model. Texture measurements for this model were all conducted in November 2011. In general, all years are modeled accurately. If the model were extended several years into the future, it is likely that additional texture measurements would need to be taken to improve the model's accuracy.

Figure 41: RoboTex Model accuracy by year. Numbers above the bars indicate the number of OBSI measurements included for that year in the model.

The average residual error by year for the CTM model is shown in Figure 42. As with the accuracy by cell, comparison of Figures 41 and 42 shows that the CTM model has higher residual errors than the RoboTex model.

66

Figure 42. CTM Model accuracy by year. Numbers above the bars indicate the number of OBSI measurements included for that year in the model.

5.4.4   Accuracy by Temperature Range

The average error separated by temperature range (in 10°C increments) is shown in Figure 43 for the RoboTex model and in Figure 44 for the CTM model. In general, OBSI levels at all temperatures are predicted accurately. The worst prediction occurs in very hot temperatures, where other noise generation mechanisms, such as adhesion between the tread blocks and asphalt, may become more prominent. Again, the CTM model generally exhibits higher overall residual errors than the RoboTex model.
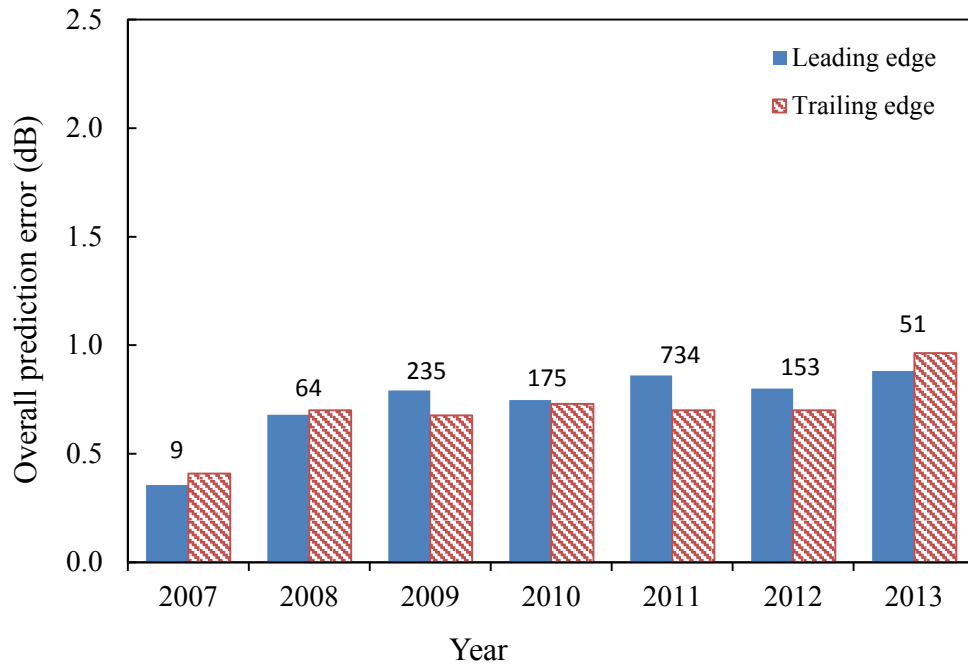
Figure 43. RoboTex Model accuracy by temperature range. Numbers above the bars indicate the number of OBSI measurements included for that temperature range in the model.
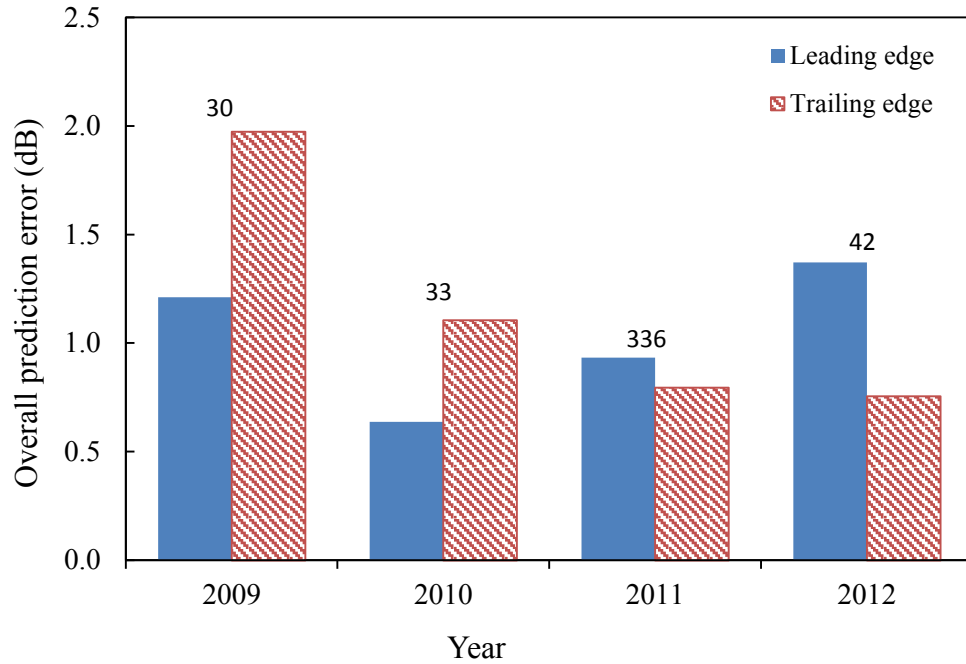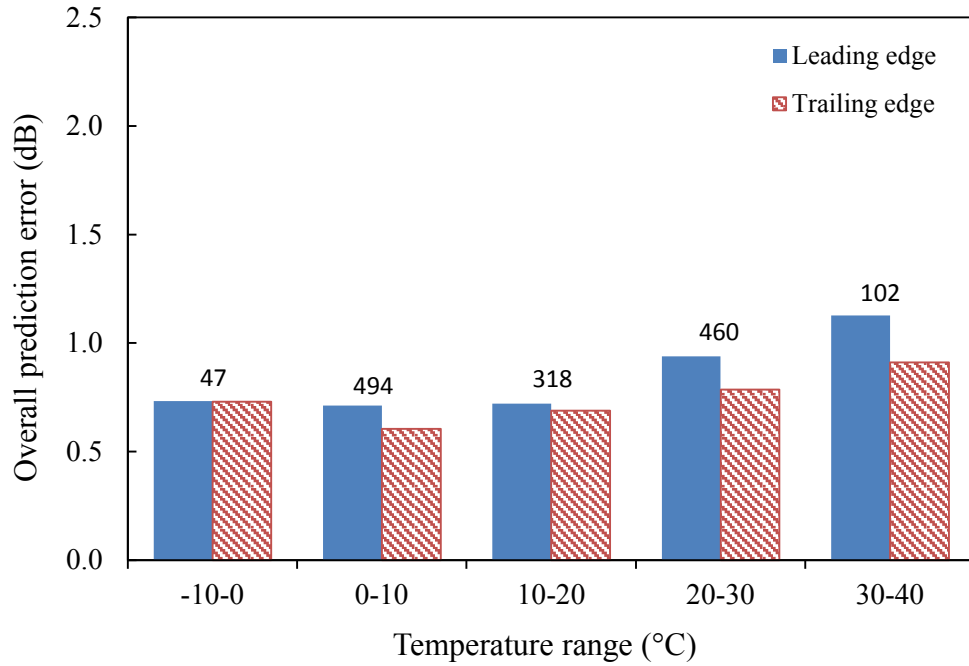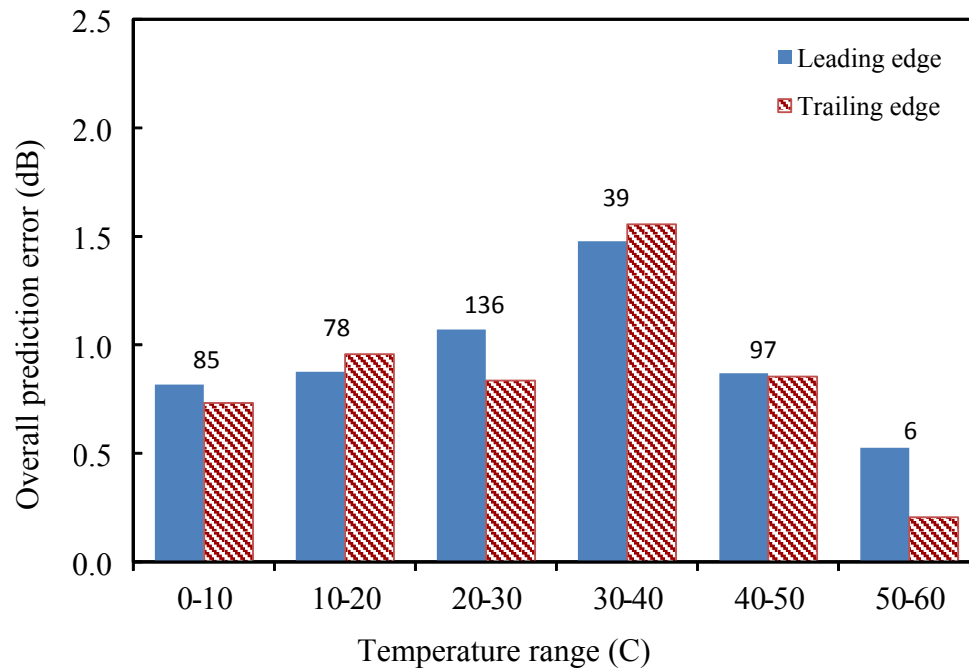

Figure 44. CTM Model accuracy by temperature range. Numbers above the bars indicate the number of OBSI measurements included for that temperature range in the model.

5.4.5 One-Third Octave Band Accuracy

The models not only predict overall OBSI levels but one-third octave band spectra as well. Figure 45 and Figure 46 compare the measured and predicted one-third octave band levels for every pavement and date for the leading and trailing edges using the RoboTex model. In general, there is good agreement between the measured and predicted cases at all frequencies. The mid-frequency range is generally predicted better than the high- and low-frequency ranges. As was seen with the overall levels, the data points with the highest residual tend to be below the 1:1 curve (shown as a dotted line), meaning that the model is predicting noise levels to be quieter than were actually measured. Average residual error separated by frequency band is shown in Figure 47. OBSI levels at most frequencies are predicted to within 2 dB on average, and the average error for all one-third octave band levels is 1.5 dB at the leading edge and 1.7 dB at the trailing edge. For comparison, the run-to-run variation in one-third octave bands for data used in this study was approximately 0.6 dB. This corresponds to the average difference in one-third octave band OBSI levels for two different measurements of the same pavement made on the same day. The worst prediction error occurs in the 400 Hz band. Data in this band can vary significantly run-to-run, which causes difficulty in modeling. However, the 400 Hz band does not have a significant effect on the overall levels.

Figure 45. Measured and predicted one-third octave band levels, leading edge, RoboTex model.

Figure 46. Measured and predicted one-third octave band levels, trailing edge, RoboTex model.

Figure 47. RoboTex Model accuracy by one-third octave bands.

The same comparisons of measured and predicted one-third octave bands are shown for the CTM model in Figures 48 and 49. The mid- and high-frequency ranges are generally predicted better than the low-frequency range with this model. Inspection of both figures shows that for frequencies up to and including 1000 Hz, the predicted OBSI levels fall in a narrower range than the measured values; that is, the cluster of data points tends towards horizontal rather than centering around the 1:1 line. This indicates that the model is not predicting the variation in OBSI levels that are measured at those frequencies.

Figure 50 shows the average residual error separated by frequency band. OBSI levels at most frequencies are predicted to within 2 dB on average, and the average residual error for all one-third octave band levels is 1.5 dB at the leading edge and 1.9 dB at the trailing edge. Recall that the run-to-run variation in one-third octave bands for data used in this study was approximately 0.6 dB.
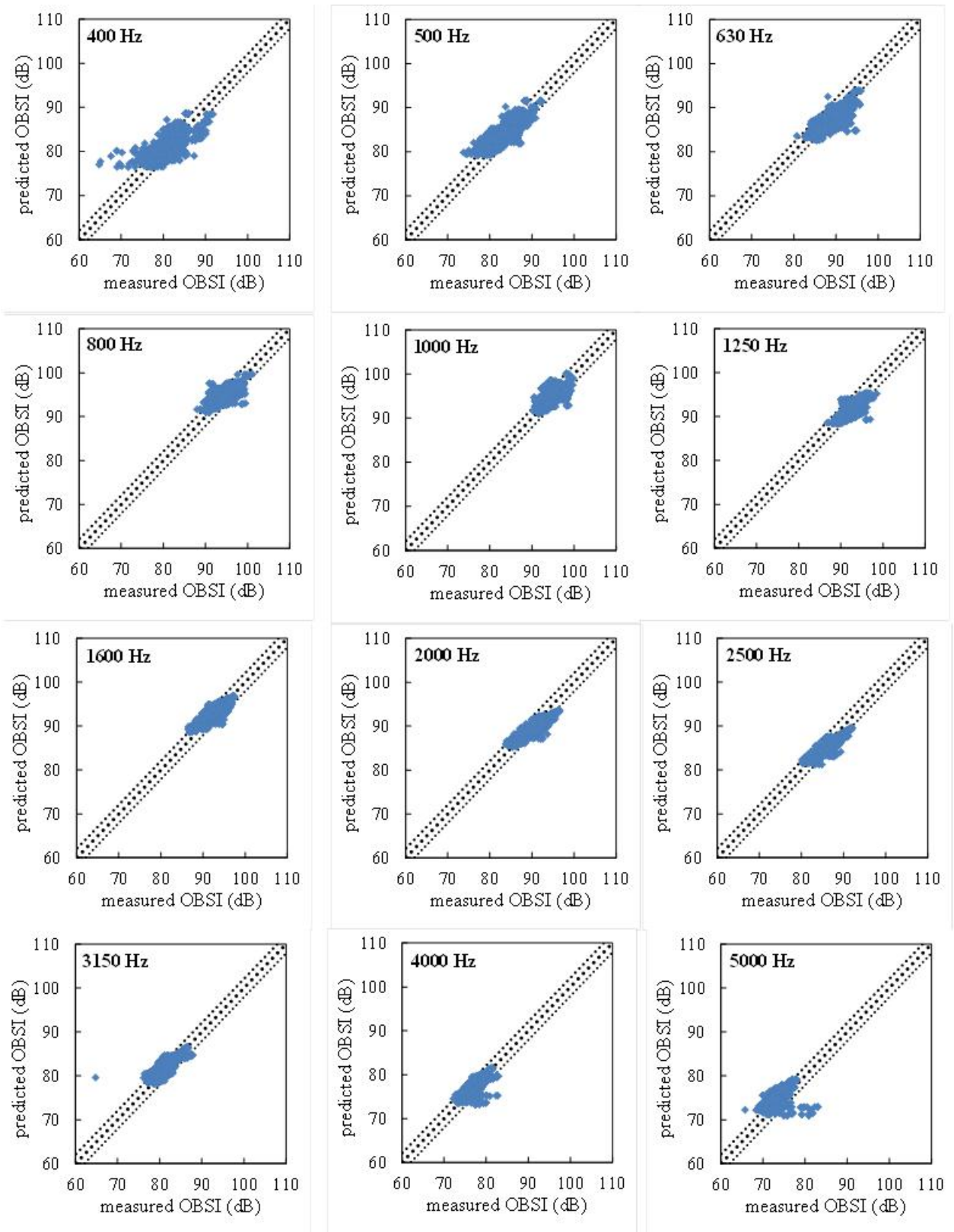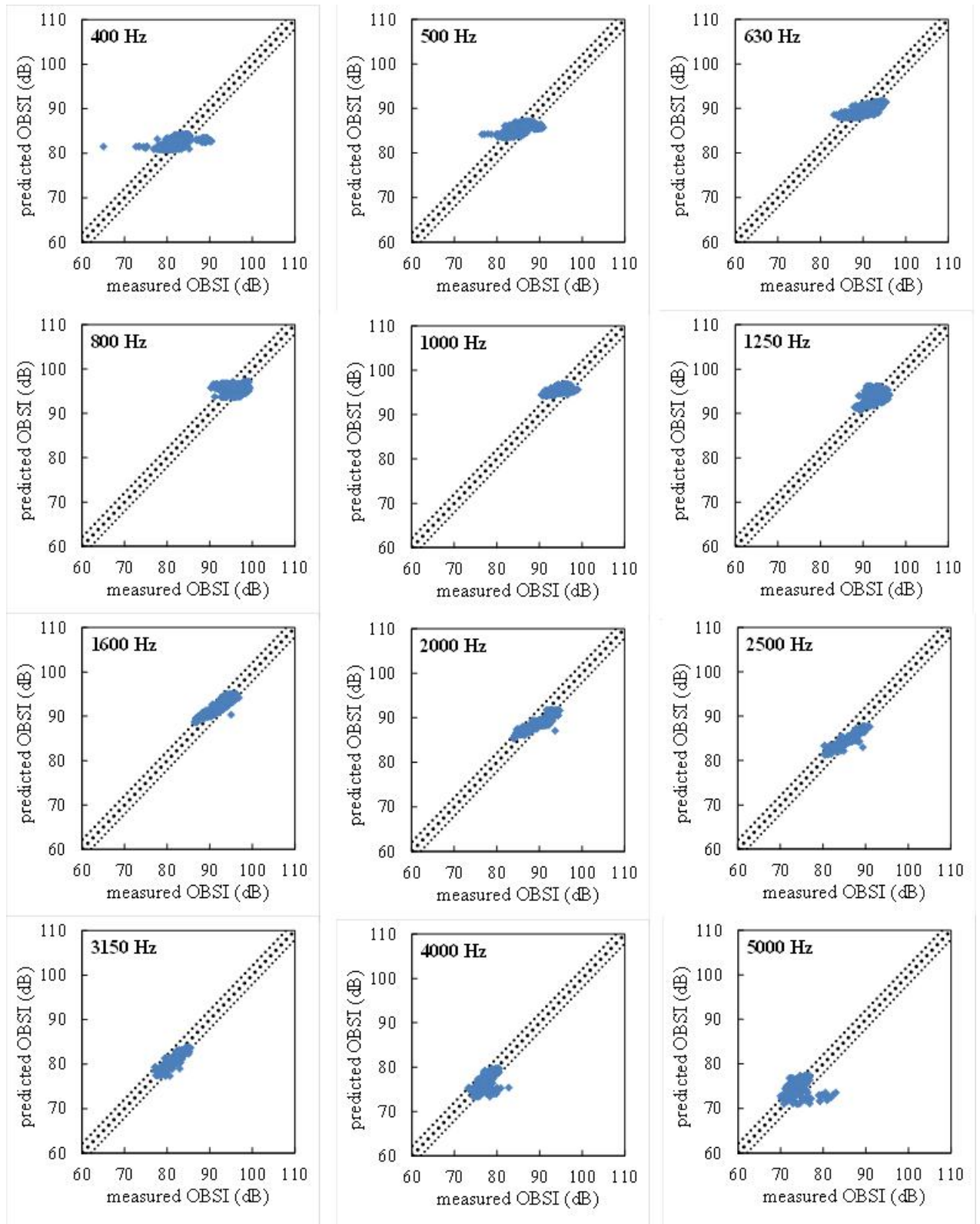
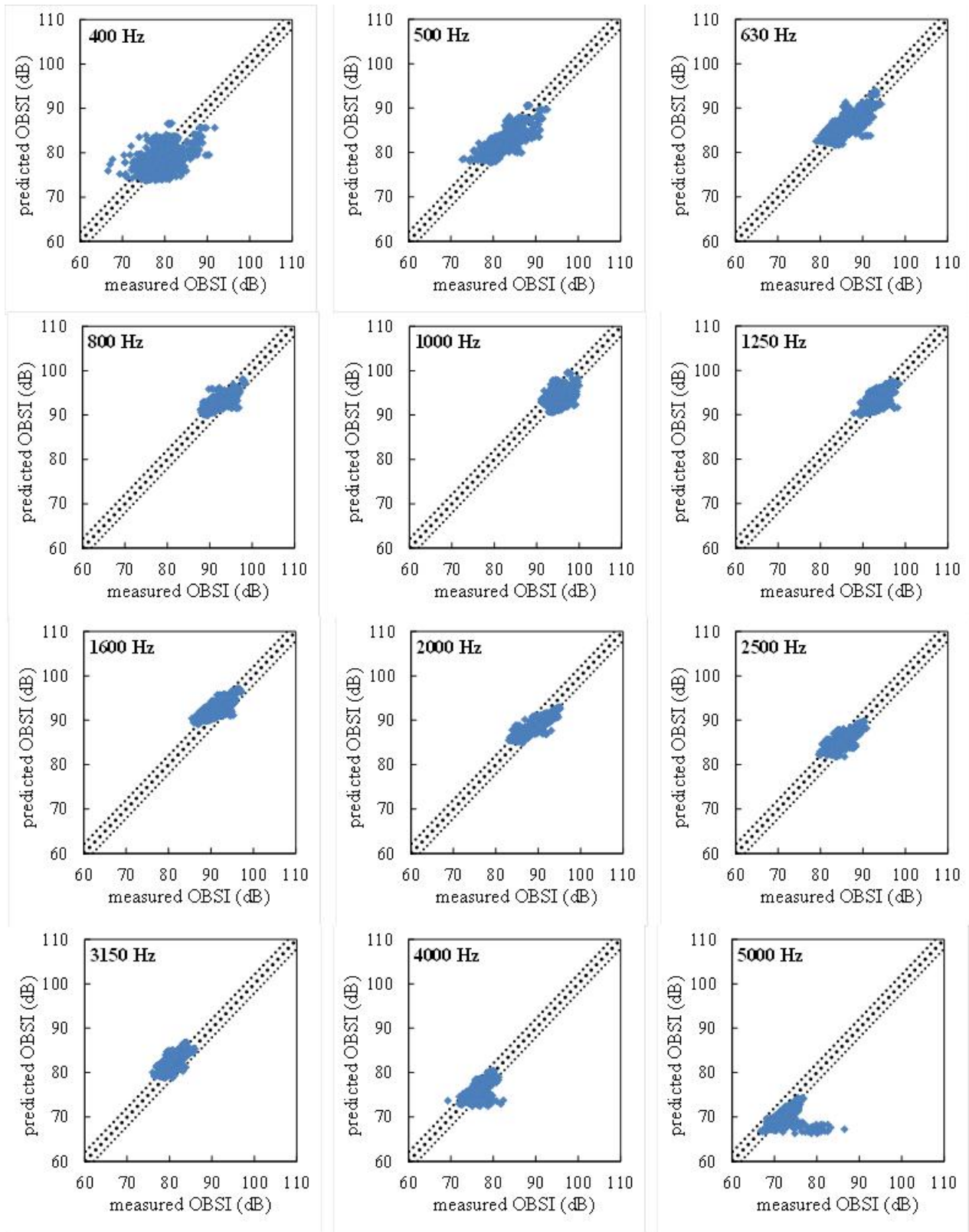Figure 48. Measured and predicted one-third octave band levels, leading edge, CTM model.

73

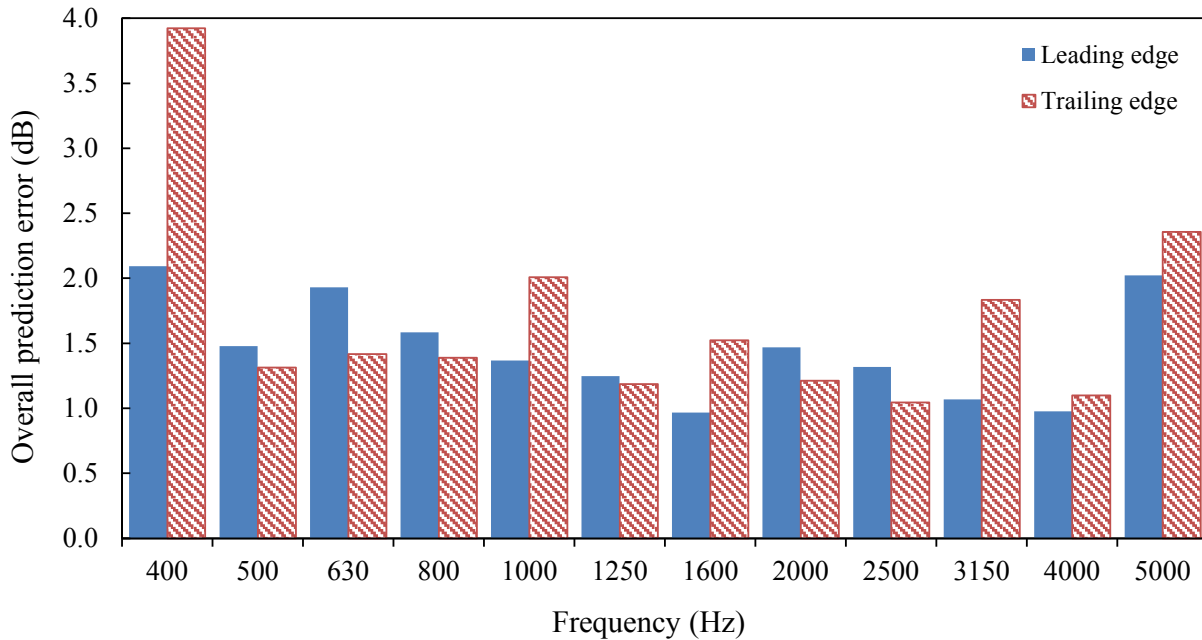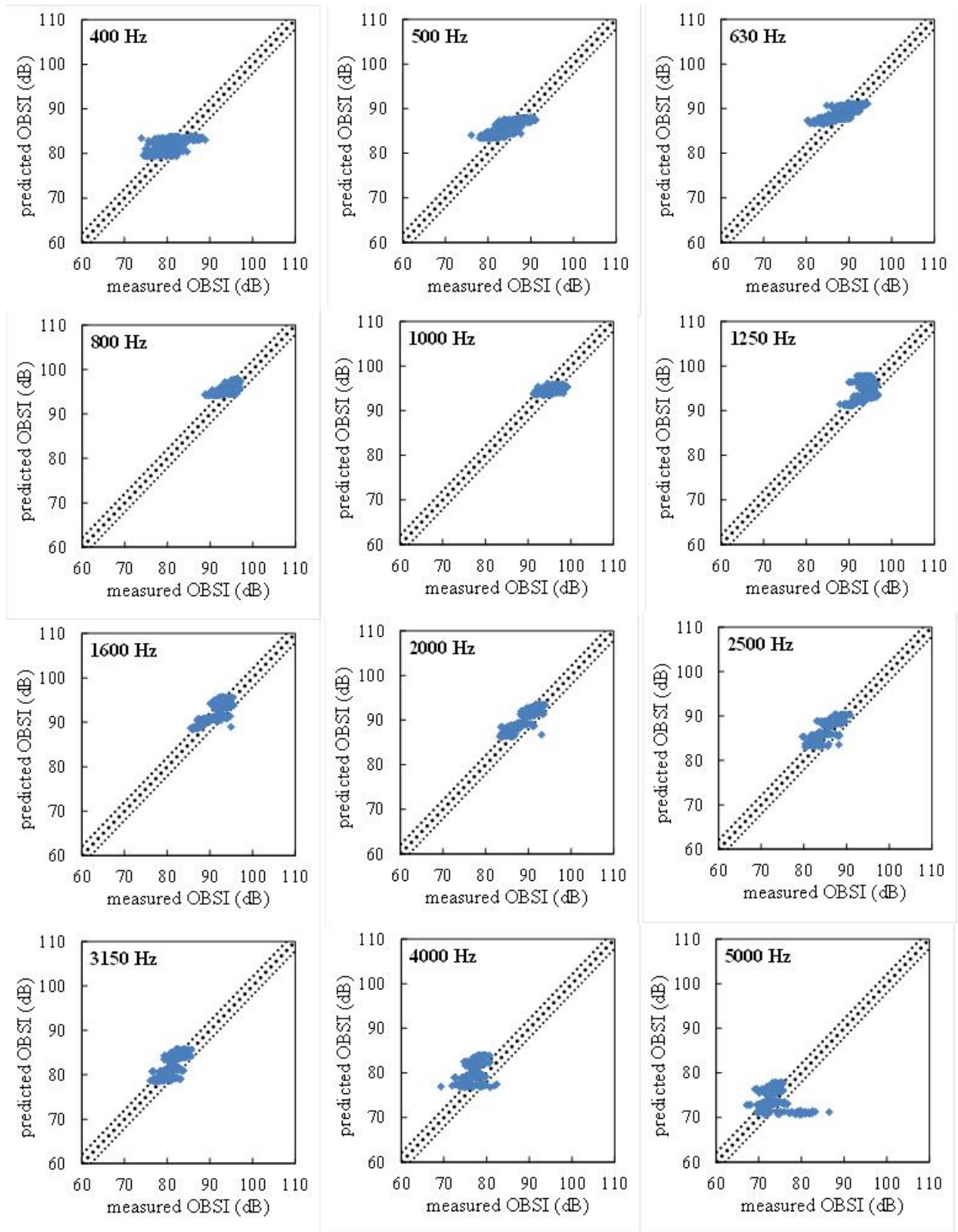Figure 49. Measured and predicted one-third octave band levels, trailing edge, CTM model.
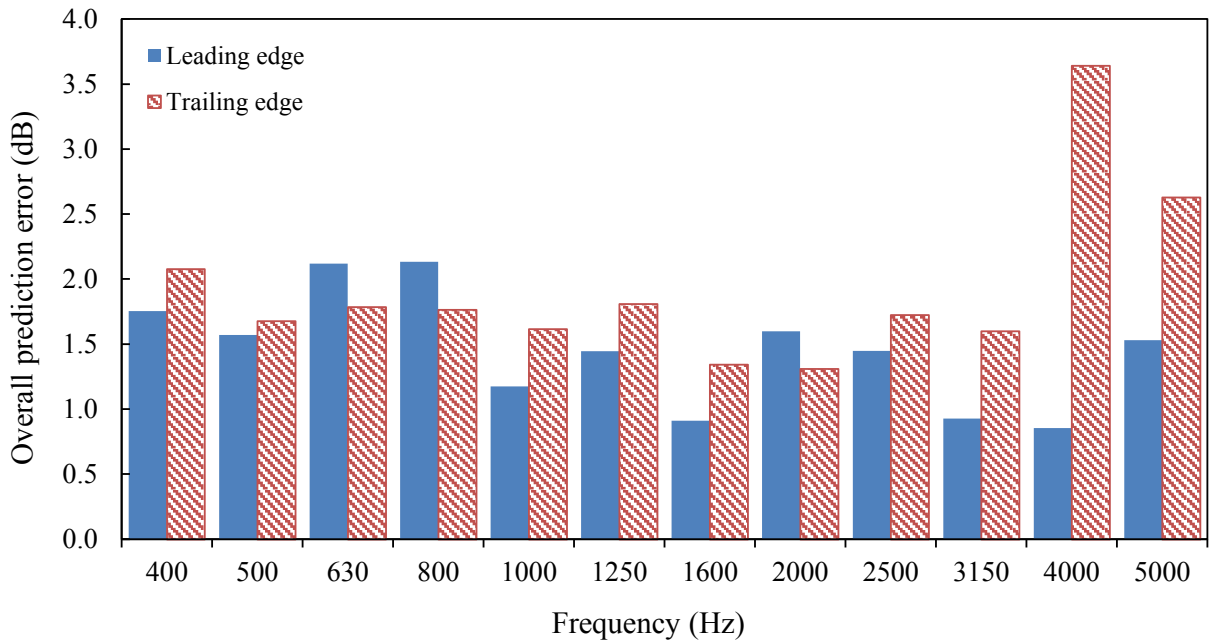
Figure 50. CTM Model accuracy by one-third octave bands.

5.5 Discussion

The information presented in Section 5.4 shows that the model developed using RoboTex data is generally more accurate than the model using the CTM data. The overall level accuracy (Section 5.4.1), summarized in Table 5, is much better for the RoboTex model. The overall prediction errors by cell, year and temperature range are all higher for the CTM model than for the RoboTex model. The one-third octave band data shows that the CTM model is not doing a good job of predicting the one-third octave band spectra for frequencies up to and including 1000 Hz.

Table 5. Percent of pavements with noise levels predicted to within 1.5 dB for the two models

Model Location	Percent of Pavements with Noise Levels Predicted to within 1.5 dB	
	RoboTex Model	CTM Model
Leading Edge	87%	81%
Trailing Edge	90%	82%

However, it is much easier, less expensive and more feasible for MnDOT to measure texture using the CTM versus the RoboTex.

The improved performance of the RoboTex method may be due to several reasons. RoboTex data was collected on 22 pavements. Noise measurements were made on these pavements multiple times over more than five years, resulting in 1421 measurements. The CTM data was available for multiple years on only 13 different asphalt pavements, where 441 different

noise measurements were collected. So, there was over three times as much data for the RoboTex model compared to the CTM model.

Perhaps an even greater impact is due to the nature of the texture measurements themselves. Texture data is inherently noisy data. The texture can change substantially from one location to another within the same test cell or pavement. The RoboTex collects 100 lines of data, resulting in approximately 15,000 m of data within a test cell; this resulted in error bars on the texture measurements of 0.1-0.2 dB. The CTM, on the other hand, was typically used to test eight locations within a test cell. Given the circumference of the circle scanned by the CTM, this resulted in approximately 7-8 m of data per cell. In other words, there was about 2000 times more texture data from the RoboTex as from the CTM. The error bars on the CTM texture data were 3-5 dB, leading to 2-3 dB variation in the predicted OBSI. It might be possible to improve the accuracy of the CTM model by performing more measurements in each test cell, but the time and labor required to do so is likely prohibitive and could not reasonably be expected to provide the same amount of data as was obtained with the RoboTex.

Understanding the limitations of the models, then, either can be used to predict tire-pavement noise based on differing input values. The RoboTex model provides better accuracy because of the extensive amount of texture data available; however, the model is more accurate when the texture measurements are more recent and collection of the RoboTex data is expected to be a one time, or certainly rare, event. The CTM data is much more feasible to collect frequently, however, the model is not as accurate because even with frequent measurements, there is not as much texture data available because of the much shorter path measured.

5.6   Using the Model

Since the model takes the form of a set of equations, it can be implemented in any data processing software. Along with this report, an Excel spreadsheet is provided to assist in future implementation of the model and to illustrate the effects of changing pavement parameters.

The model is simple to use. On one of the Model tabs (either RoboTex or CTM), three or four inputs are required:
- the 12.5 mm wavelength texture level (dB) of the subject surface,
- the temperature (°C) corresponding to the temperature at the time of OBSI testing,
- the modulus of the pavement surface (GPa) backcalculated from FWD testing results
- and, if the RoboTex model is used, the time in years between measurement of the texture and the noise.

As the spreadsheet is currently configured, up to three pavements can be compared at one time or a given pavement can be evaluated under differing conditions, such as changes in temperature and modulus values. A table of predicted A-weighted OBSI sound pressure levels at various frequencies (one-third octave bands) and the overall OBSI level is automated generated, as are graphs of the one-third octave bands and overall OBSI levels.

The Calculations tabs include all of the model equations and computations required to generate the outputs shown on the Model tab. If future research leads to changes in the model, they can be implemented by revising the calculations.

6. Discussion and Conclusions

The objective of this project was to develop a model to predict on-board sound intensity (OBSI) levels on asphalt pavements using field and laboratory data from MnROAD. The model was to consider the effects of pavement surface and material characteristics, so it was necessary first to identify which of those characteristics have significant effects on tire-pavement noise. To accomplish the objective, it was also necessary to determine the effects of seasonal variations on those characteristics that could affect noise generation.

Only asphalt surfaces were studied in this project. However, there was a fairly wide range of surface types, including dense-graded asphalt, porous asphalt, 4.75 mm surfaces, ultrathin wearing courses, and chip seals. Most of these surfaces were constructed in 2007 and 2008, so the pavement age is limited. A total of 25 test cells were used in various portions of the study.

Different noise generation and amplification mechanisms affect different frequency ranges. In addition, different pavement characteristics affect different mechanisms. This study explored the various mechanisms and related pavement characteristics using the mechanism-decomposition method, which allows the effects of changes in various parameters on the low-, mid- and high-frequency noise spectra to be predicted. The changes in the individual constituent spectra are then logarithmically added to yield estimates of overall tire-pavement noise and one-third octave bands levels.

Using the available MnROAD data, a series of reduced-parameter models was developed to investigate which factors most strongly impact noise measured at MnROAD. Each simplified model involved only one or two variables, and all of the other variables were controlled. Simplified models were developed for as many different pavement and atmospheric parameters as possible.

Using the findings from these simplified models, a set of significant variables was identified. In general, the low-frequency spectrum was found to be affected most by macrotexture parameters and less by microtexture, absorption, and temperature. The mid-frequency spectrum was affected by all texture parameters and absorption. The high-frequency spectrum was most affected by microtexture and air temperature. Using the two-parameter age-temperature model, it was shown that age significantly affects the low- and mid-frequency spectra but not the high-frequency spectrum. The two-parameter temperature-modulus model was used to show that modulus and temperature must both be considered for the high-frequency spectrum but not necessarily for the low-frequency spectrum. Some variables were found not to be necessary for each of the three constituent spectra, so they were eliminated from further model development at the appropriate frequency ranges. Many pairs of remaining parameters were highly correlated, so the need to include both in the final model was explored.

The significant variables identified through the reduced parameter models were used as preliminary inputs to the model for subsequent development of two full models. (The models differ in the type of texture data used as an input parameter.) Ultimately, it was found necessary for the models to consider the effects of pavement macrotexture, air temperature, modulus of the pavement surface layer and the combined effect of temperature and modulus. Only two porous pavements were included in the data set; if more porous pavements were included, an absorption parameter might be found to be significant.

The models are provided in an Excel spreadsheet requiring three or four input values: 12.5 mm texture level, air temperature and surface modulus. When laser profiler data is used for the texture metric, the time between the texture measurement and the noise determination is also

77

required. Changing the inputs results in automatic changes in the predicted overall OBSI sound intensity level and one-third octave band levels. Sound intensity levels are predicted for both the leading and trailing edges of the tire.

The models show that to achieve a low noise pavement, a smooth surface with a low stiffness is preferable. As the macrotexture and stiffness decrease, the peak and overall OBSI levels also decrease. As modulus is related to temperature, increasing the temperature results in a decrease in the modulus, but some surface materials are more sensitive to changes in temperature than others. In general, stiffer materials tend to experience greater decreases in stiffness than softer materials. In this study, the ultrathin wearing courses were among the stiffer materials and produced some of the higher noise levels. The sections with chip or surface seals had higher texture and also higher noise levels. The warm mix asphalt and lower traffic volume mixtures tended to have lower stiffness values and lower noise. The warm mix sections used a fairly soft binder grade (PG58-28) and may have experienced reduced aging during construction. Mixes designed for lower traffic volumes may not have as strong an aggregate structure, which could affect the overall surface stiffness. The models also reflect that noise tends to increase as pavements age, but none of the cells tested were approaching the end of their service life or exhibiting high levels of distress.

The models were developed for the types of asphalt surfaces tested at MnROAD and based on the types of test data available. Because the models rely heavily on modulus, they would not be reliably used on other pavement types that have different stiffness values and respond differently to changes in temperature compared to asphalt mixtures. A wide range of asphalt mixtures was studied, so the models are applicable to a wide range of types of asphalt surfaces, but high levels of distress and old pavements were not tested.

In addition, the models were developed to predict noise as measured by the OBSI method; attempts to correlate OBSI data to other types of noise data have yielded mixed results. For example, OBSI data can be used to predict CPB data for some types of pavements to within 0.5 dB. Correlating OBSI data, which is measured at the source of the noise, to farfield noise, as measured with the pass-by techniques, is less reliable, especially for porous pavements, which affect noise propagation. Applying these models to other surface types, with different input variables or to predict other noise measurements would require validation and perhaps revision of the models. However, the models were formulated and implemented (in an Excel spreadsheet) in such a way that future revisions can be readily accommodated.

The models have been found to predict the overall OBSI sound intensity level to within 1.5 dB and the one-third octave bands to within 2 dB for most of the pavements tested. Other metrics and evaluation of the model accuracy by cell, year, temperature and other factors are also reported and are generally favorable.

7. References

1. International Organization for Standardization, "Acoustics - Method for measuring the influence of road surfaces on traffic noise - Part 1: The Statistical Pass-By Method", ISO 11819-1, ISO, Geneva, Switzerland, 1997.

2. International Organization for Standardization, "Acoustics - Method for measuring the influence of road surfaces on traffic noise - Part 2: "The Close Proximity Method", ISO 11819-2, ISO, Geneva, Switzerland, 2000.

3. American Association of State Highway and Transportation Officials, "Standard Method of Test for Measurement of Tire/Pavement Noise Using the On-Board Sound Intensity (OBSI) Method," AASHTO TP 76, AASHTO, Washington, DC, 2008.

4. Ulf Sandberg and Jerzy A. Ejsmont, *Tyre/Road Noise Reference Book,* Kisa, Sweden: INFORMEX, 2002.

5. Jerzy A. Ejsmont and Ulf Sandberg, "Tire/road noise: Trailer measurements in practice," in *Proceedings of Inter-Noise 1985*, Munich, Germany, 1985.

6. P. Donavan and B. Rymer, "Quantification of tire/pavement noise: Application of the sound intensity method," in *Proceedings of Inter-Noise 2004*, Prague, Czech Republic, 2004, p. 1465.

7. Paul R. Donavan, "The effects of porous pavements on tire/pavement noise source levels and pass-by measurements," in *Proceedings of Noise-Con 2011*, Portland, OR, 2011.

8. Nils-Aaki Nilsson, Ove Bennerhult and Stig Soederqvist, "External tire/road noise: its generation and reduction," in *Proceedings of Inter-Noise 1980*, Miami, FL, 1980, p. 245.

9. Kenneth J. Plotkin, Mark L. Montroll and William R. Fuller, "The generation of tire noise by air pumping and carcass vibration," in *Proceedings of Inter-Noise 1980*, Miami, FL, 1980, p. 273.

10. W. A. Leasure, "Tire-road interaction noise," in *Proceedings of Inter-Noise 1973*, Copenhagen, Denmark, 1973, p. 421.

11. A. C. Eberhardt, "Development of a transient response model for tire/pavement interaction," in *Proceedings of Inter-Noise 1984*, Honolulu, HI, 1984, p. 77.

12. T. Fujikawa, H. Koike, Y. Oshino and H. Tachibana, "Road texture for abating truck tire noise generation," in *Proceedings of Inter-Noise 2006*, Honolulu, HI, 2006, p. 1191.

13. P. R. Donavan and L. J. Oswald, "The identification and quantification of truck tire noise sources under on-road operating conditions," in *Proceedings of Inter-Noise 1980*, Miami, FL, 1980, p. 253.

14. Paul Donavan and Dana M. Lodico, "Tire/pavement noise of test track surfaces designed to replicate California highways," in *Proceedings of Inter-Noise 2009*, Ottawa, Canada, 2009, p. 3884.

15. Sungtae Kim, Wontae Jeong, Yonghwan Park and Sogab Lee, "Prediction method for tire air-pumping noise using a hybrid technique," *Journal of the Acoustical Society of America*, Vol. 119, No. 6, p. 3799, June 2006.

16. Nils Ake Nilsson, "Principles in the control of external tire/road noise," in *Proceedings of Inter-Noise 1982*, San Francisco, CA, 1982, p. 123.

17.   G. Descornet and U. Sandberg, "Road surface influence on tire noise - II," in *Proceedings of Inter-Noise 1980*, Miami, FL, 1980, p. 267.

18.   U. Sandberg, B. Kalman and A. R. Williams, "The porous tread tire - the quietest pneumatic tire measured so far?," in *Proceedings of Inter-Noise 2005*, Rio de Janeiro, Brazil, 2005.

19.   Ryszard Wozniak, "Measurement of tyre/road noise in longitudinal slip conditions," in *Proceedings of Inter-Noise 2001*, The Hague, Holland, 2001, p. 556.

20.   R. Wozniak and S. Taryma, "Investigations in tyre/road noise in longitudinal slip conditions," in *Proceedings of Inter-Noise 2004*, Prague, Czech Republic, 2004, p. 2300.

21.   Ard Kuijpers and Gijsjan van Blokland, "Tyre/road noise models in the last two decades: A critical evaluation," in *Proceedings of Inter-Noise 2001*, The Hague, Holland, 2001, p. 2494.

22.   Richard J. Ruhala and Courtney B. Burroughs, "Separation of leading edge, trailing edge, and sidewall noise sources from rolling tires," in *Proceedings of Noise-Con 1998*, Ypsilanti, MI, 1998, p. 109.

23.   M. Kroger, M. Lindner and K. Popp, "Influence of friction on noise and vibrations of tyres," in *Proceedings of Inter-Noise 2004*, Prague, Czech Republic, 2004, p. 1457.

24.   J. Stuart Bolton, Heuk Jin Song, Yoon Ki Kim and June Kang Yeon, "The wave number decomposition approach to the analysis of tire vibration," in *Proceedings of Noise-Con 1998*, Ypsilanti, MI, 1998, p. 97.

25.   Lawrence J. Oswald and Artemis Arambages, "The noise mechanisms of cross groove tire tread pattern elements," in *Proceedings of Noise-Con 1983*, New York, NY, 1983, p. 363.

26.   H. Koiki, T. Fujikawa, Y. Oshino and H. Tachibana, "Generation mechanism of tire/road noise Part 2: Pipe resonance in tread groove of tire," in *Proceedings of Inter-Noise 1999*, Fort Lauderdale, FL, 1999, p. 199.

27.   Hyu-Sang Kwon, J. Stuart Bolton and Darren L. Hallman, "Nearfield acoustical holography applied to sound radiation from tire," in *Proceedings of Noise-Con 1998*, Ypsilanti, MI, 1998, p. 103.

28.   P. R. Donavan, "Examination of tire/road noise at frequencies above 630 hertz," in *Proceedings of Inter-Noise 2002*, Dearborn, MI, 2002, p. 241.

29.   Takeo Fujii, Shigeo Iwai and Miki Kuroki, "Behavior or tire tread groove relating to generation of tire/road noise at the contact patch," in *Proceedings of Inter-Noise 2003*, Jeju, South Korea, 2003, p. 885.

30.   Lawrence E. Kinsler, Austin R. Frey, Alan B. Coppens and James V. Sanders, *Fundamentals of Acoustics*, 4th ed. New York, NY: John Wiley & Sons, Inc., 2000.

31.   Klaus Schaaf and Dirk Ronneberger, "Noise radiation from rolling tires - sound amplification by the "horn-effect"," in *Proceedings of Inter-Noise 1982*, San Francisco, CA, 1982, p. 131.

32.   Kiho Yum and J. Stuart Bolton, "Sound radiation modes of a tire on a reflecting surface," in *Proceedings of Noise-Con 2004*, Baltimore, MD, 2004, p. 161.

33.   Shigeo Iwai, Yuji Miura, Hidetomo Koike and Georges Levy, "Influence of porous asphalt pavement characteristics on the horn amplification of tire/road contact noise," in

Proceedings of Inter-Noise 1994, Yokohama, Japan, 1994, p. 431.

34. Wai Keung Lui and Kai Ming Li, "A theoretical study for the propagation of rolling noise over a porous road pavement," *Journal of the Acoustical Society of America*, Vol. 116, No. 1, July 2004, p. 313.

35. J. J. Henry, "Overview of the International PIARC Experiment to Compare and Harmonize Texture and Skid Resistance Measurements: The International Friction Index," proceedings of the *Third International Symposium on Pavement Surface Characteristics: Christchurch*, New Zealand, 3-4 September 1996.

36. J. C. Wambold, C. E. Antle, J. J. Henry and Z. Rado, *International PIARC Experiment to Compare and Harmonize Texture and Skid Resistance Measurement*, Permanent International Association of Road Congress, Paris, France, 1995.

37. International Organization for Standardization, "Characterization of pavement texture by use of surface profiles - Part 4: Spectral analysis of surface profiles," , ISO 13473-4, ISO, Geneva, Switzerland, 2008.

38. ASTM International, "Standard Test Method for Measuring Pavement Macrotexture Properties Using the Circular Track Meter," ASTM E2157, ASTM, West Conshohocken, PA, 2009.

39. J. Fujikawa, Y. Oshino, T. Mikami and H. Tachibana, "Examination on effects of road roughness parameters for abating tire/road noise," in *Proceedings of Inter-Noise 2004*, Prague, Czech Republic, 2004, p. 1122.

40. S. A. Storeheier, "Investigation on road surface texture levels in tyre/road noise mitigation," in *Proceedings of Inter-Noise 2004*, Prague, Czech Republic, 2004, p. 3403.

41. Tatsuo Fujikawa, Yasuo Oshino and Hideki Tachibana, "Effect of road roughness on tire/road noise - Approach by frequency analysis," in *Proceedings of Inter-Noise 2007*, Istanbul, Turkey, 2007, p. 708.

42. ASTM International, "Standard Practice for Calculating Pavement Macrotexture Mean Profile Depth," ASTM E1845, ASTM, West Conshohocken, PA, 2009.

43. Tyler Dare and Robert Bernhard, "Predicting tire-pavement noise on longitudinally ground pavements using a nonlinear model," in *Proceedings of Inter-Noise 2009*, Ottawa, Canada, 2009, p. 4047.

44. Ulf Sandberg and Jerzy A. Ejsmont, "Texturing of cement concrete pavements to reduce traffic noise," *Noise Control Engineering Journal*, Vol. 46, No. 6, November 1998, p. 231.

45. I. A. Fulop, I. Bogardi, A. Gulyas and M. Csicsely-Tarpay, "Use of Friction and Texture in Pavement Performance Modelling," *ASCE Journal of Transportation Engineering*, Vol. 126, No. 3, 2000, pp. 243-248.

46. D. I. Hanson and B. D. Prowell, *Evaluation of Circular Texture Meter for Measuring Surface Texture of Pavements*, NCAT Report No. 04-05, National Center for Asphalt Technology, Auburn, AL, 2004.

47. Robert Rasmussen, Eric Mun, Ted Farragut and Paul Wiegand, "A comprehensive field study on concrete pavement solutions for reducing tire-pavement noise," in *Proceedings of Inter-Noise 2006*, Honolulu, HI, 2006, p. 3900.

48. Robert Rasmussen, Eric Mun, Steven Karamihas and George Chang, "Relating pavement texture to tire-pavement noise," in *Proceedings of Inter-Noise 2006*, Honolulu, HI, 2006,

p. 3910.

49. Julien Cesbron, Fabienne Anfosso-Ledee, Denis Duhamel, Hai Ping Yin and Donatien Le Houedec, "Experimental study of tyre/road contact forces in rolling condictions for noise prediction," *Journal of Sound and Vibration*, Vol. 320, No. 1-2, February 2009, p. 125.

50. Federal Highway Administration (FHWA), *Technical Advisory T 5040.36 – Surface Texture for Asphalt and Concrete Pavements*, FHWA, Washington, DC, June 17, 2005, 7 pp.

51. Michael W. Sayers and Steven M. Karamihas, *The Little Book of Profiling,* The Regent of the University of Michigan, Ann Arbor, MI, 1998.

52. Lev Khazanovich and Bernard I. Izevbekhai, "Implication of time-dependent texture-degradation on pavement on board sound intensity patterns in MnROAD test cells," in *Proceedings of Noise-Con 2008*, Dearborn, MI, 2008.

53. Aybike Ongel, Erwin Kohler and John Harvey, "Principal Components Regression of Onboard Sound Intensity Levels," *Journal of Transportation Engineering*, Vol. 134, No. 11, 2008.

54. R. J. Bernhard and R. S. McDaniel, "Basics of Noise Generation for Pavement Engineers," *Transportation Research Record, Journal of the Transportation Research Board, No. 1941,* TRB, National Research Council, Washington, DC., 1996, pp. 161-166.

55. Thomas Beckenbauer and Ark Kuijpers, "Prediction of pass-by levels depending on road surface parameters by means of a hybrid model," in *Proceedings of Inter-Noise 2001*, The Hague, Holland, 2001, p. 2528.

56. Tatsuo Fujikawa, Yasuo Oshino, Tetsuo Mikami and Hideki Tachibana, "Examination of road roughness parameters for abating tire vibration and radiated noise," *Noise Control Engineering Journal*, Vol. 57, No. 2, p. 77, March 2009.

57. Ard Kuijpers and Gijsjan van Blokland, "Tyre/road noise modeling: The road from a tyre's point-of-view," in *Proceedings of Inter-Noise 2003*, Jeju, South Korea, 2003, p. 249.

58. J.-F. Hamet and P. Klein, "Road texture and tire noise," in *Proceedings of Inter-Noise 2000*, Nice, France, 2000, p. 2517.

59. F Wullens, W. Kropp and P. Jean, "Quasi-3D versus 3D contact modelling for tyre/road interaction," in *Proceedings of Inter-Noise 2004*, Prague, Czech Republic, 2004, p. 3318.

60. ASTM International, "Standard Test Method for Skid Resistance of Pavement Surfaces Using a Full-Scale Tire," ASTM, E274, ASTM, West Conshohocken, PA, 2011.

61. ASTM International, "Standard Test Method for Measuring Paved Surface Frictional Properties Using the Dynamic Friction Tester," ASTM E1911, ASTM, West Conshohocken, PA, 2009.

62. ASTM International, "Standard Practice for Calculating International Friction Index of a Pavement Surface," ASTM E1960, ASTM, West Conshohocken, PA, 2011

63. Truls Berge and Svein A. Storeheier, "Low noise pavements in a Nordic climate. Results from a four year project in Norway," in *Proceedings of Inter-Noise 2009*, Ottawa, Canada, 2009, p. 1936.

64. American Association of State Highway and Transportation Officials, "Standard Method of Test for Determining Dynamic Modulus for Hot Mix Asphalt (HMA)," AASHTO T 342, AASHTO, Washington, DC, 2011.

65.   American Association of State Highway and Transportation Officials, "Standard Practice for Developing Dynamic Modulus Master Curves for Hot Mix Asphalt," AASHTO PP 62, AASHTO, Washington, DC, 2010.

66.   J. F. Shook and B. F. Kallas, "Factors Influencing Dynamic Modulus of Asphalt Concrete," *Journal of Association of Asphalt Paving Technologists*, Vol. 38, 1969.

67.   J. Bari and M. W. Witczak, "Development of a New Revised Version of the Witczak E* Predictive Model for Hot Mix Asphalt," *Journal of Association of Asphalt Paving Technologists*, Vol. 75, 2006.

68.   D. W. Christensen, T. K. Pellinen and R. F. Bonaquist, "Hirsch Model for Estimating the Modulus of Asphalt Concrete," *Journal of Association of Asphalt Paving Technologists*, Vol. 72, 2003.

69.   R. Dongre, L. Myers, J. D'Angelo, C. Paugh and J. Gudimettla, "Field Evaluation of Witczak and Hirsch Models for Predicting Dynamic Modulus of Hot-Mix Asphalt," *Journal of Association of Asphalt Paving Technologists*, Vol. 74, 2005.

70.   C. W. Schwartz, "Evaluation of the Witczak Dynamic Modulus Prediction Model," in *Proceedings of the 84th Annual Meeting of the Transportation Research Board*, Washington, DC, 2005.

71.   N. H. Tran and K. D. Hall, "Evaluating the Predictive Equation in Determining Dynamic Moduli of Typical Asphalt Mixtures Used in Arkansas," *Journal of Association of Asphalt Paving Technologists*, Vol. 74, 2005.

72.   G. Garcia and M. Thompson, *HMA Dynamic Modulus Predictive Models - A Review*, FHWA-ICT-07-006, Federal Highway Administration, Washington, DC, 2007.

73.   G. Garcia and M. Thompson, *HMA Dynamic Modulus - Temperature Relations*, FHWA-ICT-07-006, Federal Highway Administration, Washington, DC, 2007.

74.   Chetana Rao and Harold L. Von Quintus, *Determination of In Place Elastic Layer Modulus – Selection and Demonstration of Backcalculation Methodology and Practice: Phase I Interim Report*, Long Term Pavement Performance Program, Federal Highway Administration, Washington, DC, May 2012.

75.   International Organization for Standardization, "Acoustics - Materials for Acoustical Applications - Determination of Airflow Resistance," ISO 9053, ISO, Geneva, Switzerland, 1991.

76.   Minnesota Department of Transportation, Office of Materials and Road Research, *MnDOT Distress Identification Manual*, Minnesota Department of Transportation, Maplewood, MN, 2003.

77.   American Association of State Highway and Transportation Officials, "Theoretical Maximum Specific Gravity and Density of Hot Mix Asphalt (HMA)," AASHTO T 209, AASHTO, Washington, D.C.,2011.

78.   American Association of State Highway and Transportation Officials, "Bulk Specific Gravity and Density of Compacted Hot Mix Asphalt (HMA) Using Automatic Vacuum Sealing Method," AASHTO T 331, AASHTO, Washington, D.C., 2010.

79.   ASTM International, "Standard Test Method for Impedance and Absorption of Acoustical Materials Using a Tube, Two Microphones and a Digital Frequency Analysis System," ASTM E1050, ASTM, West Conshohocken, PA, 2010.

80.   K. J. Kowalski, R. S. McDaniel and J. Olek, *Identification of Laboratory Technique to Optimize Superpave HMA Surface Friction Characteristics,* Publication FHWA/IN/JTRP-2010/06, Joint Transportation Research Program, Indiana Department of Transportation and Purdue University, West Lafayette, IN, 2010.

81.   R. S. McDaniel, K. J. Kowalski, A. Shah, J. Olek and R. J. Bernhard, *Long-Term Performance of a Porous Friction Course,* Publication FHWA/IN/JTRP-2009/22, Joint Transportation Research Program, Indiana Department of Transportation and Purdue University, West Lafayette, IN, 2010.

82.   S. Kocak and M. E. Kutay, "Relationship between Material Characteristics of Asphalt Mixtures and Highway Noise," Paper No. 12-4309, *TRB 91st Annual Meeting Compendium of Papers*, TRB, National Research Council, 2012.

83.   G. Descornet, "Low-noise road surface techniques and materials," in *Proceedings of Inter-Noise 2000*, Nice, France, 2000, p. 4867.

84.   S. Huschek, "Influence of Road Surface Roughness on Tire Noise Generation in the Federal Republic of Germany," *Surface Characteristics of Roadways: International Research and Technologies,* ASTM STP 1031, W.E. Meyer and J. Reichert, Eds., American Society for Testing and Materials, Philadelphia, 1990.

85.   P. M. Nelson, "Designing Porous Road Surfaces to Reduce Traffic Noise," *TRL Annual Review*, Crowthorne, Berkshire, United Kingdom, 1994.

86.   F. E. Perez Jimenez and M. A. Calzada Perez, "Analysis and Evaluation of the Performance of Porous Asphalt: The Spanish Experience," *Surface Characteristics of Roadways: International Research and Technologies*, ASTM STP 1031, W.E. Meyer and J. Reichert, Eds., American Society for Testing and Materials, Philadelphia, 1990.

87.   R. L. Wayson, Synthesis of Highway Practice 268. *Relationship Between Pavement Surface and Highway Traffic Noise*, National Cooperative Highway Research Program, National Academy Press, Washington, D.C., 1998.

88.   Ulf Sandberg, "Semi-generic temperature corrections for tyre/road noise," in *Proceedings of Inter-Noise 2004*, Prague, Czech Republic, 2004, p. 3302.

89.   J. J. Hajek, L. Kwan and C. T. Blaney, "Comparison of tire/pavement noise measurements method," in *Proceedings of Inter-Noise 1982*, San Francisco, CA, 1982, p. 119.

90.   S. M. Bazlamit and F. Reza, "Changes in Asphalt Pavement Friction Components and Adjustments of Skid Number for Temperature," *ASCE Journal of Transportation Engineering*, Vol. 131, No. 6, pp. 470-476, 2005.

91.   G. W. Flintsch, Y. Luo and I. L. Al-Qadi, "Analysis of the Effect of Pavement Temperature on the Frictional Properties of Flexible Pavement Surfaces," in *Proceedings of the 84th Annual Meeting of the Transportation Research Board*, Washington, DC, 2005.

92.   T. Gargett, "The Introduction of a Skidding-Resistance Policy in Great Britain," *Surface Characteristics of Roadways: International Research and Technologies,* ASTM STP 1031, W.E. Meyer and J. Reichert, Eds., American Society for Testing and Materials, Philadelphia, 1990.

93.   J. J. Henry, K. Saito and R. Blackburn, *Predictor Model for Seasonal Variations in Skid Resistance*, Vol. I: Summary Report and Vol. II Comprehensive Report FHWA/RD-83/004 and FHWA/RD-83/005, Federal Highway Administration, Washington, DC,

1984.

94. B. J. Hill and J. J. Henry, "Surface Materials and Properties Related to Seasonal Variations in Skid Resistance," *Pavement Surface Characteristics and Materials*, ASTM STP 763, C. M. Hayden, Ed., ASTM, Washington, DC, 1982, pp. 45-60.

95. J. C. Wambold, J. J. Henry, C. E. Antle, B. T. Kulakowski, W. E. Meyer, A. J. Stocker, J. W. Button and D. A. Anderson, *Pavement Friction Measurement Normalized for Operational, Seasonal, and Weather Effects*, FHWA-RD-88-069, Federal Highway Administration, Washington, DC, 1989.

96. H. Wang and G. W. Flitsch, "Investigation of Short and Long-Term Variations of Pavement Surface Characteristics at the Virginia Smart Road," in *Proceedings of the 86th Annual Meeting of the Transportation Research Board*, Washington, DC, 2007.

97. K. T. Diringer and R. T. Barros, "Predicting the Skid Resistance of Bituminous Pavements Through Accelerated Laboratory Testing of Aggregates," *Surface Characteristics of Roadways: International Research and Technologies,* ASTM STP 1031, W.E. Meyer and J. Reichert, Eds., American Society for Testing and Materials, Philadelphia, 1990.

98. X. Huihua and J. J. Henry, "The Use of Fuzzy-Sets Mathematics for Analysis of Pavement Skid Resistance," *Surface Characteristics of Roadways: International Research and Technologies,* ASTM STP 1031, W.E. Meyer and J. Reichert, Eds., American Society for Testing and Materials, Philadelphia, 1990.

99. J. Donbavand and D. Cook, "Procedure for Correcting Seasonal Variations," in *Proceedings of the International Conference on Surface Friction*, Christchurch, New Zealand, 2005.

100. J. W. Shupe, "Pavement Slipperiness," in *Highway Engineering Handbook*, K. B. Woods, D. S. Berry and W. H. Goetz, Eds. New York, NY: McGraw-Hill, 1960.

101. K. Saito, T. Horiguchi, A. Kasahara, H. Abe and J. J. Henry, "Development of Portable Tester for Measuring Skid Resistance and its Speed Dependency on Pavement Surfaces," *Transportation Research Record, Journal of the Transportation Research Board*, Vol. 1536, TRB, National Research Council, Washington, DC, 1996, pp. 45-51.

102. T. W. Vollor and D. I. Hanson, *Development of Laboratory Procedure for Measuring Friction of HMA Mixtures - Phase I*, NCAT Report No. 06-06, National Center for Asphalt Technology, Auburn, AL, 2006.

103. Applied Research Associates, Inc., *Environmental Effects in the Absence of Heavy Loads*, Interim Report, Long-Term Pavement Performance Division, Federal Highway Administration, McLean, VA, April 2012, 203 pp.

104. B. L. Elkin, K. J. Kercher and S. Gulen, "Seasonal Variation in Skid Resistance of Bituminous Surfaces in Indiana," *Transportation Research Record, Journal of the Transportation Research Board,* No. 777, TRB, National Research Council, Washington, DC., 1980, p. 50-58.

105. B. J. Hill and J. J. Henry, "Short-Term, Weather-Related Skid Resistance Variations," *Transportation Research Record, Journal of the Transportation Research Board,* No. 836, TRB, National Research Council, Washington, DC., 1981, pp. 76-81.

106. K. Saito and J. J. Henry, "Mechanistic Model for Predicting Seasonal Variations in Skid Resistance," *Transportation Research Record, Journal of the Transportation Research Board,* No. 946, TRB, National Research Council, Washington, DC, 1983, pp. 29-38.

107. Kidd, S. Q., *Skid Resistance and Wear Properties of Aggregates for Asphalt Paving Mixtures*, Final Report, Mississippi State Highway Department, Report No. MSHD-RD-89-55, Jackson, MS, 1989.

108. E. J. Dickinson, "The Effect of Climate on the Seasonal Variation of Pavement Skid Resistance," *Australian Road Research*, Vol. 19, Issue 2, Australian Road Research Board, Melbourne, Australia, 1989, pp. 129-144.

109. P. W. Jayawickrama and B. Thomas, "Correction of Field Skid Measurements ofr Seasonal Variations in Texas," *Transportation Research Record, Journal of the Transportation Research Board,* No. 1639, TRB, National Research Council, Washington, DC, 1986, pp. 147-154.

110. M. A. Ahammad and S. L. Tighe, "Effect of Short-Term and Long-Term Weather on Pavement Surface Friction," *International Journal of Pavement Research and Technology*, Vol. 3, No. 6, November 2010, Taiwan, China, pp. 295-302.

111. H. A. Ali and A. Lopez, "Statistical Analysis of Temperature and Moisture Effects on Pavement Structural Properties Based on Seasonal Monitoring Data," *Transportation Research Record, Journal of the Transportation Research Board,* No. 1540, TRB, National Research Council, Washington, DC., 1996, pp. 48-55.

112. H. A. Ali and N. A. Parker, "Using Time Series to Incorporate Seasonal Variations in Pavement Design," *Transportation Research Record, Journal of the Transportation Research Board,* No. 1539, TRB, National Research Council, Washington, DC., 1996, pp. 33-43.

113. H. M. Salem, F. M. Bayomy, M. G. Al-Taher and I. H. Genc, "Using Long-Term Pavement Performance Data to Predict Seasonal Variation in Asphalt Concrete Modulus," *Transportation Research Record, Journal of the Transportation Research Board,* No. 1896, TRB, National Research Council, Washington, DC., 2004, pp. 119-128.

114. A. Bae, S. M. Stoffels and S. W. Lee, "Observed Effects of Subgrade Moisture on Longitudinal Profile," Paper No. 06-2312, *TRB 85th Annual Meeting Compendium of Papers* CD-ROM, TRB, National Research Council, Washington, DC., 2006, 19 pp.

115. ASTM International, "Standard Specification for P225/60R16 97S Radial Standard Reference Test Tire," ASTM F2493, ASTM, West Conshohocken, PA, 2008.

116. Robert Rasmussen, "Measuring and modeling tire-pavement noise on various concrete pavement textures," *Noise Control Engineering Journal*, Vol. 57, No. 2, p. 139, March 2009.

117. International Organization for Standardization, "Characterization of pavement texture by use of surface profiles – Part 4; Spectral analysis of surface profiles," ISO 13473-4, ISO, Geneva, Switzerland, 2008.

118. American Society of Mechanical Engineers, Surface Texture (Surface Roughness, Waviness and Lay," ASME B46.1, ASME, New York, NY, 2009.

119. International Organization for Standardization, "Geometrical Product Specifications (GPS) – Surface Texture: Profile Method; Surfaces Having Stratified Functional Properties – Part 2: Height Characterization Using the Linear Material Ratio Curve," ISO 11819-1, ISO, Geneva, Switzerland, 1996.

120. Carlos H. Reyes and John Harvey, "A method for prediction sound intensity noise levels

using laboratory pavement cores," in *Proceedings of Noise-Con 2011*, Portland, OR, 2011.

121. M. Brinkmeier, U. Nackenhorst, O. von Estorff and S. Petersen, "Physically Based Modelling of Tire-Rolling-Noise by a Finite Element Approach," in *Proceedings of Inter-Noise 2004*, Prague, Czech Republic, 2004.

122. Maik Brinkmeier, Udo Nackenhorst, Jan Biermann and Otto von Estorff, "Prediction of tire/road noise - modelling and validation," in *Proceedings of Inter-Noise 2007*, Istanbul, Turkey, 2007.

123. Tatsuo Fujikawa, Hiroshi Koike and Yasuo Oshino, "Relation between Road Roughness Parameters and Tyre Vibration Noise - Examination Using a Simple Tyre Model," in *Proceedings of Inter-Noise 2003*, Seogwipo, Korea, 2003.

124. Tatsuo Fujikawa, Yasuo Oshino and Hideki Tachibana, "Development of Method to Predict Tire/Road Noise Reduction by Road-Surface Improvements," in *Proceedings of Inter-Noise 2008*, Shanghai, China, 2008.

125. Tatsuo Fujikawa, Yasuo Oshino and Hideki Tachibana, "Application of road-profile enveloping procedure to height-unevenness method for prediction tire/road noise," in *Proceedings of Inter-Noise 2010*, Lisbon, Portugal, 2010.

126. Tatsuo Fujikawa and Hideki Tachibana, "Prediction of tire/road noise reduction by road-surface improvements," in *Proceedings of Inter-Noise 2009*, Ottawa, Canada, 2009.

127. Gijsjan van Blokland and Peter The, "Test sections for development of a hybrid tyre/road interaction noise model," in *Proceedings of Inter-Noise 2007*, Istanbul, Turkey, 2007.

128. T. Beckenbauer, P. Klein, J.-F. Hamet and W. Kropp, "Tyre/road noise prediction: A comparison between the SPERoN and HyRoNE models - Part 1," in *Proceedings of Acoustics08*, Paris, France, 2008.

129. P. Klein, T. Beckenbauer, J.-F. Hamet and W. Kropp, "Tyre/road noise prediction: A comparison between the SPERoN and HyRoNE models - Part 2," in *Proceedings of Acoustics08*, Paris, France, 2008.

130. Philippe Klein and Jean-Francois Hamet, "Tyre/road prediction with the HyRoNE model," in *Proceedings of Inter-Noise 2007*, Istanbul, Turkey, 2007, p. 191.

131. Eddy Gerretsen, Erik Salomons and Foort de Roo, "State of the art in tyre-road noise modelling," in *Proceedings of Inter-Noise 1997*, Budapest, Hungary, 1997.

132. Foort de Roo, Eddy Gerretsen, Werner G.J. Hoffmans and Niek J. Doelman, "Dutch tyre-road noise emission model -- Adjustments and validation," in *Proceedings of Inter-Noise 1999*, Fort Lauderdale, FL, 1999.

133. F. de Roo and E. Gerretsen, "TRIAS - Tyre Road Interaction Acoustic Simulation Model," in *Proceedings of Inter-Noise 2000*, Nice, France, 2000.

134. Foort de Roo, Eddy Gerretsen and Era H. Mulder, "Predictive performance of the tyre-road noise model TRIAS," in *Proceedings of Inter-Noise 2001*, The Hague, Holland, 2001.

135. F.J.M. van der Eerden, E. Gerretsen, F. de Roo, E.H. Mulder and E.D. Schoen, "A parameter study with the tyre-road noise simulation tool TRIAS," in *Proceedings of Inter-Noise 2002*, Dearborn, MI, 2002.

136. N.J. Doelman, E.H. Mulder, F.J.M. van der Eerden and F. de Roo, "3-D characterisation

of road surface textures in TRIAS," in *Proceedings of Inter-Noise 2004*, Prague, Czech Republic, 2004.

137. Washington State Department of Transportation (WSDOT), *EVERSERIES Users Guide: Pavement Analysis Computer Software and Case Studies*, Seattle, WA, 2005.

138. Tyler P. Dare, "Generation Mechanisms of Tire-Pavement Noise, Purdue University, West Lafayette, IN, Ph.D. Dissertation, 2012.

139. Paul R. Donavan, "The Acoustic Longevity of Various Pavement for Noise Reduction Performance Based on On-Board Sound Intensity Measurement," in *Proceedings of Noise-Con 2010*, Balitmore, MD, 2010.

Appendix A – Definitions

Tire directional terms

- **Radial:** along a line pointing from the wheel's hub outward towards the treadband

- **Tangential** or **circumferential:** around the tire, along the direction of the treadband

- **Axial:** in the direction of a wheel's axle; perpendicular to the line of travel

Pavement directional terms

- **Longitudinal:** in the direction of travel

- **Transverse:** perpendicular to the direction of travel

Pavement texture terms

- **Microtexture:** texture features with wavelength less than 0.5 mm

- **Macrotexture:** texture features with wavelength between 0.5 mm and 50 mm

- **Megatexture:** texture features with wavelength greater than 50 mm

- **Positive texture:** texture features above the mean pavement level

- **Negative texture:** texture features below the mean pavement level
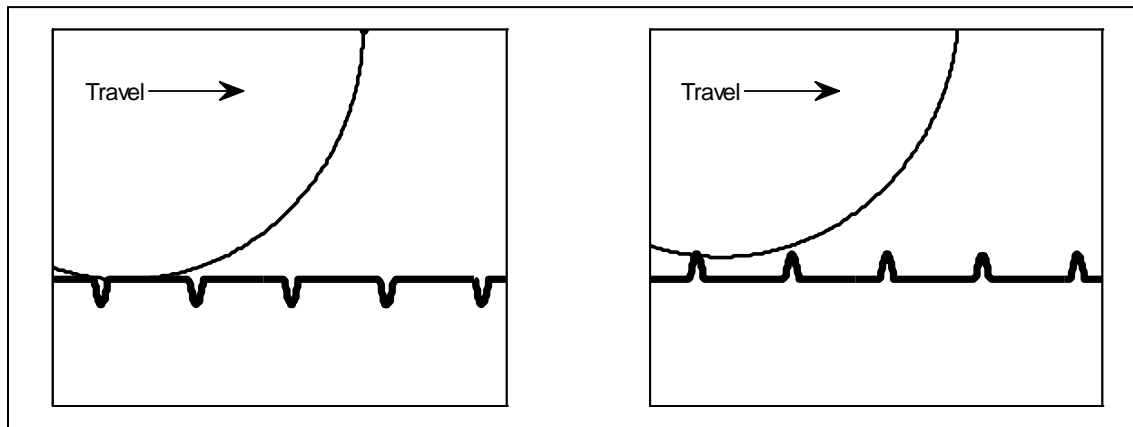
Figure A 1: Positive and negative texture for two pavements with identical texture spectra. Left: Negative texture. Right: Positive texture.

Appendix B – FWD Backcalculation Using Evercalc 5.0

The Evercalc software (developed by Washington State DOT) was used to determine pavement stiffness using Falling Weight Deflectometer (FWD) data and the corresponding surface temperature data provided by MnDOT.

Only specific test cells were analyzed. The cells were selected after discussion with MnROAD personnel regarding the materials at MnROAD and the limitations of backcalculation. Consequently, some cells were not analyzed because the asphalt layers were too thin to analyze reliably, such as Cells 106 and 206 with only 2 in. of asphalt. For some cells, layers of similar materials were grouped together, since it is better to analyze no more than four or five layers. There is a water table at 4 to 10 ft. in some locations, however, this was not modeled as a stiff layer for this analysis because of uncertainty as to the actual depth at the time of FWD testing.

While a vast amount of deflection data was collected over the years, for ease of processing and to allow comparison to the OBSI data, only data from 2009 to 2011 were used for the analysis. Only the data from the outer wheel path drop locations were extracted and used in determining the modulus of the pavement.

Three load drops and deflection measurements were taken at each location. For each test, a specific *.gen file was created which contains general information, such as plate radius, sensor spacing, minimum and maximum modulus, etc., as shown in Figure B1. In addition, the user is also given the option of choosing the location where the stresses and strains are to be computed, such as top, middle or bottom of the pavement layer. In this analysis, the calculations were conducted at the bottom of the top layer, middle of the second layer and top of the third layer. Following the creation of the general file, a deflection file (*.def) tied to the corresponding general file data was created. In this file, the loads and measured deflections at each of the sensor locations corresponding to each load drop was entered manually. Other information, such as surface temperature and layer thickness, was also provided. Figure B2 shows a typical example of this file. After the data was entered, it was also possible to generate a plot of the deflection basins for the three loading conditions (Figure B3). Figure B4 shows the deflection basins for Cell 19 measured at different times of the year. These basins clearly show seasonal differences in the deflections and hence the stiffness of the pavements.

Backcalculation of the pavement modulus using Evercalc software was then conducted by selecting each general file and the corresponding deflection file. A seed modulus was chosen and then the software varied the moduli to yield calculated deflections that matched the measured deflections. The summary output file shows the modulus of each layer, temperature-adjusted modulus, load-normalized modulus and percent RMS error. It is preferred that the RMS is low, typically less than 3%. While this condition was hard to satisfy given the inherent variability in the data set, the %RMS for the data used in this study was less than 9%.

It is known that asphalt pavement modulus decreases with increasing temperature as the binder mastic softens. Thus the material behaves as a viscoelastic material at warmer temperatures and elastic at lower temperatures. A plot of modulus of the top layer (E_1) versus surface temperature from one of the test cells reflects this expected trend (Figure B5). In most cases, the r-squared value for the regression line was high indicating a strong correlation between the estimated pavement modulus and surface temperature. The E_1 results were used to explore the relationship between modulus and noise.

Figure B 1: Example of general information file (*.gen). (Cell 19)
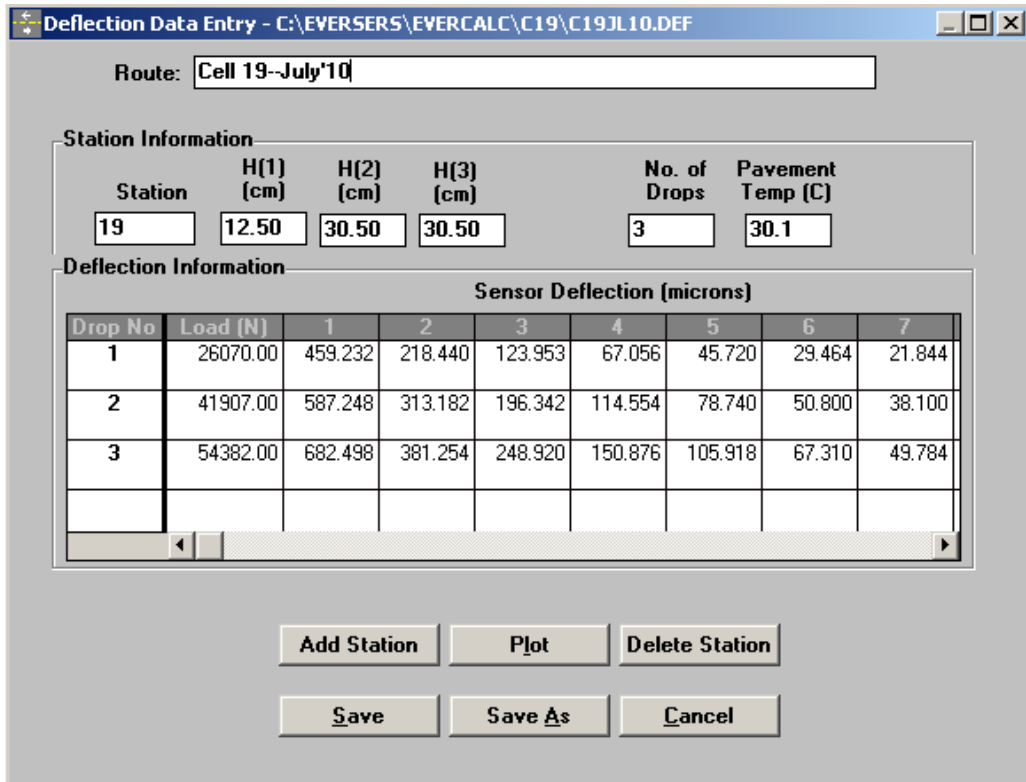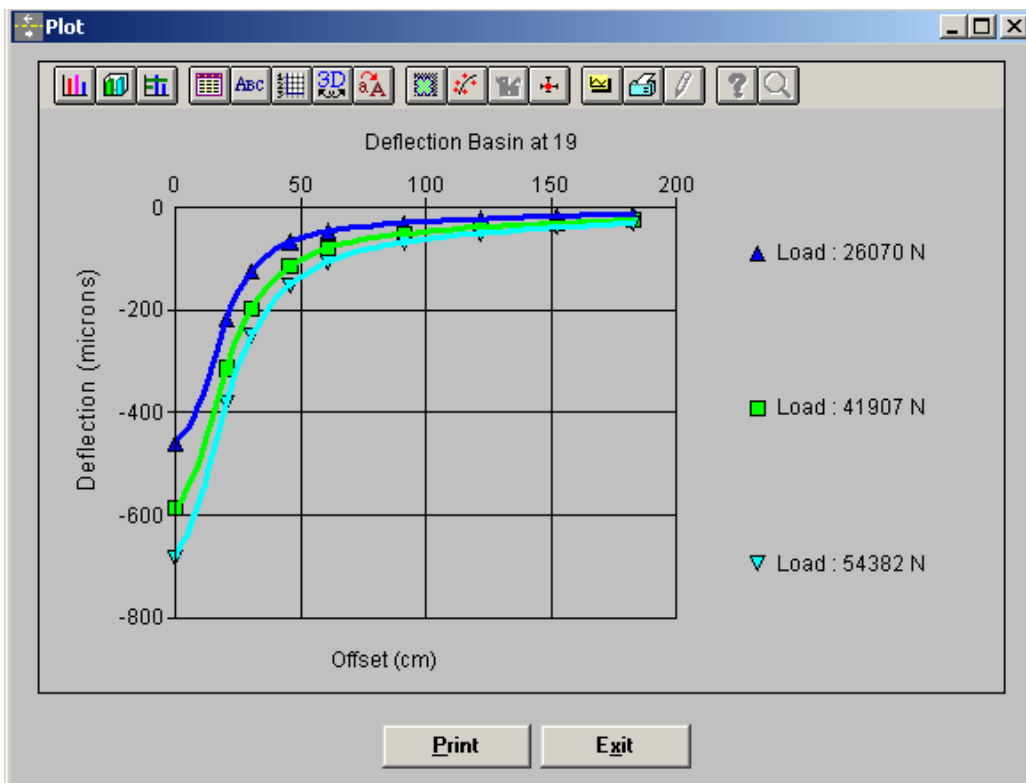
Figure B 2: Example of deflection file (Cell 19).

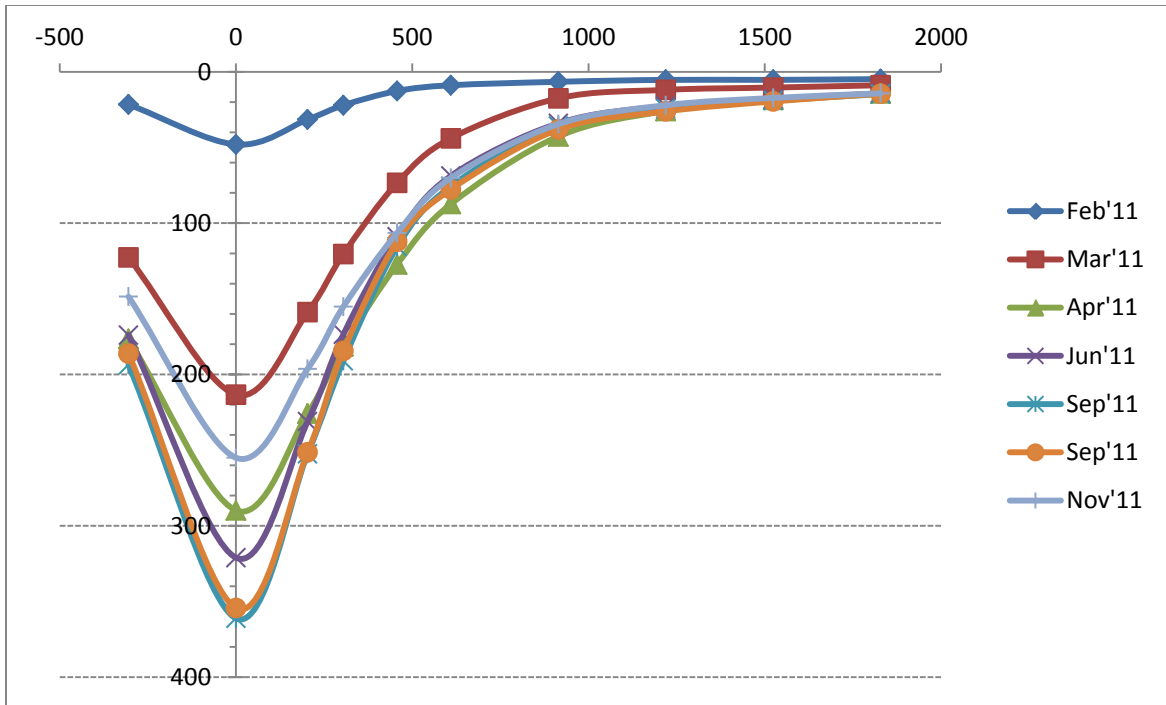Figure B 3: Plot of deflections basins measured for Cell 19 at different loads.

B-3

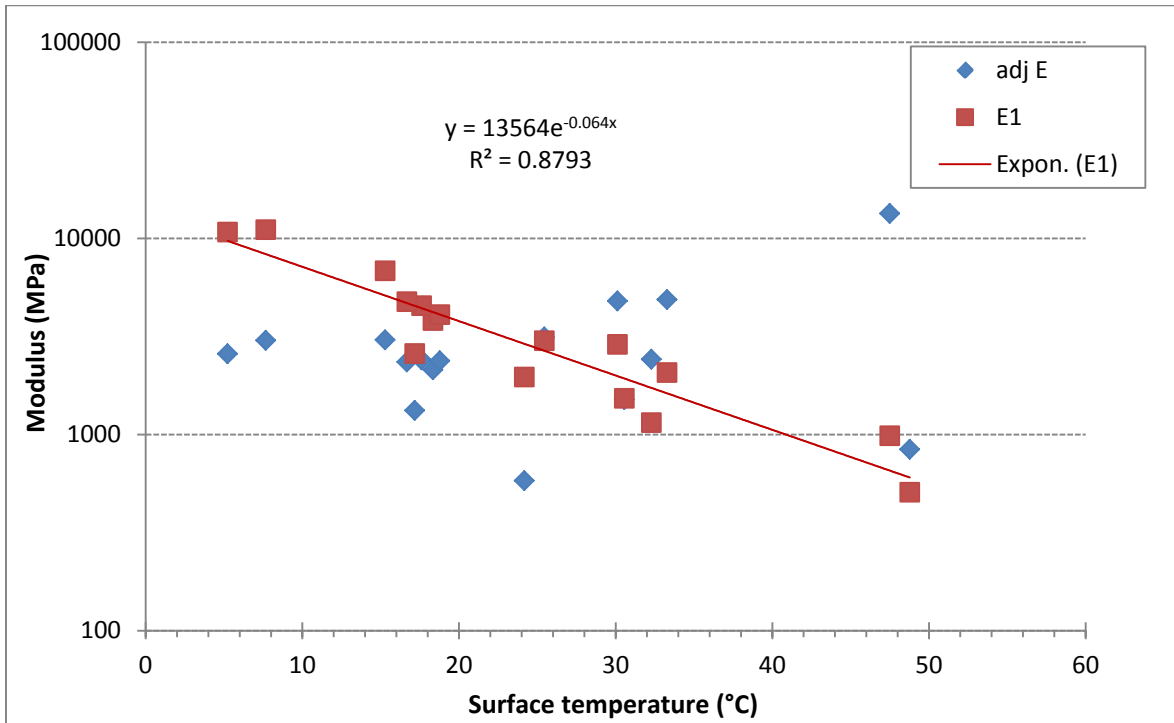Figure B 4: Deflection basins for Cell 19 measured at different times, showing seasonal effects.

Figure B 5: Plot of E1 and adjusted E1 versus surface temperature (Cell 19).

$$y = 13564e^{-0.064x}$$
$$R^2 = 0.8793$$

Appendix C – Results for Trailing Edge OBSI Probe
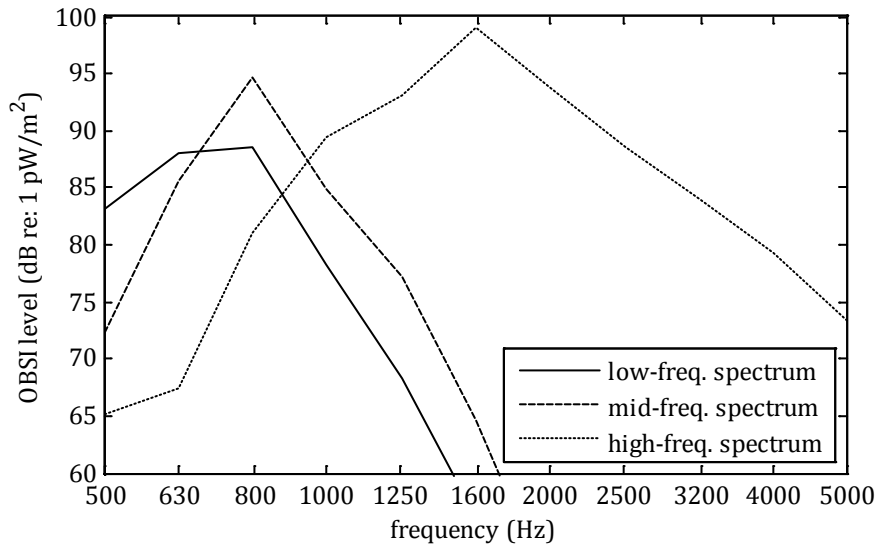
Figure C 1: Low-, mid-, and high-frequency constituent spectra (trailing edge).
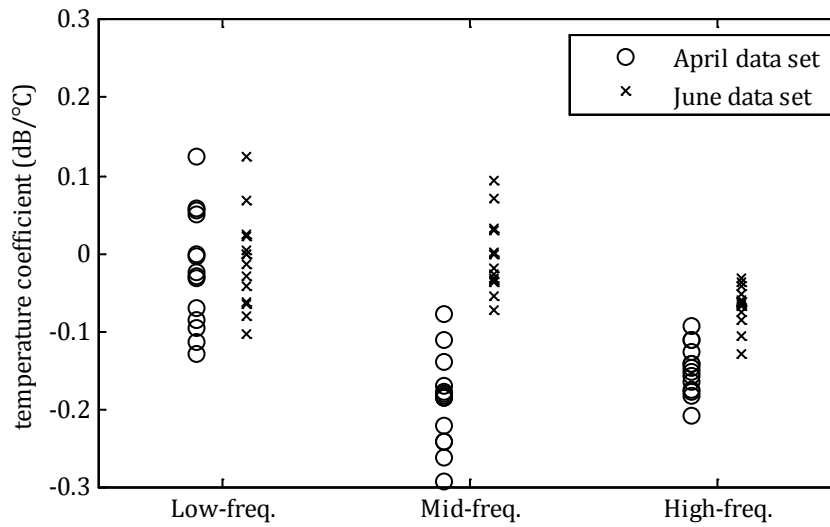
Figure C 2: Constituent spectra temperature coefficients using air temperature (trailing edge).
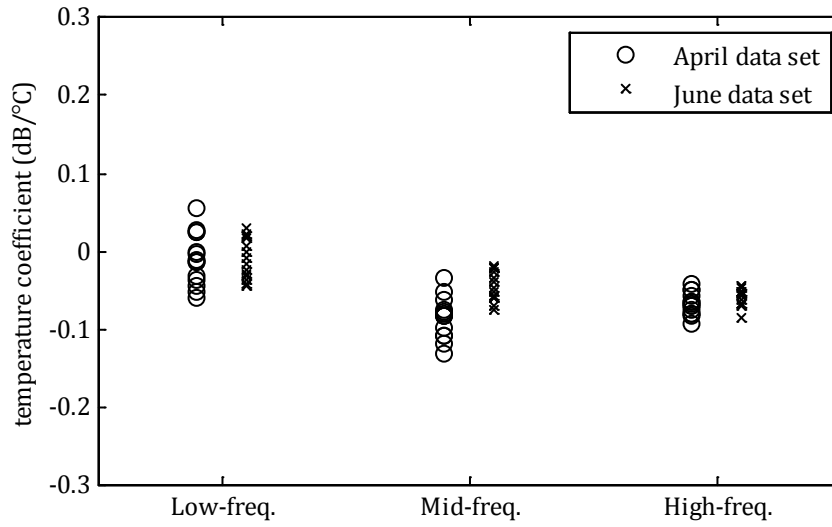
Figure C 3: Constituent spectra temperature coefficients using pavement temperature (trailing edge).
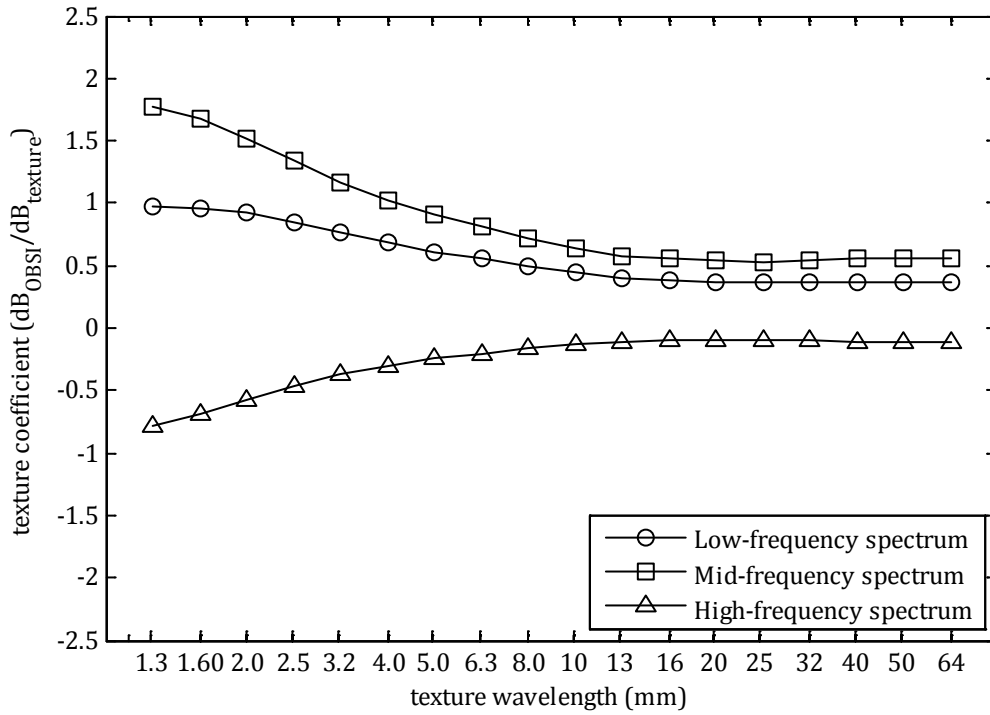
Figure C 4: Best-fit texture coefficients for each texture wavelength (trailing edge).
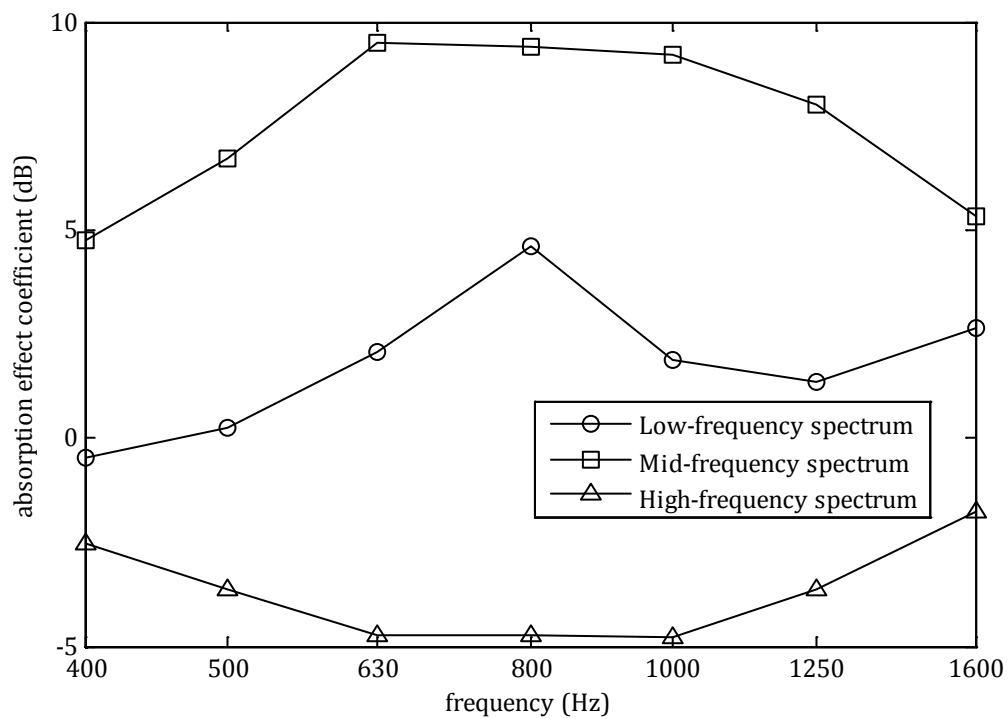
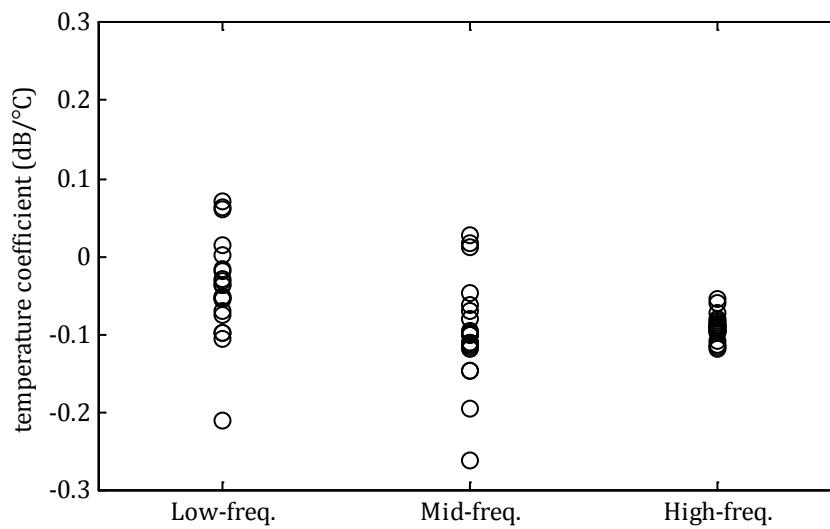Figure C 5: Best-fit coefficients for each absorption frequency (trailing edge).

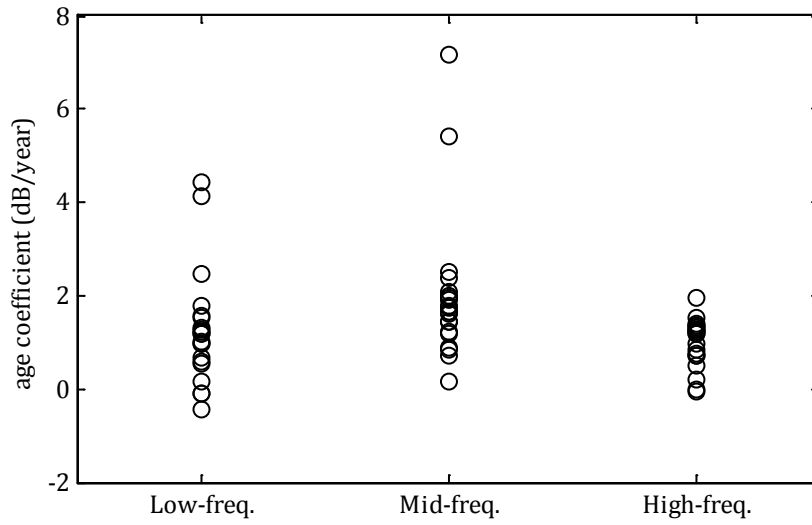Figure C 6: Best-fit temperature coefficients for two-parameter age-temperature model (trailing edge).

.

C-3

Figure C 7: Best-fit pavement age coefficients for two-parameter age-temperature model (trailing edge).
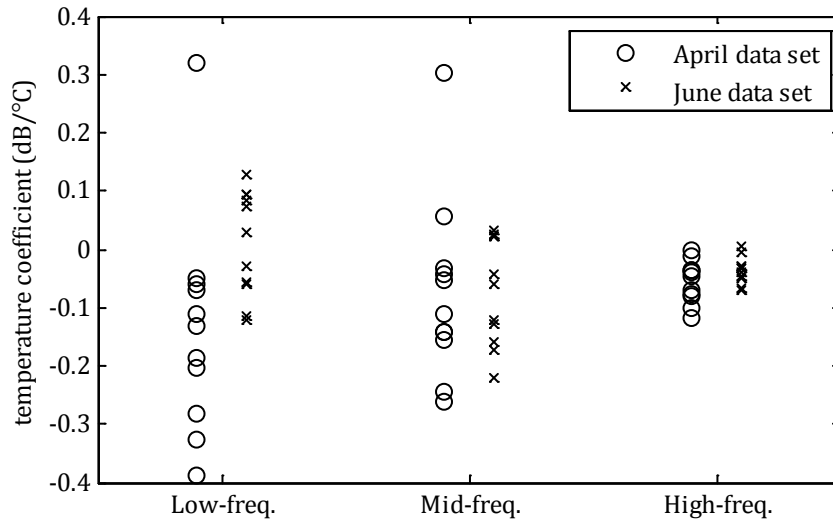

Figure C 8: Best-fit pavement temperature coefficients for two-parameter temperature-modulus model (trailing edge).
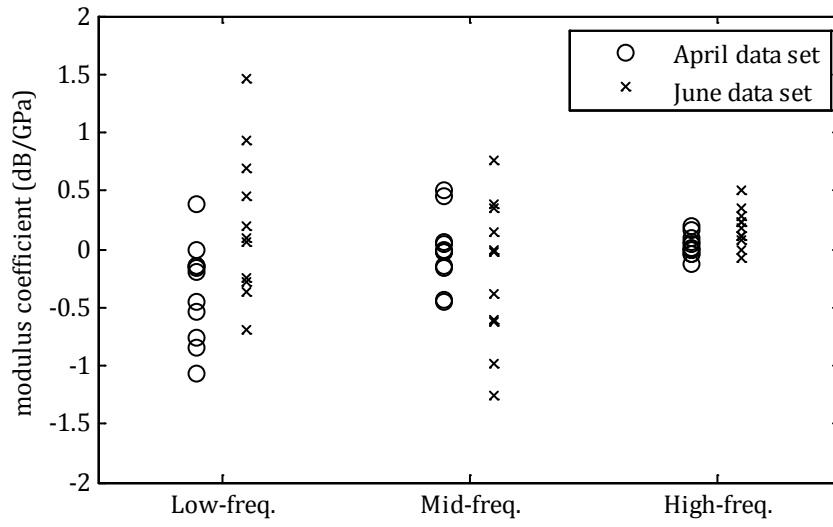
Figure C 9: Best-fit modulus coefficients for two-parameter temperature-modulus model.